

Molecular mechanisms of DELLA action and its partners during secondary growth

Dissertation

der Mathematisch-Naturwissenschaftlichen Fakultät
der Eberhard Karls Universität Tübingen
zur Erlangung des Grades eines
Doktors der Naturwissenschaften
(Dr. rer. nat.)

vorgelegt von
Mehdi BEN TARGEM
aus Tunis/TUNESIEN

Tübingen
2018

Gedruckt mit Genehmigung der Mathematisch-Naturwissenschaftlichen Fakultät
der Eberhard Karls Universität Tübingen.

Tag der mündlichen Qualifikation:	30.11.2018
Dekan:	Prof. Dr. Wolfgang Rosenstiel
1. Berichterstatter:	Dr. Laura Ragni
2. Berichterstatterin:	Prof. Dr. Gerd Jürgens

Dedication

To my family: my mother Fethia, my father Ahmed, my sister and brother: Imen and Mohamed, they are my constant source of love motivation and strength. None of this would have been possible without their unconditional love and constant support.

To the soul of my grandmother Aziza for all the sweet memories.

To all who contribute to make this world a better place with their intentions and attitudes.

Acknowledgements

First and foremost I offer my sincerest gratitude to Dr. Laura Ragni for the great opportunity to explore the molecular mechanisms of secondary growth as a Doctoral researcher in her Lab. I would like to thank her for the continuous support and encouragement, for all what I learned during my stay among her group, for her willingness to discuss scientific ideas, giving me the room to test hypothesis that I propose. It was a pleasure to work with her and one simply could not wish for a more caring and dedicated supervisor.

I would like to express my gratitude to Prof. Dr. Gerd Jürgens and Dr. Martin Bayer for all the scientific input they gave through my progress report presentations and committee meetings. For the nice and friendly collaboration, I had been doing on RNA sequencing with Dr. Martin Bayer from Max Planck Institute for Developmental Biology.

Many thanks go to my friendly and cheerful fellow Lab mates, to all my colleagues in the developmental genetic department and ZMBP as well as all the staff of each facility.

I would not miss to thank Prof. Dr. Klaus Harter and Prof. Dr. Claudia Oecking for accepting to be part of the jury.

A special appreciation goes to all my Professors during my Agriculture Engineering studies in TUNISIA and my Master of Science studies in GREECE.

Mehdi

Table of Contents

1 Summary:	2
2 Zusammenfassung	4
3 Introduction	6
3.1 Secondary growth and wood formation in plants	6
3.2 The Arabidopsis hypocotyl as a model to study secondary growth	7
3.3 Secondary growth and cambium regulaion	8
3.3.1 Regulation through peptides and receptors.....	8
3.3.2 Hormonal regulation	9
3.4 DELLA mode of action:.....	11
3.4 DELLA cross-talk with Auxin, Cytocinin and Jasmonate:	12
4 Aim of the thesis.....	13
5 Draft manuscripts	15
5.1 Draft manuscript 1:	15
5.2 Draft manuscript 2:	54
6 Discussion	80
7 References	87
8 Appendices	94
8.1 Published article 1:.....	94
8.2 Published article 2:.....	102

1 Summary

Secondary growth or the increase in girth of plant organs is a primordial developmental process in seed plants as vascular expansion limits the transport of water and solute and provides mechanical support for the plant. Secondary growth involves the vascular cambium which is a cylindrical meristematic tissue producing inwards the xylem and outwards the phloem. It leads to thickening of plant organs and formation of secondary xylem or wood. Wood is the principal sink for excess atmospheric CO₂ and fundamental source of natural renewable energy. Arabidopsis hypocotyl provides a good model to study secondary growth where two phases can be distinguished: an early phase in which xylem and phloem are produced at roughly the same rate, followed by a later phase of xylem expansion, in which xylem is produced at higher rate accompanied by fiber differentiation. Gibberellin (GA) triggers the shift between the two phases upon flowering, it moves from the shoot apex to the hypocotyl where it induces locally the degradation of DELLA proteins which are known to act as repressors of secondary growth. Although secondary growth is crucial for the plant and environment, it is surprising that little is known about the molecular mechanisms underlying it. In this study, we found that among the DELLA gene family *REPRESSOR OF gal-3 (RGA)* and *GA INSENSITIVE (GAI)* mediate most of the GA related secondary growth, with a more pronounced role of RGA as repressor. The role of RGA and GAI seems to be conserved across ecotypes, which greatly differ in xylem occupancy.

We identified novel regulators of secondary growth through evaluating DELLA known interactors as well as analyzing the transcriptome related to RGA upon transition to the xylem expansion phase. We found that *AUXIN RESPONSIVE FACTOR (ARF6)*, *ARF7* and *ARF8* act as positive regulators of xylem expansion and fiber differentiation whereas *type-B ARABIDOPSIS RESPONSE REGULATORS (ARR1)* and *ARR2*, *CORONATINE-INSENSITIVE 1 (COI1)* and *TRANSCRIPTION FACTOR MYC2 (MYC2)* activate phloem proliferation with a specific role for *ARR1* and *ARR2* in repressing fiber differentiation in the hypocotyl. Our genetic interaction analyses indicate that DELLA sequesters the identified ARF's and possibly *BREVIPEDICELLUS/KNAT1/ (BP/KNAT1)* during the early phase. During the second phase *ARF6*, *ARF7*, *ARF8* and probably *BP* are released from DELLA repression. We also showed that *BP* expression does not depend on *ARF6* and *ARF8* in the hypocotyl, instead our data indicate a

possible interaction between BP and ARF's to regulate cambium activity. We performed RNA seq experiments in order to gain more insights into the regulatory network related to the positive regulation of xylem expansion mediated by *ARF6* and *ARF8*, we identified several candidates involved in xylem development. Apart from the DELLA mediated control of secondary growth; we also identified a specific role for Jasmonate in promoting fiber formation, in the xylem and ectopically in the phloem, without altering the Xylem/Total area (X/A) ratio.

Taken together, our findings shed light on a complex hormone cross-talk between GA, Auxin, Cytokinin and Jasmonate where DELLA function as central hub regulating xylem expansion and fiber differentiation.

2 Zusammenfassung

Sekundäres Dickenwachstum ist ein grundlegender Entwicklungsprozess in Samenpflanzen, da die Entwicklung des vaskulären Gewebes den Transport von Wasser als auch löslichen Nährstoffen steuert, und den Pflanzen zusätzlich mechanische Stützkraft verleiht. Das vaskuläre Kambium, ein zylinderförmiges, meristematisches Gewebe, ist am sekundären Dickenwachstum beteiligt. Es produziert nach innen Xylem- und nach außen Phloemgewebe, was zu einer Verdickung der Pflanzenorgane führt. Zudem wird sekundäres Xylem oder Holz gebildet. Holz ist Hauptspeicher für atmosphärisches CO₂ und eine der Hauptquellen zur Gewinnung erneuerbarer Energien. Im Hypokotyl von *Arabidopsis thaliana* lassen sich zwei Phasen des sekundären Dickenwachstums unterscheiden, was *Arabidopsis* zu einem geeigneten Modell für das Studium des selbigen macht. In der frühen Phase des Dickenwachstums werden Xylem und Phloem zu gleichen Anteilen gebildet, wohingegen in der späteren Wachstumsphase sich das Xylem, begleitet von Faserbildung, vergrößert. Der Übergang von der frühen in die späte Entwicklungsphase wird bei Blühbeginn durch Gibberellinsäure (GA) ausgelöst. GA wandert von der Spitze des Sprosses zum Hypokotyl, wo sie lokal den Abbau von DELLA Proteinen induziert, welche wiederum als Repressoren des sekundären Dickenwachstums bekannt sind.

Trotz der hohen Relevanz von sekundärem Dickenwachstum für Pflanze und Umwelt, ist überraschenderweise wenig über die zu Grunde liegenden Regulationsmechanismen bekannt. In dieser Forschungsarbeit haben wir herausgefunden, dass ein Großteil des GA-abhängigen Dickenwachstums innerhalb der DELLA-Genfamilie durch REPRESSOR OF *ga1-3* (RGA) und GA INSENSITIVE (GAI) vermittelt wird, wobei RGA vornehmlich als Repressor agiert. Die Rolle von RGA und GAI scheint zudem innerhalb verschiedener Ökotypen, die sich in ihrem Xylemvorkommen unterscheiden, konserviert zu sein.

Durch die Auswertung von bekannten Della-Interaktoren sowie Transkriptomanalysen zu RGA im Übergang zur Xylemausdehnung, war es möglich neue Regulatoren des sekundären Dickenwachstums zu identifizieren. *AUXIN RESPONSIVE FACTOR (ARF) 6*, *ARF7* und *ARF8* agieren als positive Regulatoren in der Xylemausdehnung und Faserdifferenzierung, wohingegen *Typ-B ARABIDOPSIS RESPONSE REGULATORS (ARR) 1* und *ARR2*, *CORONATINE-INSENSITIVE 1 (COI1)* und *TRANSCRIPTION FACTOR MYC2 (MYC2)* die Phloem Proliferation aktivieren. Durch die Hemmung der Faserdifferenzierung im Hypokotyl spielen *ARR1* und *ARR2*

hierbei eine spezifische Rolle. Unsere genetischen Interaktionsanalysen lassen darauf schließen, dass DELLA die identifizierten ARFs und wahrscheinlich auch BREVIPEDICELLUS/KNAT1/ (BP/KNAT1) während der frühen Phase sequestriert.

Während der zweiten Phase werden ARF6, ARF7, ARF8 und wahrscheinlich auch BP von der DELLA Repression freigegeben. Wir konnten ebenfalls zeigen, dass die Expression von BP im Hypokotyl nicht ARF6 und ARF8 abhängig ist. Unsere Daten lassen jedoch vermuten, dass eine mögliche Interaktion zwischen BP und ARFs zur Regulation der Kambiumaktivität beiträgt. Um mehr Einblick in die Maschinerie zu erhalten, welche die ARF6- und ARF8-abhängige Xylemausdehnung positiv reguliert, haben wir RNA sequenziert und konnten hierdurch einige Kandidatengene für die Xylementwicklung identifizieren. Unabhängig von der DELLA-gesteuerten Kontrolle des sekundären Dickenwachstums konnte auch eine spezifische Rolle für Jasmonate in der Förderung der Faserdifferenzierung im Xylem und ektopisch im Phloem nachgewiesen werden, wobei der Xylem/Gesamtfläche-Anteil gleich bleibt.

Zusammengefasst bringen unsere Ergebnisse Licht in das Dunkel des komplexen hormonellen Zusammenspiels zwischen GA, Auxin, Cytokinin und Jasmonat, in dem DELLA als zentraler Knotenpunkt bezüglich der Regulation der Xylemausdehnung sowie der Faserdifferenzierung agiert.

3 Introduction

3.1 Secondary growth and wood formation in plants

Evolution of life on earth witnessed a marking event, the looming of the plant vascular system, allowing long distance transport of water and nutrients and enabling plants to increase in size and invade more land. The plant vascular system consists of xylem and phloem (Ye, 2002). Xylem conducts water and solutes, acquired by the roots, up to the shoots, in addition to its important role as structural support. Whereas phloem, transports the products of photosynthesis, from source tissues to sink tissues (Dinneny and Yanofsky, 2004). As plant vasculature size and shape are key factors limiting plant growth, another important invention in evolution, is the increase in girth of plant organs or secondary growth, restricted to seed plants in extant taxa (Ragni and Greb, 2017). Secondary growth results in the thickening of plant organs and formation of secondary xylem (Wood), the main source of natural renewable energy (Plomion et al., 2001). Wood biosynthesis follows five major steps, starting from cell division, cell expansion, cell wall thickening (biosynthesis and deposition of cellulose, hemicellulose, lignin, and cell wall proteins), programmed cell death, and heartwood (HW) formation (Chaffey, 1999, Plomion et al., 2001).

Secondary growth is orchestrated by the vascular cambium, a meristematic tissue that lies between the xylem and phloem. In a thickening stem both radial and periclinal divisions occur within the cambium. Cells produced by periclinal divisions mature into phloem on the outside and xylem (wood) on the inside. With a higher division rate for xylem mother cells comparing to phloem mother cells, explaining the disproportion existing between phloem and xylem tissues (Murmanis, 1970, Elo *et al.*, 2009). The cambial zone has few cell layers. Consisting of elongated and highly vacuolated cells with a thin cell wall. Two cell types are present, short radial initials and elongated fusiform initials, they divide respectively into rays conducting nutrients between phloem and xylem radially, and through periclinal divisions to produce secondary vascular tissues: xylem elements towards the center or pith consisting mainly of tracheids (in gymnosperms), vessel elements, vessel associated cells, axial parenchyma and fibers (in dicotyledons). Phloem cells towards the periphery, consisting of sieve tubes, companion cells, axial parenchyma, and fibers. To maintain the vascular cambium, the two types of initials are produced continuously, fusiform initials are produced by anticlinal (radial) divisions of the mother cells, subsequently, new ray initials are issued. (Plomion et al., 2001)

The phellogen or cork cambium is another lateral meristem that contributes to secondary growth. It produces inwards the phelloderm cells and outwards the phellem cells (cork) (Esau, 1977). Thereby forming the so-called periderm surrounding the vascular cylinder and protecting the plant against biotic and abiotic stresses during secondary growth (Lulai and Freeman, 2001, Groh *et al.*, 2002, Lendzian, 2006).

3.2 The Arabidopsis hypocotyl as a model to study secondary growth

Several studies suggest that Arabidopsis is a good model to study secondary development and wood production (Chaffey *et al.*, 2002, Sibout *et al.*, 2008b, Zhang *et al.*, 2011), as it has been shown that key regulators are conserved between herbaceous and woody plants. For example, in both Arabidopsis and Populus, ectopic expression of *VASCULAR-RELATED NAC-DOMAIN 6* (*VND6*) and *VND7* promotes xylem vessel differentiation (Kubo *et al.*, 2005), while HD- ZIP Class III transcription factors control cambium establishment and xylem formation (Zhong and Ye, 1999, Carlsbecker *et al.*, 2010b, Robischon *et al.*, 2011).

In Arabidopsis, secondary growth occurs in roots, hypocotyls and stems. A key advantage on working on the hypocotyl is that radial growth is not masked by ongoing elongation as the hypocotyl stops to elongate few days after germination (Chaffey *et al.*, 2002, Sibout *et al.*, 2008b, Ragni and Hardtke, 2014). In addition, extensive amounts of secondary xylem fibers and vessel elements are produced, having structural and ultra-structural characteristics similar to those found in an angiosperm tree (Chaffey *et al.*, 2002). The cambium comprises uniseriate rays suggesting the presence of fusiform initials and ray initials similarly to trees (Mazur and Kurczynska, 2012). Based on the morphology of the vasculature tissues and their production rate, two phases of hypocotyl secondary growth can be distinguished: an early phase in which xylem and phloem are produced at roughly the same rate, followed by a later phase of xylem expansion, in which xylem is produced at higher rate and accompanied by fiber differentiation. The shift between the two phases is triggered by flowering (Figure 1) (Sibout *et al.*, 2008b), which is a general requirement for hypocotyl xylem expansion in herbaceous annual plants with rosette habitus (Ragni *et al.*, 2011).

However, analyses of flowering mutants showed that flower specification and bolting are not necessary for xylem expansion, the transition is actually mediated by the GA flow coming from the shoot triggering xylem expansion in the hypocotyl upon flowering (Ragni *et al.* 2011).

Taken together, these observations render the *Arabidopsis* hypocotyl a very attractive model to study secondary growth.

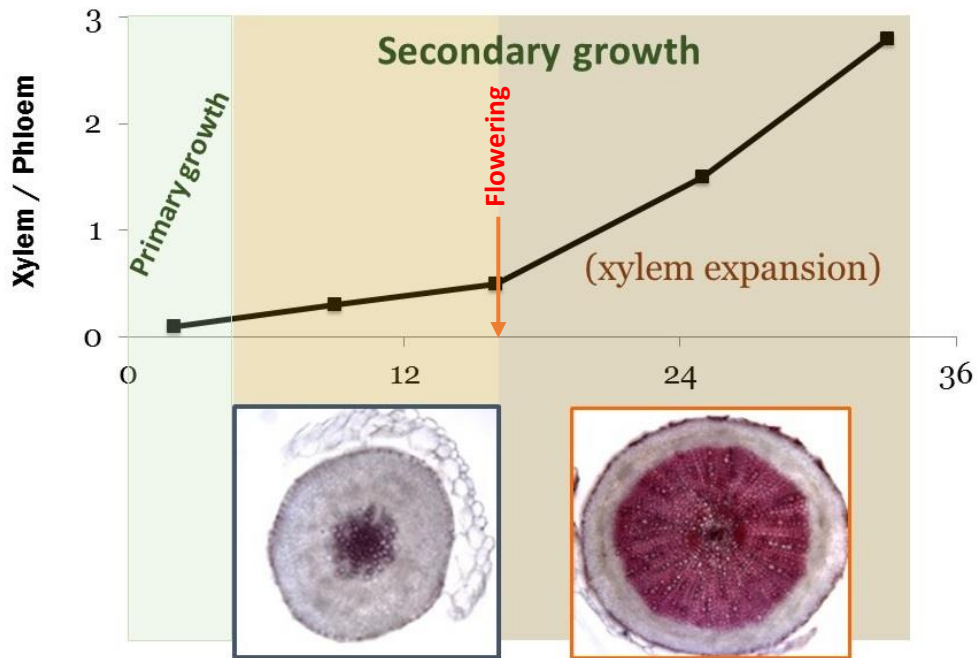


Fig. 1 Secondary growth dynamics in *Arabidopsis* hypocotyl. Adapted from (Sibout *et al.*, 2008b)

3.3 Secondary growth and cambium regulation

3.3.1 Regulation through peptides and receptors

Several Leucine-rich repeat receptor-like kinases (LRR-RLKs) especially CLV1-like LRR-RLKs have an important role regulating cambium activity, the well conserved CLE41-PXY/TDR loop is a very known example, in principle PXY/TDR receptor binds The CLV3/EMBRYO SURROUNDING REGION (CLE) related peptide CLE41 ligand and activates downstream *WUSCHEL-RELATED HOMEBOX 4* (*WOX4*) and *WOX14* genes (Hirakawa *et al.*, 2010, Morita *et al.*, 2016). CLE41 peptide and its close redundant homologue CLE44, are expressed in the phloem and move to the cambium where they are perceived by PXY/TDR receptors. *WOX4* and *WOX14* are expressed in the cambium domain, they physically interact with transcriptional regulators belonging to the HAIRY MERISTEM family, regulating stem cell proliferation (Hirakawa *et al.*, 2010, Suer *et al.*, 2011, Etchells *et al.*, 2013, Zhou *et al.*, 2014).

MORE LATERAL GROWTH 1 (MOL1) is also a CLV1-like LRR-RLKs receptor, it is expressed in a different domain comparing to the PXY/TDR, in the cambial distal part towards the phloem, repressing cambium activity via a yet unknown mechanism.

Other LRR-RLKs receptors non clustered in the CLV1 subgroup regulate cambium activity as well. For instance, *REDUCED IN LATERAL GROWTH1 (RUL1)* is known to promote cambium activity (Agusti *et al.*, 2011b), PXY-CORRELATED1 (PXC1) positively regulates secondary cell wall formation in xylem fibers (Wang *et al.*, 2013) and *ERECTA (ER)* and *ER-LIKE1 (ERL1)* repress xylem production, as in *er erl1* double mutants, xylem production and fiber formation is strongly increased in the hypocotyl (Ikematsu *et al.*, 2017).

3.3.2 Hormonal regulation

Auxin has a positive effect on cambial activity (Snow, 1935), it is also required to maintain cambial identity in pine (Savidge, 1983), Auxin transport through certain auxin efflux carriers (PINs) and ATP-binding cassette transporters (ABCs) plays also an important role in promoting cambium activity and secondary growth (Agusti *et al.*, 2011a, Kaneda *et al.*, 2011, Bennett *et al.*, 2016). The transcription factor WUSCHEL-RELATED HOMEODOMAIN 4 (WOX4) promoting cambium proliferation, has been placed downstream of the Auxin signaling pathway (Suer *et al.*, 2011). In a recent study, the *AUXIN RESPONSE FACTOR (ARF5)* which has a negative effect on cambium activity has been suggested to mainly promote the transition of cambium stem cells to xylem cells by directly activating xylem-related genes and by repressing WOX4, this doesn't exclude Other ARFs from being involved in activating WOX4 at the same time. *ARF3* and *ARF4* however, are positive regulators of cambium independently from WOX4 (Brackmann *et al.*, 2018). A direct regulator of MP has recently emerged, *BIN2-LIKE 1 (BIL1)*, which is a member of the Glycogen synthase kinase 3 (GSK3) family. BIL1 enhances the negative effect of MP on vascular development via its direct phosphorylation, this suppresses cytokinin responses by inducing the A-type Arabidopsis response regulators (ARRs) which function as negative regulators of Cytokinin signaling. BIL1 is in turn inhibited by PXY (Han *et al.*, 2018).

Despite the evidences for a role of Strigolactones SLs in regulating cambium downstream of auxin signaling (Agusti *et al.*, 2011a). Also the fact that Thermospermine (Tspm) a recently discovered signaling molecule controlling xylem differentiation (Milhinhos *et al.*, 2013) is subject to an auxin-responsive transcription factor MONOPTEROS (MP) as well as its direct target gene *ATHB8* encoding for an HD-Zip III transcription factor (Baima *et al.*, 2014). The molecular cascade from

auxin perception, all the way down to the actual cambial control in the context of secondary growth is poorly enlightened.

Cytokinins (CK), also have a positive role on secondary growth via regulating cambial activity, in fact *Arabidopsis* and poplar impaired in CK biosynthesis (mutant in isopentenyltransferase genes) showed a dramatic reduction of secondary growth (Matsumoto-Kitano *et al.*, 2008), consistently, overexpressing one of isopentenyltransferase genes in poplar increased the number of cambial cells and the total biomass (Immanen *et al.*, 2016). Furthermore, overexpressing a CK catabolic enzyme reducing CK levels resulted in down-regulation of the transcription factor *AINTEGUMENTA* and the cell cycle regulator *CYCLIN D3 (CYCD3)*, two cambium regulators promoting secondary growth and increasing cambium cell number. Whereas CK application increase their expression (Randall *et al.*, 2015).

Brassinosteroids (BR) appear also have a positive role on secondary growth and cambium activity, for instance xylem differentiation was repressed in xylogenic *Zinnia elegans* cell cultures upon application of the BR biosynthesis inhibitor (unicazol)(Yamamoto *et al.*, 1997). Consistently trans-differentiation of *Zinnia* mesophyll cells into tracheary elements was accompanied by accumulation of BR biosynthesis genes (Yamamoto *et al.*, 2007). Moreover, the xylem to phloem ratio in the stem vascular bundles show significant reduction in *Arabidopsis* BR signaling and biosynthesis mutants (Cano-Delgado *et al.*, 2004). Suggesting a conserved role of BR among species. Additionally, BR cross-talk with other pathways in controlling xylem differentiation has been proposed. In fact, The BR responsive factor *BRI1-EMS suppressor 1 (BES1)* was recently found to be a target of the PXY/TDR signaling network, through *GLYCOGEN SYNTHASE KINASE 3(GSK3)-like kinases* and the *BRASSINOSTEROID-INSENSITIVE 2 (BIN2)*(Kondo *et al.*, 2014).

Jasmonate also promote cambium proliferation and secondary growth, as the positive mediators of JA signalling *Coronatine-insensitive 1 COI1* and Transcription factor *MYC2 (MYC2)* promote secondary growth in *Arabidopsis* stem whereas *JASMONATE ZIM-DOMAIN (JAZ7)* and *JAZ10* repress it (Sehr *et al.*, 2010). Additionally, jasmonate biosynthesis/signaling genes are up-regulated in the perennial and woody *soc1 ful* double mutant (Melzer *et al.*, 2008, Davin *et al.*, 2016). Most recently, it has been shown that in response to blue light, *MYC2* and *MYC4* directly bind to the *NST1* promoter, thus fine-tuning its transcriptional programming for secondary cell wall thickening formation in *Arabidopsis* fiber cells (Zhang *et al.*, 2018).

Last but not least, Gibberellins (GA) have been shown to promote secondary growth both in trees and Arabidopsis, mutants overproducing GA and GA treated plants showed enhanced fiber elongation and overall secondary growth in trees (Digby and Wareing, 1966, Eriksson *et al.*, 2000b). Whereas in Arabidopsis GA is able to promote wood formation through enhancing polar transport of auxin and fiber elongation in the developing xylem (Björklund *et al.*, 2007, Mauriat and Moritz, 2009).

GA is involved in promoting xylem expansion and fiber differentiation through the degradation of DELLA proteins upon flowering in Arabidopsis hypocotyl, in fact in *della* quadruple mutant, xylem expansion is significantly increased comparing to the wild type at flowering, consistently ectopic expression of dominant DELLA dramatically suppressed xylem expansion (Ragni *et al.*, 2011).

The competency to respond to GA depend on the homeobox transcription factor BREVIPEDICELLUS/KNAT1 (BP) (Ikematsu *et al.*, 2017). BP positively regulates cambium maintenance and fiber formation in the root and hypocotyl (Liebsch *et al.*, 2014, Woerlen *et al.*, 2017). The fiber phenotype in the hypocotyls of bp mutant can be attributed to the decreased expression levels of *NAC SECONDARY WALL THICKENING PROMOTING FACTOR1 (NST1)* and *NST3*, key regulators of the formation of secondary walls in woody tissues of Arabidopsis thaliana (Mitsuda *et al.*, 2007). Furthermore GA signaling induces expression of *NST1* and *NST3* to trigger fiber differentiation in the hypocotyl (Ikematsu *et al.*, 2017).

3.4 DELLA mode of action:

The DELLA proteins act downstream of the receptor GIBBERELLIN-INSENSITIVE DWARF1 (GID1) upon GA perception to modulate various aspects of growth and development in plants (Thomas and Sun, 2004, Griffiths *et al.*, 2006, Nakajima *et al.*, 2006). There are five members of the DELLA gene family in Arabidopsis: *REPRESSOR OF gal-3 (RGA)*, *GA-INSENSITIVE (GAI)*, *RGA-LIKE1 (RGL1)*, *RGL2*, and *RGL3*. Characterization of mutant combinations of null alleles in each *DELLA* gene demonstrates the overlapping and distinct functions of these genes in plant development (Dill and Sun, 2001, Cao *et al.*, 2005). DELLA can interact with many TFs belonging to diverse families and regulate various transcriptional networks, suggesting their role as central signaling hubs connecting different signaling cascades (Claeys *et al.*, 2014, Marin-de la Rosa *et*

al., 2014). Based on experimental evidences reviewed through various molecular genetic studies, DELLAs regulate gene expression through various mechanisms: DELLA can Sequester DNA-binding transcription factors that induce or repress target genes bHLH transcription factors of the PIF family, BES1 and BRASSINAZOLE-RESISTANT 1 (BZR1) transcription factors, ETHYLENE-INSENSITIVE3 (EIN3), SQUAMOSA PROMOTER BINDING PROTEIN-LIKE 9 (SPL9) and other SPLs, ALCATRAZ (ALC)). DELLA can interact with negative transcriptional regulators, therefore releasing certain transcriptional regulators from being repressed, (DELLA interaction with JAZ releasing MYC2 transcriptional activity). DELLA can be present in transcriptional complexes; this is suggested by chromatin immunoprecipitation studies. BOIRING finger proteins might act through this mechanism. Additionally, the ability of DELLA to interact with DNA-binding transcription factors might be modulated through its interactors (SCARECROW-LIKE 3 (SCL3) and INDETERMINATE DOMAIN 1 (IDD1) might affect DELLA ability to bind PHYTOCHROME INTERACTING FACTORS PIFs and others) (Locascio *et al.*, 2013). Recent studies revealed the existence of other regulatory mechanisms underlying DELLA-regulated plant growth and development processes (Fukazawa *et al.*, 2014, Yoshida *et al.*, 2014). For example, DELLAs function as a transcriptional coactivator through interaction with other transcription factor(s): type-B ARRs and DELLAs jointly promote transcription of the target genes (Marin-de la Rosa *et al.*, 2015). The most recently discovered layer of DELLA action mode, suggests that DELLAs may also act as co-repressors to suppress gene transcription by interacting with a negative transcription factor, DELLAs binding to FLOWERING LOCUS C (FLC) enhances transcriptional repression of FLC on *FLOWERING LOCUS T (FT)* and *SUPPRESSOR OF OVEREXPRESSION OF CO 1 (SOC1)* genes (Li *et al.*, 2016).

3.4 DELLA cross-talk with Auxin, Cytokinin and Jasmonate:

The GA signaling pathway can be modulated by other hormones such as auxins, cytokinins or ethylene (Jasinski *et al.*, 2005, Frigerio *et al.*, 2006), placing it as central regulator in plant growth and development (Claeys *et al.*, 2014).

This cross-talk can be mediated through DELLA. In fact a recent study by (Oh *et al.*, 2014) show that RGA and GAI inhibit AUXIN RESPONSE FACTOR (ARF6), ARF7 and ARF8 from binding to target genes *in vivo*. In fact DELLA physically interact with ARF's in the context of hypocotyl cell elongation, particularly RGA and GAI interact with ARFs activators (ARF6, ARF7 and ARF8), but not the repressor ARF1 (Oh *et al.*, 2014). ARF6 and ARF8 are also known to negatively

regulate hypocotyl elongation (Tian et al., 2004). In addition, ARF6 and ARF8, are positive regulators of adventitious rooting (emerging from the hypocotyl) (Wu *et al.*, 2006, Gutierrez *et al.*, 2009, Gutierrez *et al.*, 2012).

Additionally, DELLA proteins interact with type-B Arabidopsis response regulators: (ARR1, ARR2 and ARR14). Particularly GAI and RGA enhance the transactivation ability of ARR1 in vivo and ARR1 mediates the presence of RGA at target downstream promoters. ARR1 and DELLA act as transcriptional co-regulators in Arabidopsis (Marin-de la Rosa et al., 2015).

DELLA competitive binding to JAZ1 prevents MYC2-JAZ1 interaction, thus enabling MYC2 to regulate its target set of genes (Hou et al., 2010). But most importantly MYC2 is able to directly interact with DELLA Proteins in the context of Sesquiterpene Synthase Gene Expression Regulation (Hong et al., 2012).

4 Aim of the thesis

The occurrence of secondary growth or the increase in girth of plant organs, is a crucial point that marked the evolution of plants on earth. It is restricted to seed plants in extant taxa (Ragni and Greb, 2017). It largely relies on the interdependent processes of cell proliferation, expansion and differentiation originated in the meristem (Scheres, 2007). Meristems provide a protected microenvironment necessary to keep stem cell population sheltered from differentiation signals, while being central control regions for growth and development, receiving, integrating, responding to and broadcasting growth regulating signals (Grieneisen *et al.*, 2007, Petersson *et al.*, 2009, Hohm *et al.*, 2010, Uyttewaal *et al.*, 2010, Zhao *et al.*, 2010).

Secondary growth results in the thickening of plant organs and formation of secondary xylem or Wood: principal sink for carbon and fundamental source of natural renewable energy (Plomion et al., 2001). Despite the crucial importance of such a developmental process in the plant, it is surprising that very little is known about the molecular mechanisms underlying secondary growth. The use of Arabidopsis hypocotyl as model to study secondary growth facilitated many aspects and created new possibilities toward its understanding. Morphology studies of the vascular tissues and its dynamics revealed two phases of secondary growth in Arabidopsis. A first phase where xylem and phloem are produced with the same rate, and a second phase where xylem is produced in a higher rate comparing to the phloem, the second phase is called xylem expansion phase. Although

the shift between the two phases is marked by flowering. The shift to the xylem expansion phase is mediated by GA signaling which leads to DELLA degradation. The DELLA gene family in *Arabidopsis* comprise five members: *RGA*, *GAI*, *RGL1*, *RGL2*, and *RGL3*.

The aim of this thesis was first to study the spatio-temporal activity of *DELLA* genes individually. We also aimed to determine their distinct functions during different phases of hypocotyl secondary growth.

We focused on understanding the molecular mechanisms through which *DELLA* act to mediate the shift to the xylem expansion phase. As *DELLAs* are known to act via transcriptional complexes, we opted to identify the transcriptional regulators involved with *DELLA* on regulating secondary growth, the nature of their interaction with *DELLA*.

We next determined single and combined effects of the identified *DELLA* downstream interactors on secondary growth.

We then addressed the question, whether the identified *DELLA* downstream factors interact amongst each other to regulate secondary growth.

We also analyzed the transcriptome profile caused by inactivation of *DELLA* downstream interactors in order to identify their downstream target genes.

Ultimately, we aimed to shed more light on the networks controlling xylem expansion and fiber differentiation in the context of *DELLA* mediated hormonal cross-talk, and to further explain secondary growth phenotypes before and after flowering, paving the road for future researches using our model as a fulcrum.

5 Draft manuscripts

5.1 Draft manuscript 1:

AUXIN RESPONSIVE FACTOR 6 (ARF6) and ARF8 promotes Gibberellins mediated hypocotyl xylem expansion by repressing phloem proliferation.

Contribution:

All experiments were performed by MBT except:

SM made the RGA and GAI, GFP and GUS transgenic lines

MB generated the library for sequencing and LR analyzed the sequencing data

LR took the confocal pictures

DR helped in the embedding / learning of the samples and generating multiple mutants

The interpretation of the results as well as the writing of the manuscript were done

By MBT and LR.

Author	Author position	Scientific ideas %	Data generation %	Analysis & interpretation %	Paper writing %
Mehdi Ben Targem (MBT)	1	50	70	45	50
Dagmar Ripper (DR)	2		10		
Stefan Mann (SM)	3		5		
Martin Bayer (MB)	4		5	10	
Laura Ragni (LR)	5	50	10	45	50
Title of paper: <i>AUXIN RESPONSIVE FACTOR 6 (ARF6) and ARF8 promotes Gibberellins mediated</i> <u>d</u> <i>hypocotyl xylem expansion by repressing phloem proliferation</i>					
Status in publication process: Draft					

AUXIN RESPONSIVE FACTOR 6 (ARF6) and ARF8 promotes Gibberellins mediated hypocotyl xylem expansion by repressing phloem proliferation.

Authors: Mehdi Ben-Targem¹, Dagmar Ripper¹, Stefan Mahn¹, Martin Bayer² and Laura Ragni^{1*}

Affiliations:

¹ZMBP- Center for Plant Molecular Biology, University of Tübingen, Auf der Morgenstelle 32, D-72076 Tübingen, Germany

²Max Planck Institute for Developmental Biology, Max-Planck-Ring 5, 72076 Tübingen

* Corresponding author: laura.ragni@zmbp.uni-tuebingen.de +49 (0)7071 - 29 76677

Summary

Secondary growth is a crucial developmental process that occurs in seed plants. It results in the thickening of plant organs and formation of secondary xylem or wood: which represent the principal sink for carbon assimilation and a fundamental source of natural renewable energy. Two phases mark secondary growth in *Arabidopsis thaliana* hypocotyls: a first phase in which xylem and phloem are produced at the same rate and a second phase referred to as xylem expansion in which xylem production is accelerated and xylem fibers are formed. Upon flowering Gibberellins (GA) triggers the xylem expansion phase, locally inducing DELLA degradation. Despite its crucial importance, it is surprising that little is known about the molecular mechanisms underlying GA mediated secondary growth.

In this study, we found that REPRESSOR OF *ga1-3* (RGA) and GA INSENSITIVE (GAI) are the main DELLAs regulating xylem expansion, with a greater contribution for RGA. This role seems to be conserved across ecotypes, which greatly differ in xylem expansion and secondary growth such as Col and Ler. We also identified a novel role for AUXIN RESPONSIVE FACTOR (ARF6) and ARF8 as positive regulators of xylem expansion. RGA and GAI expression pattern overlaps in the phloem with its known interactors ARF6 and ARF8 during secondary growth, and *arf6 arf8* mutants are characterized by enhanced phloem production. Our genetic analyses suggest that ARFs are downstream DELLA in regulating xylem expansion. Moreover, ARF6 and ARF8 promote cambium formation together with *BREVIPEDICELLUS/KNAT1/ (BP/KNAT1)*. Overall, our results shed light on a pivotal hormone cross-talk between GA and Auxin in the context of plant secondary growth.

Keywords: Phloem Xylem Cambium secondary growth, auxin Gibberellin

Introduction:

Secondary growth, the increase in girth of plant organ largely contributed to the success of land plants and continuously produces xylem tissue (wood), which in perennial dicotyledons represents the principal form of biomass accumulation (Demura and Ye, 2010, Spicer and Groover, 2010). The vasculature not only contribute to the transport of assimilate, ions, water and signaling molecules but it confers mechanical strength. Secondary growth is mainly driven by the vascular cambium, a post-embryonic meristem, which divides in a strictly bifacial manner, producing xylem inward and phloem outward (Ragni and Greb, 2018).

Several studies suggest that *Arabidopsis* is a good model to study secondary development and wood production (Chaffey *et al.*, 2002, Ragni and Hardtke, 2014), as it has been shown that key regulators are conserved between herbaceous and woody plants. For instance, in both *Arabidopsis* and poplar, ectopic expression of VASCULAR-RELATED NAC-DOMAIN 6 (VND6) and VND7 promotes xylem vessel differentiation (Kubo *et al.*, 2005), while HD- ZIP Class III transcription factors control cambium establishment and xylem formation in both species (Carlsbecker *et al.*, 2010a, Du *et al.*, 2011, Robischon *et al.*, 2011). In *Arabidopsis*, secondary growth occurs in roots, hypocotyls and stems. Moreover, studying the *Arabidopsis* hypocotyl offers a key advantage as radial growth is not masked by ongoing elongation (Chaffey *et al.*, 2002, Ragni and Hardtke, 2014). In addition, extensive amounts of secondary xylem fibers and vessel elements are produced in the hypocotyl, with structural and ultra-structural characteristics similar to those found in an angiosperm tree (Chaffey *et al.*, 2002).

Based on the morphology of the vascular tissues and their production rate, two phases of hypocotyl secondary growth can be distinguished in *Arabidopsis*: an early phase in which xylem and phloem are produced at roughly the same rate, followed by a later phase of so call “xylem expansion”, in which xylem is produced at higher rate and fibers differentiate. The shift between the two phases is triggered by flowering (Sibout *et al.*, 2008a), which is a general condition for hypocotyl xylem expansion in herbaceous annual plants with rosette habitus (Ragni *et al.*, 2011). However, neither bolting nor flower specification are necessary for this developmental transition (Ragni *et al.*, 2011). Grafting experiments suggested the presence of a mobile signal which at flowering is translocated from the shoot to the hypocotyl to induce xylem expansion (Sibout *et al.*, 2008a). Our recent findings revealed that Gibberellins (GAs) might act as the mobile cue, and that

GA signaling promote locally xylem occupancy and fiber production. In fact, xylem expansion is enhanced in *della* quadruple mutant (in which GA signaling is constitutively on), whereas the induction of a dominant version of DELLA (which cannot be degraded by GA) abolished xylem expansion (Ragni *et al.*, 2011).

DELLA proteins are conserved components of the GA signaling pathway acting immediately downstream of the GA receptor, regulating a plethora of developmental processes, (Locascio *et al.*, 2013, Colebrook *et al.*, 2014, Davière and Achard, 2016). In Arabidopsis, the *DELLA* gene family comprises five members: *REPRESSOR OF gal-3 (RGA)*, *GA-INSENSITIVE (GAI)*, *RGA-LIKE1 (RGL1)*, *RGL2*, and *RGL3*. They control gene expression through at least three mechanisms: 1) sequestering transcription factors 2) and negative regulators/repressors thereby repressing and activating the repression of certain genes 3) participating in transcriptional complexes (Locascio *et al.*, 2013). Consistently they have been shown to interact with several transcription factor families (Marin-de la Rosa *et al.*, 2014). For instance, RGA interacts with ARFs activators (ARF6, ARF7 and ARF8), but not the repressor ARF1 to regulate hypocotyl elongation (Oh *et al.*, 2014).

However, DELLA interacting proteins and their mode of action during secondary growth are largely unknown. In this work we investigated the GA signaling downstream factors, which regulate hypocotyl xylem expansion. We reveal that ARF6 and ARF8 two bona fide RGA interaction proteins promote xylem expansion, repressing phloem proliferation. In addition, we show that *ARF6* and *ARF8* might regulate cambium activity as their inactivation enhanced the cambial defect of *brevipedicellus/knat1* mutant.

Results:

GA signaling controls hypocotyl secondary growth, mostly through RGA and GAI, in Ler and Col-0 ecotypes.

We previously showed that *della* quadruple mutants are characterized by an increased xylem expansion and fiber production (Ragni *et al.*, 2011), however, the specific effect of each DELLA during secondary growth, is yet to be determined. To address this question, we first analyzed *della* single knock-out mutants. Only *rga* mutants showed a mild increase of xylem occupancy (Figure S1a,b). As *RGA* has been shown to work together with *GAI* in several developmental processes such as stem elongation (Dill and Sun, 2001, Cheng *et al.*, 2004), we then

investigated the *rga-24- gai-t6* double mutants. *rga-24 gai-t6* mutants showed a strong increase in xylem occupancy and fiber formation (Figure S1c, d), whereas knocking out all *DELLAs* (*dellako*) it only slightly enhanced the *rga gai* phenotype, suggesting that *RGA* and *GAI* are the major regulators of xylem expansion (Figure S1c, d).

It has been recently shown that *rga gai* double mutant in Col background (*rga-28 gai-td1*) is entirely male sterile, whereas the equivalent double mutant in Ler background is fertile and this is not due to the inactivation of *ERECTA* (Plackett *et al.*, 2014). As Ler and Col differs in secondary growth morphodynamics with Col displaying more overall secondary growth and Ler more xylem expansion, we wonder whether, *della* mutants have the same vascular phenotype in both ecotypes (Ragni *et al.*, 2011, Sankar *et al.*, 2014). The *rga-24 gai-t6* mutants, showed enhanced xylem to phloem ratio (xylem occupancy) and fiber production when compared to its WT counterpart Ler (Figure 1a, b). Likewise the *rga-28 gai-td1* double mutant plants show the same increase in xylem occupancy and fiber production when compared to Col. However, the absolute values reflect the differences between the two backgrounds (Ler 35% vs. Col 15%) with *rga-24 gai-t6* having 50% xylem occupancy compared to 30% for *rga-28 gai-td1* (Figure 1a, b). Interestingly, the triple mutant *rga-28 gai-td1 er-105* was undistinguishable from the *rga-28 gai-td1* double mutant in term of xylem expansion (Figure 1a, b). This is consistent with previous results, which showed that the loss of function of *ERECTA* in Col background does not explain the differences in secondary growth between the two ecotypes (Ikematsu *et al.*, 2017) (Figure 1a, b)

To corroborate our results we compared *GAI:gaiD-GR* and *RGA:rgaD-GR* dominant lines, in the two ecotypes. To this extent, the original *GAI:gaiD-GR* and *RGA:rgaD-GR* Ler lines have been backcrossed 6 times to Col background. Induction, upon flowering, of a DELLA version that cannot be degraded in presence of GA resulted in reduced xylem occupancy (40% less) and abolishes fiber formation in both accessions (Figure 1c, d and S2). Interestingly, we also observed ectopic cell divisions at the phloem poles of the Col induced plants. This phenotype was not observed in the Ler lines, probably due to the reduced phloem proliferation that is characteristic of the Ler ecotype (Sankar *et al.*, 2014) (Figure 1c and S2).

To conclude, our data suggest that *RGA* and *GAI* are the major DELLA regulating xylem expansion and display similar phenotype in both Ler and Col background, thus to unravel the

downstream factors of GA signaling in the context of secondary growth only the *rga-28 gai-td1* will be used for subsequent experiments.

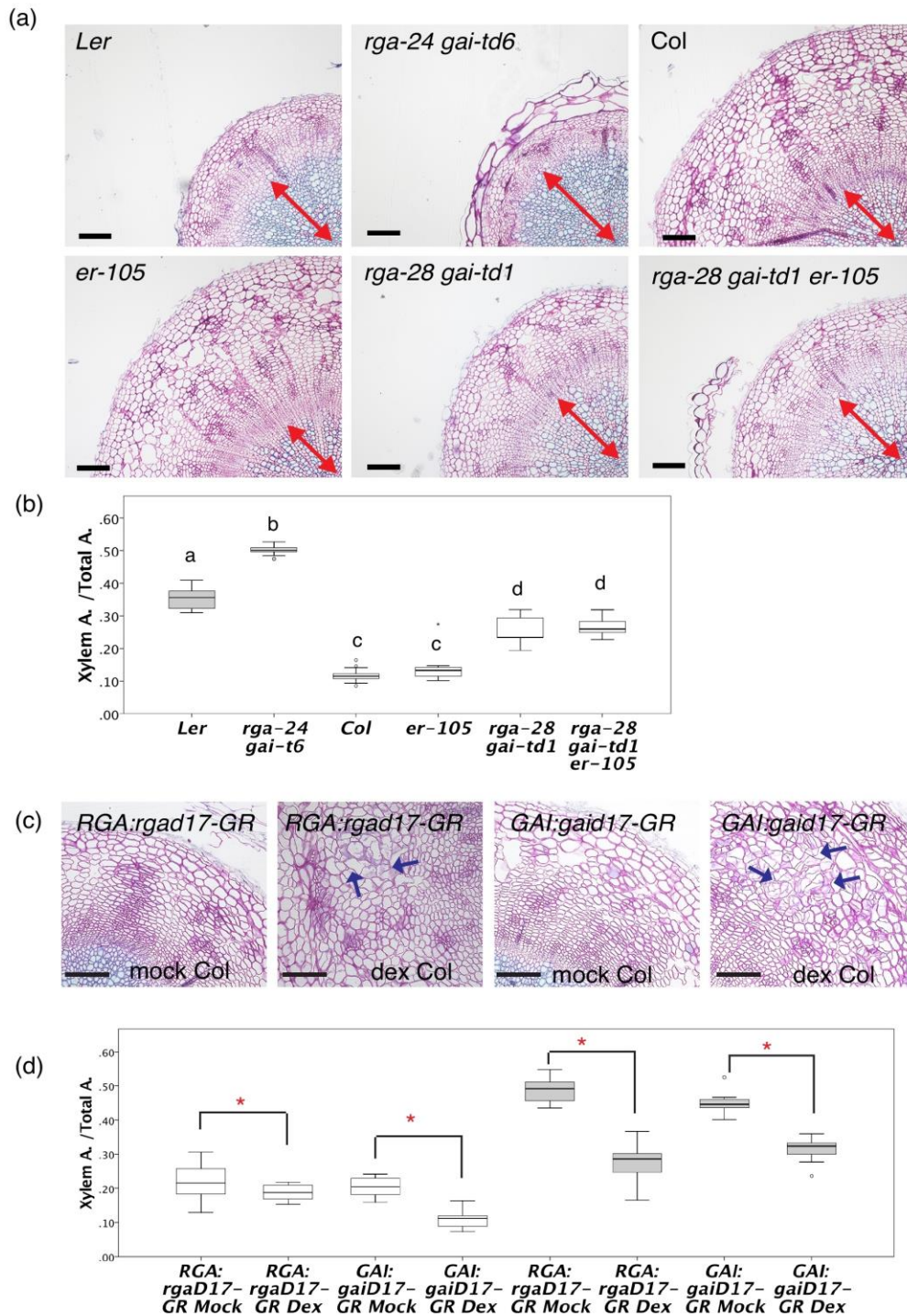


Fig. 1 GA signalling controls hypocotyl secondary growth, mostly through *RGA* and *GAI*, in Ler and Col ecotypes.

(a) Plastic cross-sections stained with toluidine blue of 10 day-after-flowering (daf) hypocotyls showing xylem expansion in *rga-24-gai-t6* (in Ler background), in *rga-28 gai-td1* (Col background) in *er-105* and *rga-28 gai-td1 er-105* (Col background). (b) Quantification of Xylem Area/Total area in the experiment illustrated by representative pictures in (a). (c) Plastic cross-sections stained with toluidine blue of 15daf hypocotyls of *rga:rga^D-GR* and *gai:gai^D-GR* in Col-0 showing ectopic cell divisions in the phloem (Blue arrow) in dex treated transgenic plants. Black bars = 100µm, double head red arrow: Xylem. (d) Quantification of Xylem Area/Total area ratio in hypocotyls of 15 daf Mock and dex treated plants carrying the constructs: *rga:rga^D-GR* and *gai:gai^D-GR* both in Col-0 and Ler backgrounds. (b, d) Box plots: the dark line in the middle of the boxes is the median, the T-bars that extend from the boxes (whiskers) include 95% of the data. Letters in the boxplots indicate statistical groups, one-way ANOVA with post hoc Bonferroni was used to determine the groups for (b) $n > 10$) and Student's or Welch t-test for (d) (red asterisk: $P < 0.05$, $n=11-16$). Grey boxes: (Col-0 background); white boxes (Col background). Black bar = 100µm, double head red arrow: xylem and blue arrow: ectopic divisions in the phloem.

ARF6, ARF7 and ARF8 expression pattern overlaps with RGA and GAI during hypocotyl secondary growth.

As Auxin is well known to control vascular patterning and xylem differentiation during thorough development (Ragni and Greb, 2018) and RGA modulates the activity of ARF6, ARF7 and ARF8 during hypocotyl elongation (Oh *et al.*, 2014), we wonder whether ARF6 and ARF8 regulate also secondary growth. To investigate whether DELLA proteins regulate xylem expansion through the interaction with ARFs, we checked if their expression patterns overlap during secondary growth. For this purpose we generated promoter reporters of RGA and GAI, as our genetic analyses point out they are the main DELLA controlling xylem expansion. *RGA* and *GAI* are broadly expressed during primary and early secondary growth in the hypocotyl (ref) (Figure S3a). During secondary growth, *RGA* and *GAI* expression get progressively restricted to the phloem and just before flowering time *RGA* and *GAI* were mainly expressed at the phloem poles. At 10 day-after-flowering during xylem expansion *RGA* and *GAI* were still expressed albeit at lower levels (Figure 2a, b). *ARF6*, *ARF7* and *ARF8* expression were also detected in the phloem elements before flowering, however *ARF6* and *ARF7* expression was broader and encompassed the cambium and the cambium and differentiating xylem respectively (Figure 2c, d, e). To summarize, *RGA* and *GAI* expression overlaps in the phloem with *ARF6*, *ARF7* and *ARF8*, suggesting that they may interact also during secondary growth.

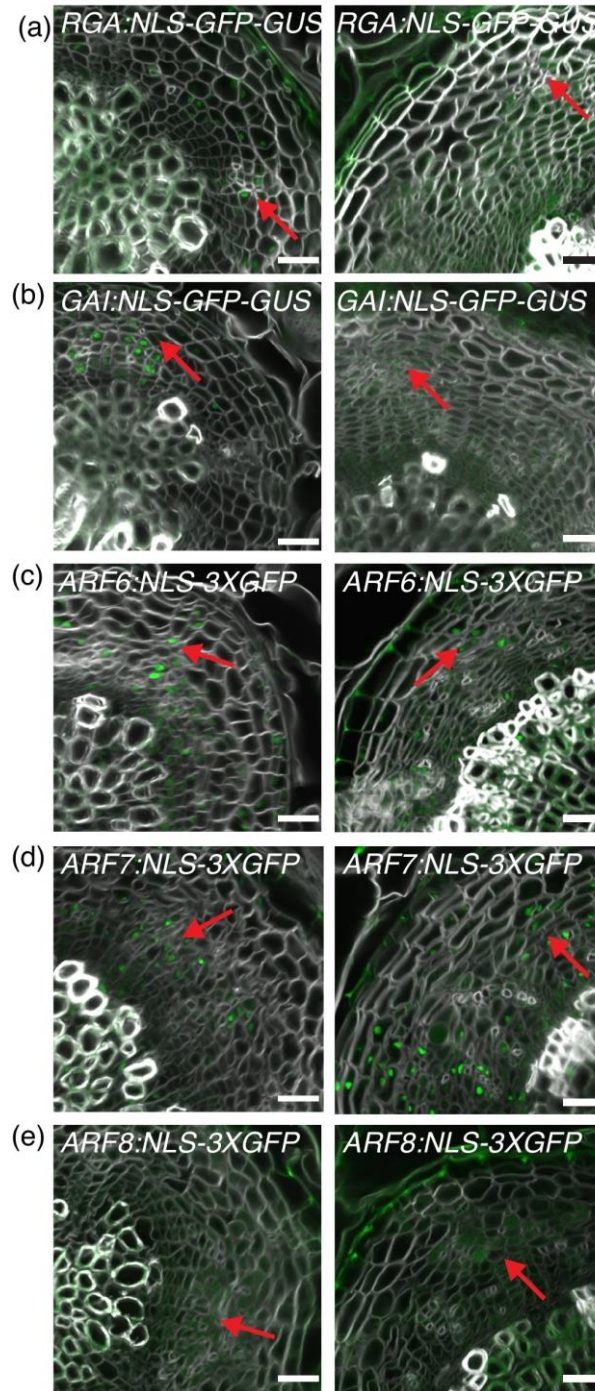


Fig. 2 *ARF6* and *ARF8* expression pattern overlaps with *RGA* and *GAI* during hypocotyl secondary growth.

(a) *RGA:NLS-GFP-GUS* and *RGA:GUS*. (b) *GAI:NLS-GFP-GUS* and *GAI:GUS* (c) *ARF6:NLS-3xGFP* and *ARF6:GUS* (d) *ARF7:NLS-3xGFP* and *ARF7:GUS*. (a-d) Hypocotyl vibratome cross-sections at 0, 8 and 20 day-after-flowering. Left and middle panels: Confocal images of section cleared with ClearSee and stained with Calcofluor-White showing GFP signal in the nuclei (red

arrows). Right panels: GUS vibratome sections stained with Phloroglucinol. White bar = 20 μm and black bar = 100 μm .

ARF6, ARF8 and to a lesser extent ARF7 promotes xylem expansion, repressing phloem proliferation.

To further investigate the ARF-DELLA interaction during secondary growth, we investigated whether *arf* mutants displayed altered xylem expansion. *arf7/nph4* mutants are characterized by reduced overall secondary growth but did not show any xylem expansion phenotype (Ragni *et al.*, 2011). *arf6* (*arf6-1* and *arf6-2*) and *arf8* (*arf8-2* and *arf8-3*) single mutants show a slight but significant inhibition of xylem expansion and less fibers compared to the Col-0 background (Fig 3 a, b and S3c), whereas the *arf6 arf8* double mutant displayed a dramatic decrease in xylem occupancy, absence of fiber accumulation until very late stages of plant growth (40 days after flowering in our growth conditions) (Figure 3a,-d). Interestingly in the double mutants, we observed an increase in number of phloem poles and ectopic cell divisions at phloem poles (Figure 3e and S4d-e) reminiscent on what happen when GA signaling is blocked in Col background (Figure 1c). We confirmed that this vascular phenotype is due to the inactivation of *ARF6* and *ARF8* taking advantage of the fact that the expression of *ARF6* and *ARF8* is tightly regulated by miR167a (Wu *et al.*, 2006, Gutierrez *et al.*, 2009). In fact, we could observe ectopic cell divisions in the phloem of F1 plants, in which we ectopically express miR167a (*UAS::miR167a x RPS5a::GALA*) (Figure S3e).

We next wonder about the temporal aspects of the *arf6 arf8* phenotype, if RGA sequesters ARFs during secondary growth, we expected that *arf6 arf8* mutants display a secondary growth phenotype only after flowering (when DELLA proteins are degraded to trigger xylem expansion). Consistently with our idea, at flowering time (*arf6 arf8* double mutants flowers on the same days in long day conditions) *arf6 arf8* hypocotyls were undistinguishable from WT plants (Figure S4a, b). After flowering, in *arf6 arf8* we did not observe the characteristic increase of xylem occupancy of WT plants that is visible from 10 daf, in contrast we observed that total hypocotyl area was bigger in *arf6 arf8* double mutants, mainly due to an increase in phloem proliferation. Another striking phenotype of the *arf6 arf8* hypocotyl is the presence of phloem fibers at plant senescence, which are normally absent in Col (Figure S3d).

As also *ARF7* is expressed at the phloem poles and it interacts with RGA, we investigated if *ARF7* can promote xylem expansion in the absence of *ARF6* and *ARF8*. The inactivation of *ARF7* in *arf6 arf8* background resulted in further reduction of xylem occupancy (Figure S4f)

whereas the ectopic cell divisions phenotype at the phloem was not enhanced (Figure 3f and S4g), suggesting only a minor role for ARF7 during xylem expansion.

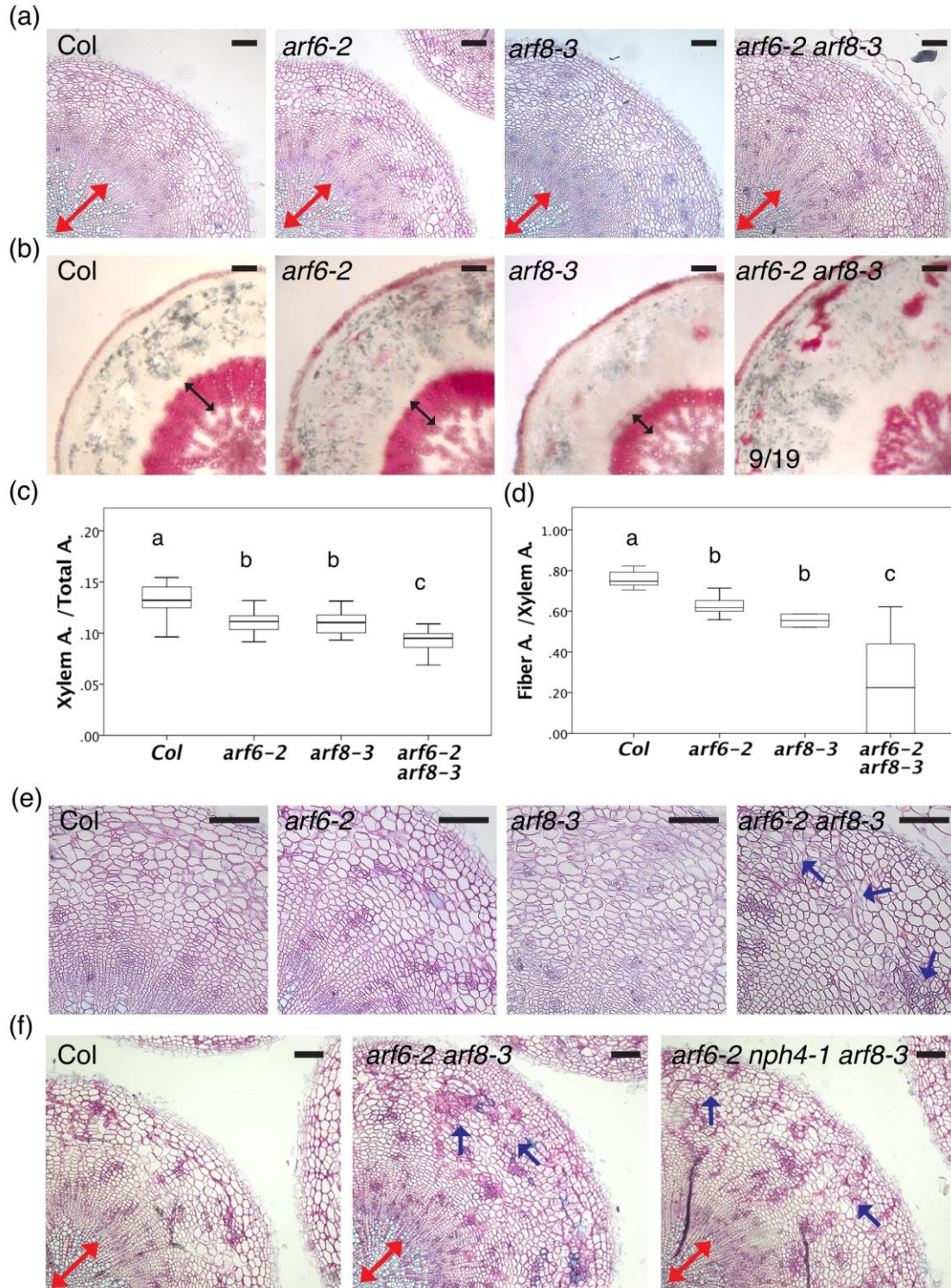


Fig. 3 ARF6, ARF8 and to a lesser extent ARF7 promotes xylem expansion, repressing phloem proliferation.

(a) Plastic hypocotyl cross-sections stained with 0.1 % toluidine blue of 10 day-after-flowering (daf), showing reduced xylem expansion in *arf6*, *arf8* and *arf6 arf8* double mutant. (b) Phloroglucinol stained vibratome sections of 40 daf hypocotyl, showing reduced fibers formation in *arf6*, *arf8* and *arf6 arf8* double mutant. (c) Quantification of the Xylem Area /Total area ratio in the experiment illustrated by representative pictures in (a). (d) Quantification of Fiber Area/Xylem Area ratio in the experiment illustrated by representative pictures in (b). (c-d) Box plots: the dark line in the middle of the boxes is the median, the T-bars that extend from the boxes (whiskers) include 95% of the data. Letters in the boxplots indicate statistical groups (one-way ANOVA post hoc Bonferroni for (c) n= 9-17, and post hoc Tamhane for (d) n=2-18). (e) Magnifications of (a) in the phloem regions. In *arf6 arf8* double mutants ectopic cell division in the phloem (blue arrow) are visible. (f) Plastic hypocotyl cross-sections stained with toluidine blue of 10 day-after-flowering, showing reduced xylem expansion and ectopic cell division in the phloem in *arf6*, *arf8* double and *arf6 nph4/arf7arf8* triple mutants. Black bars= 100µm, double head red arrow: xylem, double head black arrow: xylem fibers. Blue arrow: ectopic divisions in the phloem.

ARF6, ARF7 and ARF8 act mainly downstream GA signaling to control xylem expansion.

To better understand the role of ARF6, ARF8, downstream GA, we analyzed the GA response of *arf6 arf8* double and *arf6 nph4 ar8* triple mutants. Thus, WT and mutants plants were treated with GA at flowering time and examined at 20 daf. GA treatment, as previously shown, enhanced fibers production and xylem occupancy in WT (Ragni *et al.*, 2011) (Figure 4). Notably, *arf6 arf8* was still partially able to respond to GA as indicated by the production of fibers and higher xylem to total area ratio, however to a lesser extent than WT plants (Figure 4). The triple mutant *nph4-1 arf6-2 arf8-3* was even less responsive to GA treatment, as fiber accumulation was abolished in the majority of the plants (Figure 4a,c).

To further enforce our results we analyzed the genetic interaction between *rga gai* and *arf6 arf8* mutants. As both *rga gai* and *arf6 arf8* double mutants are sterile (Nagpal *et al.*, 2005, Plackett *et al.*, 2014) and we suspected that the quadruple mutant is gametophytic lethal, we characterized *arf6 arf8 rga* and *arf6 arf8 rga gai./+* plants. Consistently with the previous experiment, the inactivation of RGA in *arf6 arf8* slightly increased xylem occupancy but did not rescue the fiber phenotype (Figure S5). The *arf6 arf8 rga gai./+* showed a similar phenotype to *rga arf6 arf8* triple mutants (Figure S5). Over all these results confirm that ARF6 and ARF8 are downstream of DELLA in regulating xylem expansion. The partial restoration of the *arf6 arf8* phenotype caused by DELLA inactivation and or GA treatment could be explained by the fact that ARF7 is still active in *arf6 arf8* mutant and that the ARFs might not be the only DELLA interacting protein controlling xylem expansion.

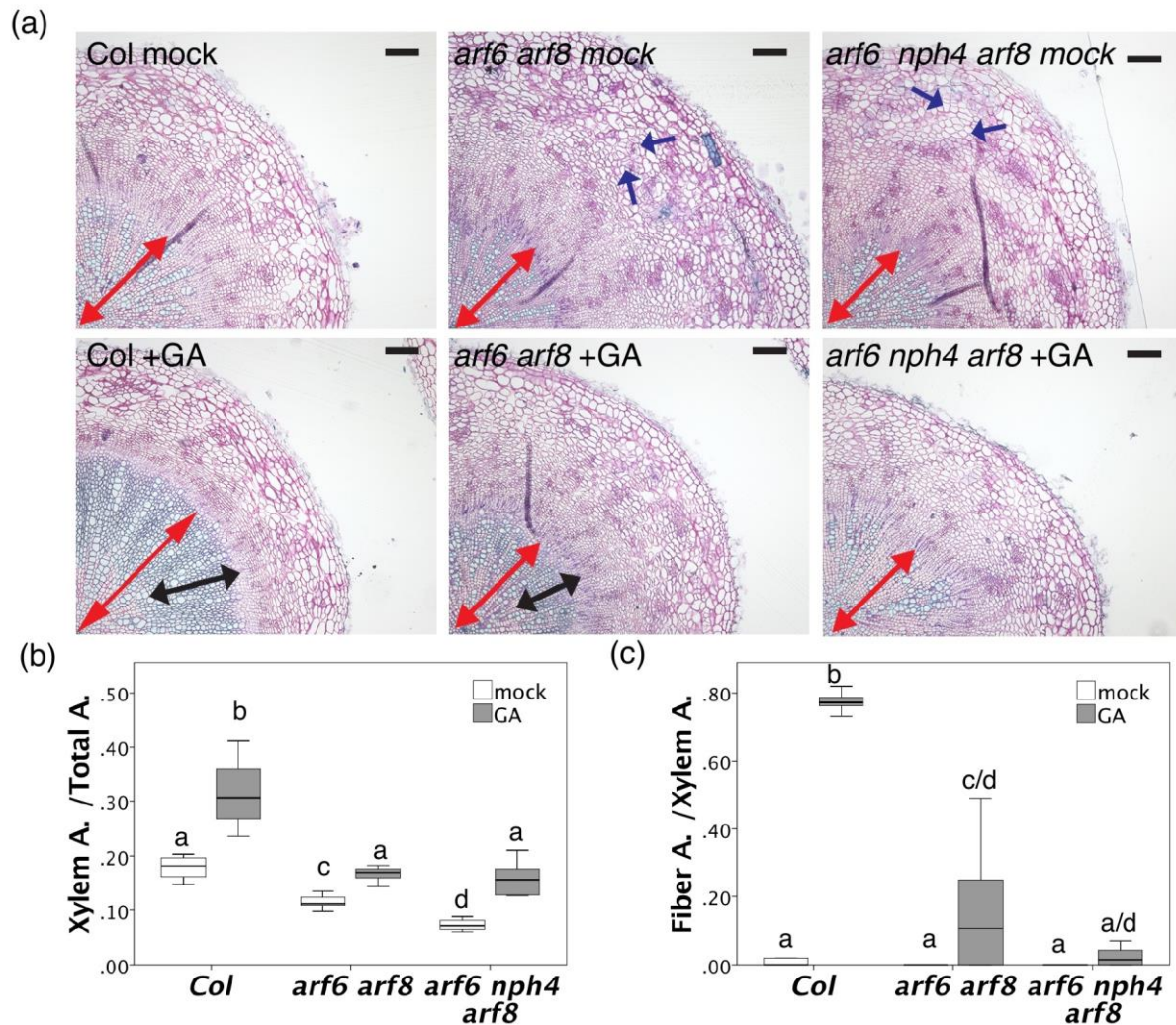


Fig. 4 ARF6, ARF7 and ARF8 act mainly downstream GA signalling to control xylem expansion.

(a) Plastic hypocotyl cross-sections stained with toluidine blue of 10 day-after-flowering, showing xylem expansion in Col-0, *arf6 arf8* and *arf6 nph4/arf7 arf8* plants treated with Mock or 10 μ M GA solution. (b) Quantification of xylem/Total area ratio in the experiment illustrated by representative examples in (a). (b) Quantification of the Xylem Area /Total area ratio in the experiment illustrated by representative pictures in (a). Quantification of Fiber Area/Xylem Area ratio in the experiment illustrated by representative pictures in (a). (b-c) Box plots: the dark line in the middle of the boxes is the median, the T-bars that extend from the boxes (whiskers) include 95% of the data. The T-bars that extend from the boxes (whiskers) are expected to include 95% of the data. Letters in the boxplots indicate statistical groups (one-way ANOVA post hoc Tamhane, n =4–13). Black bar =100 μ m, double head red arrow: xylem, double head black arrow: fibers.

BP inactivation completely abolishes xylem formation and secondary growth in *arf6 arf8*, whereas it does not fully suppresses fiber formation in *rga gai* mutants.

ARF6 and ARF8 have been shown to repress class 1 KNOX genes, such as *BP/KNAT1* and *STM* during flower development (Tabata *et al.*, 2010). Interestingly, in the root and hypocotyl BP positively regulates cambium maintenance and fiber formation (Liebsch *et al.*, 2014, Woerlen *et al.*, 2017). Moreover, the lack of fibers in *bp-9* mutants is not restored by GA application, suggesting that BP might work down stream DELLA to promote fiber formation (Ikematsu *et al.*, 2017). However, the *bp-1* allele in Ler ecotype could still respond to GA and it show a less severe phenotype in term of fibers (Figure S6a) suggesting a more complex scenario. Thus, to clarify the role of BP downstream DELLA we generated the *rga-28 gai-td1 bp-9* triple mutants. The inactivation of *RGA* and *GAI* partially rescued the height defects of *bp* mutants but not the branching phenotype (Figure S6b-c). When we examined cross-sections of hypocotyls from senescence plants, we could observe that no fibers were formed in *bp* mutants, whereas fiber formation was partially restored in the *rga-28 gai-td1 bp-9* suggesting that *BP* is not strictly required for fiber formation but it plays a major role in response to GA especially in Col background.

We then investigated the interaction of ARF6 ARF8 with BP during xylem expansion. We first checked whether *BP* is mis-expressed in *arf6 arf8* mutants. Overall BP expression was not altered in the hypocotyl of *arf6 arf8* mutants (Fig S5d). We next compared *arf6-2 arf8-3 bp-9* triple mutants with *bp-9* and *arf6-2 arf8-3* mutants during hypocotyl secondary growth. As previously reported, *bp-9* mutants are characterized by lack of fibers and reduced diameter (Liebsch *et al.*, 2014). The inactivation of *BP* in *arf6 arf8* mutants suppressed the phloem cell divisions and larger area phenotypes. In contrast, xylem occupancy was further reduced when compared to *bp* single mutant and *arf6 arf8* double mutants. Moreover, in *arf6 arf8 bp* triple mutants the morphology of the cambium and phloem cells was altered: cells in the cambial/phloem area were rounder and less differentiated, indicating that *ARF6* and *ARF8* may also control cambium proliferation together with *BP*.

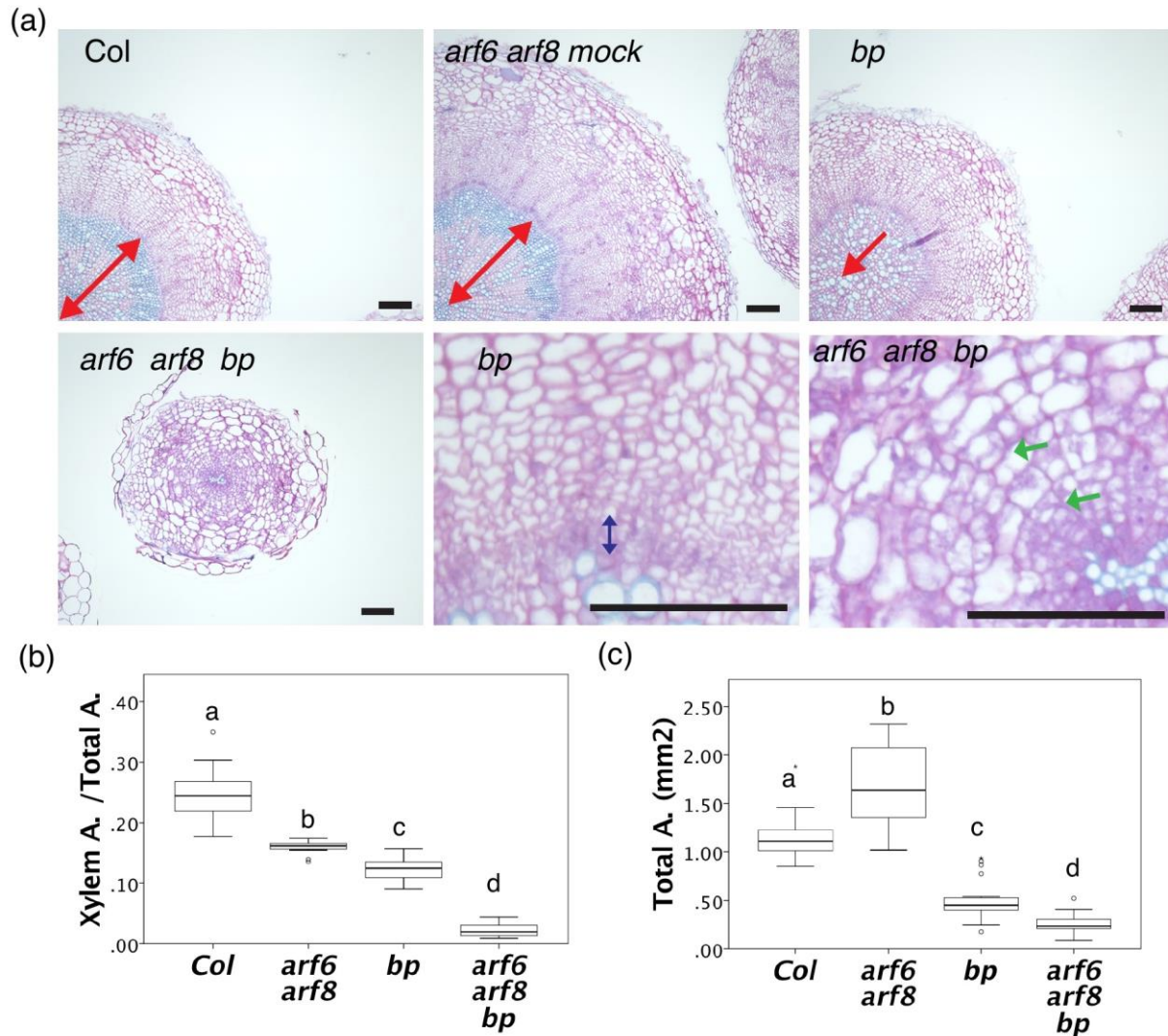


Fig. 5 BP inactivation completely abolishes xylem formation and secondary growth in *arf6 arf8*, whereas it does not suppress fibers formation in *rga gai* mutants.

Plastic hypocotyl cross-sections stained with toluidine blue of 25 day-after-flowering, showing xylem in Col-0, *bp*, *arf6 arf8* and the triple *arf6 arf8 bp* mutant. In *arf6 arf8 bp* mutant cells in the cambium/phloem region are not differentiated (green arrow). (b) Quantification of the Xylem Area / Total area ratio in the experiment illustrated by representative pictures in (a). (c) Quantification of the total area in the experiment illustrated by representative pictures in (a). (b-c) Box plots: the dark line in the middle of the boxes represents the median, the T-bars that extend from the boxes (whiskers) include 95% of the data. Letters in the boxplots indicate statistical groups (one-way ANOVA post hoc Tamhane $n=12-23$). Black bar = 100 μ m, double head red arrow: xylem, double head black arrow: fibers, double head yellow arrow: cambium.

***arf6 arf8* transcriptome reveals a major re-programming during xylem expansion.**

To gather more insights on the regulatory network underlying ARF6 and ARF8 during xylem expansion we performed an RNAseq on hypocotyls of WT and *arf6 arf8* plants. We chose two time points that reflect the progression of xylem expansion and the differences between WT and *arf6 arf8* mutants. 5daf marks the beginning of xylem expansion and precedes the phenotypic difference between *arf6 arf8*, whereas 15daf represents fiber initiation and the divergence between WT and *arf6 arf8* mutants (Figure S3c, d, e).

Consistently, when we compared the WT transcriptome at the two developmental stages we observed a major transcriptional re-programming (1574 genes were up-regulated and 1106 were downregulated in WT 15daf compared to WT 5daf). Also in *arf6 arf8* double mutants many genes were differentially expressed (617 genes were downregulated at 5daf, 1122 were downregulated at 15daf, 680 were upregulated at 5daf and 805 were upregulated at 15daf) and a set of genes were misregulated at both developmental stages (249 downregulated and 123 genes) (File S1).

Around 1/3 (428/1122) of the genes that were down regulated in in *arf6 arf8* double mutants at 15daf were normally upregulated in WT during xylem expansion, confirming a major but not exclusive role of ARF6 and ARF8 during xylem expansion. Gene ontology analyses on this set of gene revealed enrichment in cell wall processes such as: cell wall biogenesis, cell wall organization, xylan biosynthetic process. Consistently, among them we found the three cellulose synthase (CeSA4; CeSA7/ IRX3 and CeSA8/ IRX1) involved in secondary cell wall, many peroxidases and laccase. Moreover, several TFs such as *WRK12*, *MYB46*, *MYB103*, *MYB85*, and *SECONDARY WALL-ASSOCIATED NAC DOMAIN PROTEIN 2 (SND2)*, which regulate xylem differentiation (Yang and Wang, 2016) were also repressed in *arf6 arf8* mutants. The absence of xylem fibers in the hypocotyl of *arf6 arf8* double mutants could be attributed to the down-regulation of the two key fiber promoting transcription factors *NAC SECONDARY WALL THICKENING PROMOTING FACTOR1 (NST1)* and *NST3* (Mitsuda *et al.*, 2007) (Figure 6d), whereas the presence of phloem fibers might be explain by the specific downregulation in *arf6 arf8* of GH3.6 which conjugate JA in a storable inactive form (Gutierrez *et al.*, 2012).

Among the upregulated genes in *arf6 arf8*, we found GA catabolic genes such as *GA2OX2*, *GA2OX7* and *GA20OX1*, TFs such as *ERF1* and *ERF10* and the peptide *CLAVATA3/ESR-RELATED 3 (CLE3)* and *CLE6*.

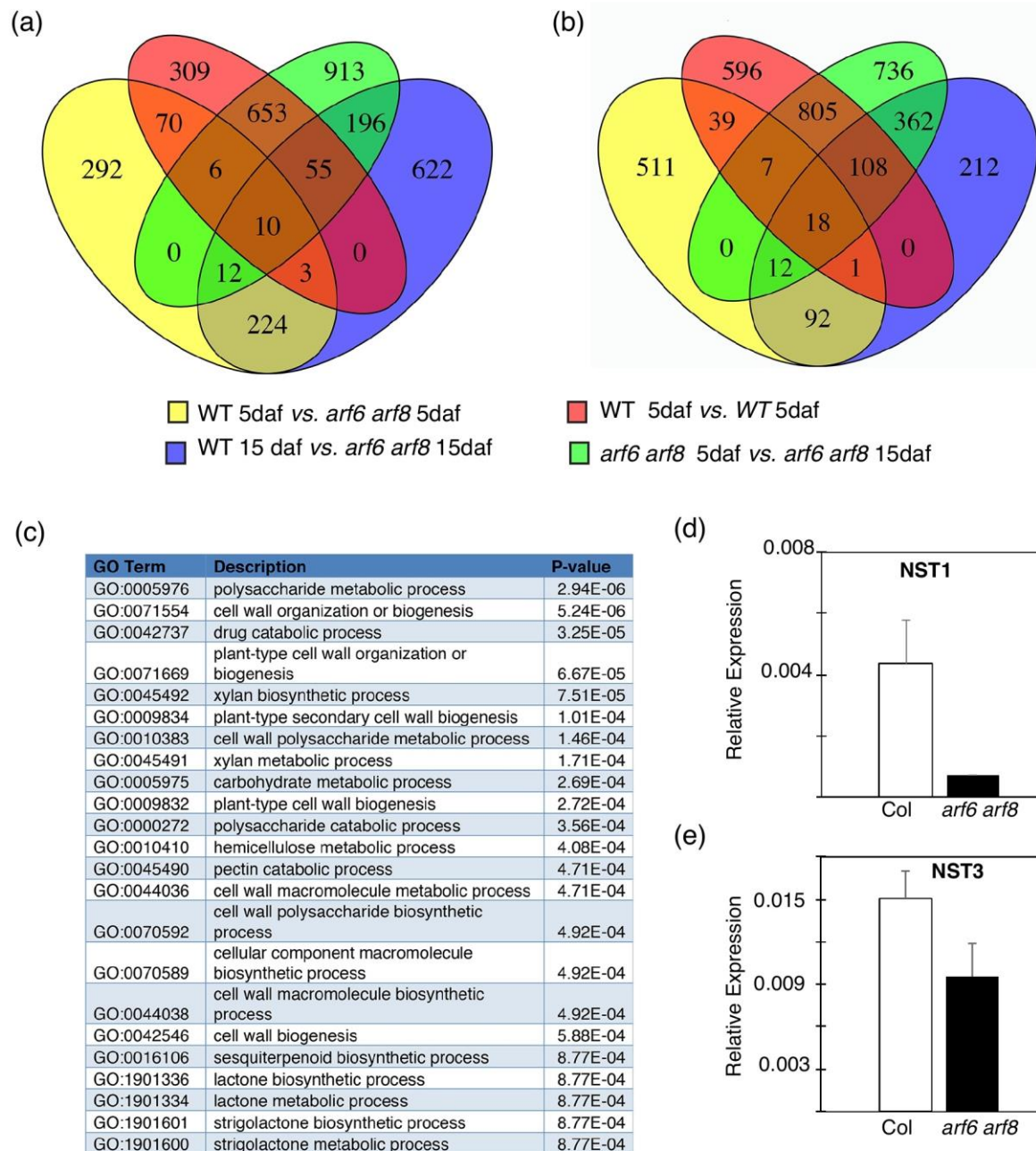


Fig. 6 *arf6 arf8* transcriptome reveals a major re-programming during xylem expansion.

(a) Venn diagram showing the genes that are upregulated in *arf6 arf8* compared to WT at 5day after flowering (daf) (yellow), in *arf6 arf8* compared to WT at 15 daf (blue), in WT at 15daf compared to WT at 5daf and in *arf6 arf8* 15daf compared to *arf6 arf8* 5daf (green). (b) Venn diagram showing the genes that are downregulated in *arf6 arf8* compared to WT at 5daf (yellow), in *arf6 arf8* compared to WT at 15 daf (blue), in WT at 15daf compared to WT at 5daf and in *arf6*

arf8 15daf compared to *arf6 arf8* 5daf (green). (c) Gene ontology of the genes that are downregulated in *arf6 arf8* at compared to WT at 15 daf and are upregulated in WT 15 daf compared to WT 5daf . (d) Q-PCR showing relative expressions, confirming that NST1 and NST3 are down regulated in *arf6 arf8* double mutants.

Discussion:

GA influences many aspects of plant growth and development from germination to senescence, including several developmental transitions. In addition, the GA signaling pathway is modulated by other hormones such as auxin, cytokinins or ethylene (Jasinski *et al.*, 2005, Frigerio *et al.*, 2006, Achard *et al.*, 2007, Weiss and Ori, 2007), placing it as major regulator of plant growth and development (Claeys *et al.*, 2014). GA signaling acts primarily through DELLAs induced degradation. DELLA proteins function mainly in protein complexes, positively or negatively modulating transcription (Locascio *et al.*, 2013). DELLA proteins interact with many TFs belonging to diverse families, suggesting a role as central signaling hubs connecting different signaling cascades (Claeys *et al.*, 2014, Colebrook *et al.*, 2014, Marin-de la Rosa *et al.*, 2014).

GA has a positive role in secondary growth, the increase in girth of plant organs, promoting wood formation and cambial activity (Eriksson *et al.*, 2000a, Björklund *et al.*, 2007). In Arabidopsis, based on the growth rates and cell types two phases of secondary growth can be distinguished. A first phase in which xylem and phloem are produced at the same rate and second phase the so-called xylem expansion in which xylem production is accelerated and xylem fiber differentiates (Ragni *et al.*, 2011). The transition between these two phases involves a major transcriptional reprogramming and it is triggered by the GA dependent degradation of DELLA proteins, which occurs upon flowering in the hypocotyl. In fact, mis-expression of a DELLA protein that cannot be degraded by GA completely abolished xylem expansion (Ragni *et al.*, 2011)(this study).

In this study, we further investigated the signaling cascade of DELLA proteins during secondary growth. In Arabidopsis the *DELLA* gene family comprises 5 members and analyses of single *della* mutants and higher order mutants pointed out that *RGA* and *GAI* are the major contributors as only *rga* single mutant showed enhanced xylem occupancy and *rga gai* double mutants displayed a stronger phenotype similar to the *della* quintuple mutants. The role of *RGA*

and *GAI* in secondary growth seems to be conserved across ecotypes, which differs in secondary growth dynamics and displays different GA responses. Col ecotype is characterized by increased overall secondary growth and reduced xylem occupancy, when compared to Ler (Ragni *et al.*, 2011, Sankar *et al.*, 2014). Interestingly, the difference in secondary growth dynamics between the two ecotypes is not due to the inactivation of *ERECTA* of the Ler background, which confers the stunted and compact inflorescence typical of Ler (Ikematsu *et al.*, 2017). *rga gai* mutants in both ecotypes displayed enhanced xylem expansion when compared to their relative WT ecotypes, whereas *rga gai* double mutant displayed higher xylem expansion in Ler background compared to Col. Consistently, *rga gai* and the *rga gai er* in Col background were undistinguishable. Altogether these results suggest that a xylem promoting factor present in Ler acts in a GA independent pathway to promote xylem expansion. In accord, we observed ectopic phloem proliferation only when we blocked GA response in Col background. A similar scenario has been observed in the context of flower fertility: a stamen elongation regulator, which is not *ERECTA*, promotes stamen elongation independently of *DELLA* in Ler background (Plackett *et al.*, 2014).

As *DELLA* proteins have been shown to interact with more than 15 different families of transcription factors, we aimed to elucidate the *DELLA* interacting partners controlling secondary growth (Marin-de la Rosa *et al.*, 2014). Among more than 60 interacting TFs, *ARF6* and *ARF8* caught our interests as they are expressed also during secondary growth and their expression pattern overlaps with *RGA* and *GAI* in the phloem. Knocking out *ARF6* and *ARF8* abolishes xylem expansion as fibers do not differentiate in the hypocotyls of *arf6 arf8* and phloem proliferation is not repressed. This is reflected in the transcriptome of *arf6 arf8* double mutants in which many, secondary cell wall biosynthesis enzymes and several transcription factors regulating xylem differentiation such as *NST1*, *NST3*, *SND2*, *SND3*, *MYB46* and *MYB83*, are downregulated. In agreement with a specific role during xylem expansion *arf6 arf8* double mutants do not show any secondary growth phenotype before flowering. Interestingly, the double mutant *arf6 arf8* has twice the number of phloem poles than wild-type plants and the phloem tissue is characterized by ectopic cell divisions and by the presence of fibers. Phloem fiber formation can be triggered by exogenous jasmonic acid (JA) application (Behr *et al.*, 2018) and *arf6 arf8* was shown to accumulate more bioactive JA during adventitious root formation, due to the downregulation of the JA conjugating enzymes (Gutierrez *et al.*, 2009). Interestingly, the same GH3 enzymes were down regulated in our

arf6 arf8 transcriptomic data, suggesting that phloem fiber formation in *arf6 arf8* is triggered by JA accumulation in the phloem.

The inactivation of *ARF7/NPH4*, which is closely related to ARF6 and ARF8, and it has been shown to physically interact with RGA (Oh *et al.*, 2014), does not affect xylem expansion even though the *arf7/nph4* mutant is characterized by reduced overall secondary growth (Ragni *et al.*, 2011) (this study). *arf6 nph4/arf7 arf8* triple mutant displayed a slightly reduced xylem occupancy when compared to *arf6 arf8* suggesting only a minor role for ARF7 in xylem expansion. To further confirm the interaction between DELLA and ARFs and its significance in controlling GA mediated xylem expansion, we proved that GA responses are attenuated in *arf6 arf8* double mutants and are even more drastically repressed in *arf6 nph4/arf7 arf8* triple mutants. This was achieved by exogenous GA application and by inactivating *RGA* and *GAI* in *arf6 arf8* background. In *arf6 arf8 rga gai/+* mutants fiber formation was not completely suppressed, suggesting that the ARFs are not the only DELLA downstream factors controlling secondary growth.

A promising candidate is the homeobox gene *BP/KNAT1*, which regulates cambium activity and xylem fiber production. In fact *bp* mutant in Col ecotype does not produce fiber even when treated with GA (Ikematsu *et al.*, 2017), whereas in Ler background GA response is attenuated. Moreover, in *rga gai bp* triple mutants fiber production is severely reduced, thus indicating that also BP works downstream DELLA mainly controlling fiber formation. Interestingly, during flower development it has been shown that ARF6 and ARF8 repress the expression of *BP* and that the inactivation of BP can partially restore the *arf6 arf8* flower phenotypes (Tabata *et al.*, 2010) however, in accord with other studies showing that BP has different functions in above and underground (root/hypocotyl) organs (Mele *et al.*, 2003, Liebsch *et al.*, 2014, Woerlen *et al.*, 2017), this was not the case during hypocotyl secondary growth. *arf6 arf8 bp* triple mutants showed even reduced xylem expansion compared to *arf6 arf8* and altered cell morphology in the cambium and differentiating phloem pointing out that they may act in parallel pathway. The remarkable cambium defects, in the *arf6 arf8 bp* triple mutants suggest that *ARF6* and *ARF8* may play a role in cambium maintenance. The fact that *arf6 arf8* double mutant do not show reduced overall secondary growth as *bp* mutant and that *arf6 arf7 arf8* triple mutants displayed a mild reduction suggest that also other ARFs maybe involved.

In conclusion, we propose a model that could explain the GA triggered shift to xylem expansion phase during secondary growth in Arabidopsis hypocotyl. Before flowering, *ARF6*, *ARF7*, *ARF8* and probably other activators of xylem expansion and fiber differentiation such as *BP* are sequestered by DELLA proteins, thus blocking their activity. After flowering when bio-active GA are higher (Talon *et al.*, 1991, Ragni *et al.*, 2011), DELLA proteins are degraded and the ARFs and other possible activators are released and starts xylem expansion (Figure 7).

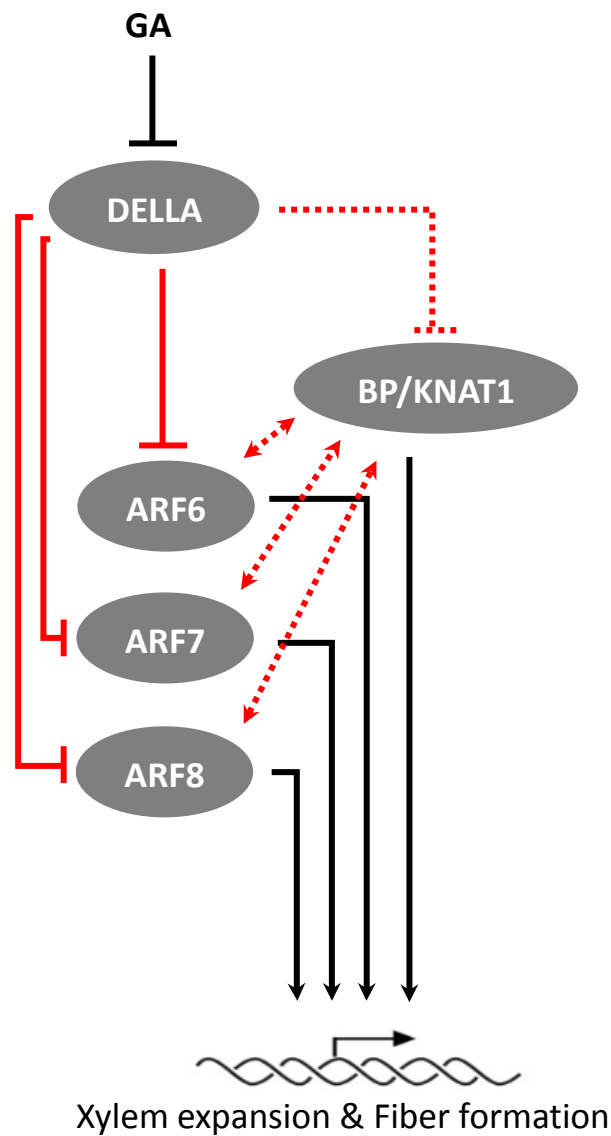


Fig.7 Proposed model on GA mediated secondary growth control and crosstalk with Auxin. Hypothesized links are illustrated with dashed lines. Red arrows represent protein-protein interactions. The lines and arrows illustrate interactions. Compare text for details.

Experimental procedure:

Plant material and growth

The majority of the lines used are in Col-0 background unless otherwise specified in the text/figure. All plants used for confocal microscopy are in Col-0 background, grown in vitro in continuous light. For all the other experiments, plants were grown in soil in long day conditions (16 hours light versus 8 hours dark) and the sampling time is stated in the text/figure. *nph4-1*, *arf6-2*, *arf8-3*, *arf6-2 nph4-1 arf8-3/+*, lines carrying *pRPS5a::GAL4* and *pUAS::MIR167* and the F1 issued from the cross between them were kindly provided by Jason Reed (University of North Carolina, USA) and described in (Nagpal *et al.*, 2005) (Stowe-Evans *et al.*, 1998), *arf8-7* (Gutierrez *et al.*, 2009) lines expressing *promARF6::GUS*, *promARF8::GUS* (Nagpal *et al.*, 2005, Wu *et al.*, 2006) were kindly sent to us by Catherine Bellini (Umeå university, Sweden). The double *rga-24 gai-t6* was a gift from Markus Schmid (Umeå university, Sweden). The *dellako* (Feng *et al.*, 2008), *er-105* (Torii *et al.*, 1996), *rga-28*, *gai-td1* and the double *rga-28 gai-td1* (Plackett *et al.*, 2014) are from S.Thomas, *bp-9* (Pautot *et al.*, 2001), *SUC2::GUS* (Schulze *et al.*, 2003), *BP::GUS* (Pautot *et al.*, 2001) are from V.Pautot (INRA Versailles), *RGA:rgaD-GR*, *GAI:gaiD-GR*, *rga-24*, *gai-t6* were previously described in (Ragni *et al.*, 2011) *ARF6::NLS-3xGFP* (N67078), *ARF7::NLS-3xGFP* (N67080), *ARF8::NLS-3xGFP* (N67082) *arf6-1*(N24606) and *arf8-2*(N24608) (Okushima *et al.*, 2005) were ordered from NASC. *RGA:rgaD-GR*, *GAI:gaiD-GR* in Col-0 background were obtained by backcrossing 6 times the original lines to Col-0. *arf6-1 arf8-2/+*, *SUC2::GUS arf6-2 arf8-3/+*, *bp-9 arf6-2 arf8-3/+*, *BP::GUS arf6-2 arf8-3/+*, *arf6-2 rga-28 gai-td1/+ arf8-3/+* were generated by crossing and genotyping, *arf6-1 arf8-2*, *SUC2::GUS arf6-2 arf8-3*, *bp-9 arf6-2 arf8-3*, *BP::GUS arf6-2 arf8-3*, *arf6-2 arf8-3 rga-28* and *arf6-2 arf8-3 rga-28 gai-td1/+* were obtained by genotyping. Primers for genotyping are listed in table S1.

GA and Dexamethasone Treatment

Induction of soil grown *RGA:rga^D-GR*, or *GAI:gai^D-GR* plants in Ler or Col-0 background was achieved by watering with a 10 µM dexamethasone solution three times per week until hypocotyl sampling. For GA and dex on soil treatments, plants were watered from flowering on, with a 100

μM GA3/ 10 μM dex or mock solution at similar frequency three times per week until hypocotyl sampling according to the experiment.

Molecular Cloning

The RGA promoter was amplified with the primers: A-pRGA F (AACAGGTCTCAACCTTATAACCTCATCCATCTATAG) and Br-pRGA R (AACAGGTCTCATGTTTCAGTACGCCGCCGTCGAGAG). The BsaI site inside the pRGA promoter was removed by overlapping PCRs and cloned in pGG-A0. The GAI promoter was amplified with the primers: A-pGAI F (AACAGGTCTCAACCTTGGGACCACAGTCTAAATGGCGT) and Br-pGAI R (AACAGGTCTCATGTTGGTTGGTTTTTTTTTCAGAGATGGA) and cloned in pGG-A0. The promoters were assembly in pZ03 with the available published modules to obtain RGA:NLS-GFP-GUS and GAI: NLS-GFP-GUS by Green Gate technologies (Lampropoulos *et al.*, 2013).

qPCR and RNA seq.

RNA was extracted from 20 hypocotyls for each genotype from plant grown on soil using the Universal RNA Purification Kit (Roboklon) according to the manufacturer protocol. C-DNA was synthesized using AMV Reverse Transcriptases (Roboklon) according to manufacturer protocol. qPCR was performed using MESA blue (Eurogentec) in a CFX96 Real-TimeSystem machine (BIO-RAD). Primers used for qPCR are listed in table S2. The relative expression was calculated using qPCR miner (<http://ewindup.info/miner/>) (Zhao and Fernald, 2005) normalizing the sample against the expression of EF1. qPCR experiment were repeated at least 2 times. For RNA-seq, RNA was extracted from hypocotyls (three biological replicates for each genotype at each time point) using the kit: Universal RNA Purification Kit (Roboklon) and RNA quality was checked at the Bioanalyzer. Libraries were prepared using the TruSeq RNA Library Prep Kit (Illumina) according to manufacturer protocol. Sequencing was performed pair ended using an Illumina HiSeq3000. Reads were aligned against the Arabidopsis genome (version TAIR10) using Tophat v2 (<http://ccb.jhu.edu/software/tophat>). After alignment, one biological replicate for each sample was discarded due to high percent multiple alignment. Read counting was done using the R package: Rsubread (Liao *et al.*, 2013) and differentially expressed gene were calculated using R package: DESeq2 (Love *et al.*, 2014). Gene ontology was performed using GOrilla (<http://cbl-gorilla.cs.technion.ac.il/>). Venn diagrams were made using the R package: VennDiagram.

Histology and stainings

GUS essay was performed according to the protocol described in (Beisson *et al.*, 2007). Vibratome sections (50–80 μm) were obtained via a Leica VT-1000 vibratome, from hypocotyls embedded in 6% agarose block, slices were collected in water in microscope slides, stained and/or imaged. For Phloroglucinol staining, a ready solution (VWR, 26337.180) was applied directly to the section. Images were taken with a Zeiss Axio M2 imager microscope. Plastic hypocotyl cross-sections (5 μm) were obtained as described in (Barbier de Reuille & Ragni, 2017) and stained with 0.1 % toluidine blue.

For sections of fluorescent lines the ClearSee protocol described in (Ursache *et al.*, 2018) was applied. Briefly, the hypocotyls were first fixed in a 4% PFA solution with 0.01% Triton for 1 hour. and then embedded in 5% Agarose for vibratome cutting. Vibratome sections are then directly collected in 1x PBS solution. After incubation, the 1x PBS solution is removed and replaced by ClearSee solution. The sections are subsequently kept at room temperature in ClearSee solution for at least 1 to 2 days. Finally is the samples are incubated for 20 min at RT in 0,05 % Calcofluor White then washed and mounted on a slides in ClearSee solution (Kurihara *et al.*, 2015).

Images acquisition

A Zeiss Axio M2 imager microscope or a Zeiss Axiophot microscope was used to take images at different magnifications of vibratome sections (50–80 μm) as well as 5 μm sections obtained from plastic embedded hypocotyls as previously described by (de Reuille and Ragni, 2017) and stained with 0.1% toluidine blue solution. Pictures of vibratome sections of fluorescent lines were acquired using the Zeiss LSM880 confocal microscope. GFP ex. 488 em. 490-520. Calcofluor White ex 404 em: 430-450.

Image analyses and statistical analyses

The total hypocotyl cross section area, the xylem area and the fiber area were analyzed using ImageJ software as previously described (Sibout *et al.*, 2008b). Statistical analyses were performed using IBM SPSS Statistics version 24-25 (IBM). We first tested all datasets for homogeneity of variances using Levene's Test of Equality of Variances. For multiple comparison, we calculated

the significant differences between each dataset using One way ANOVA with Tamhane's post hoc (equal variance not assumed) or a Bonferroni correction (equal variance assumed). For comparing two groups, we used Welch's t-test (not homogenous variance) or a Student's t-test (homogeneous variance). The significance threshold was set to p-value < 0.05.

Acknowledgement:

L.R. is indebted to the Baden-Württemberg Stiftung for financial support of this research project by the Elite program for Postdocs. This project was also partially supported by the seed funding of the SFB1101.

Conflict of Interest

The authors declare no conflict of interest

Supporting Information

Fig. S1 RGA and GAI are the main DELLA regulators of secondary growth.

Fig S2 RGA and GAI dominant negative lines repress xylem expansion in both Col and Ler ecotypes.

Fig S3 The phloem poles are the sites of DELLA and ARF expression and ectopic cell division in *arf6 arf8* mutant.

Fig. S4 Secondary growth dynamics in *arf* mutants.

Fig. S5 Genetic interaction between ARFs and DELLA in the regulation of secondary growth.

Fig. S6 Genetic interaction between *DELLAs* and *BP*.

Table S1 Primers used for genotyping.

Table S2 Primers used for qPCR.

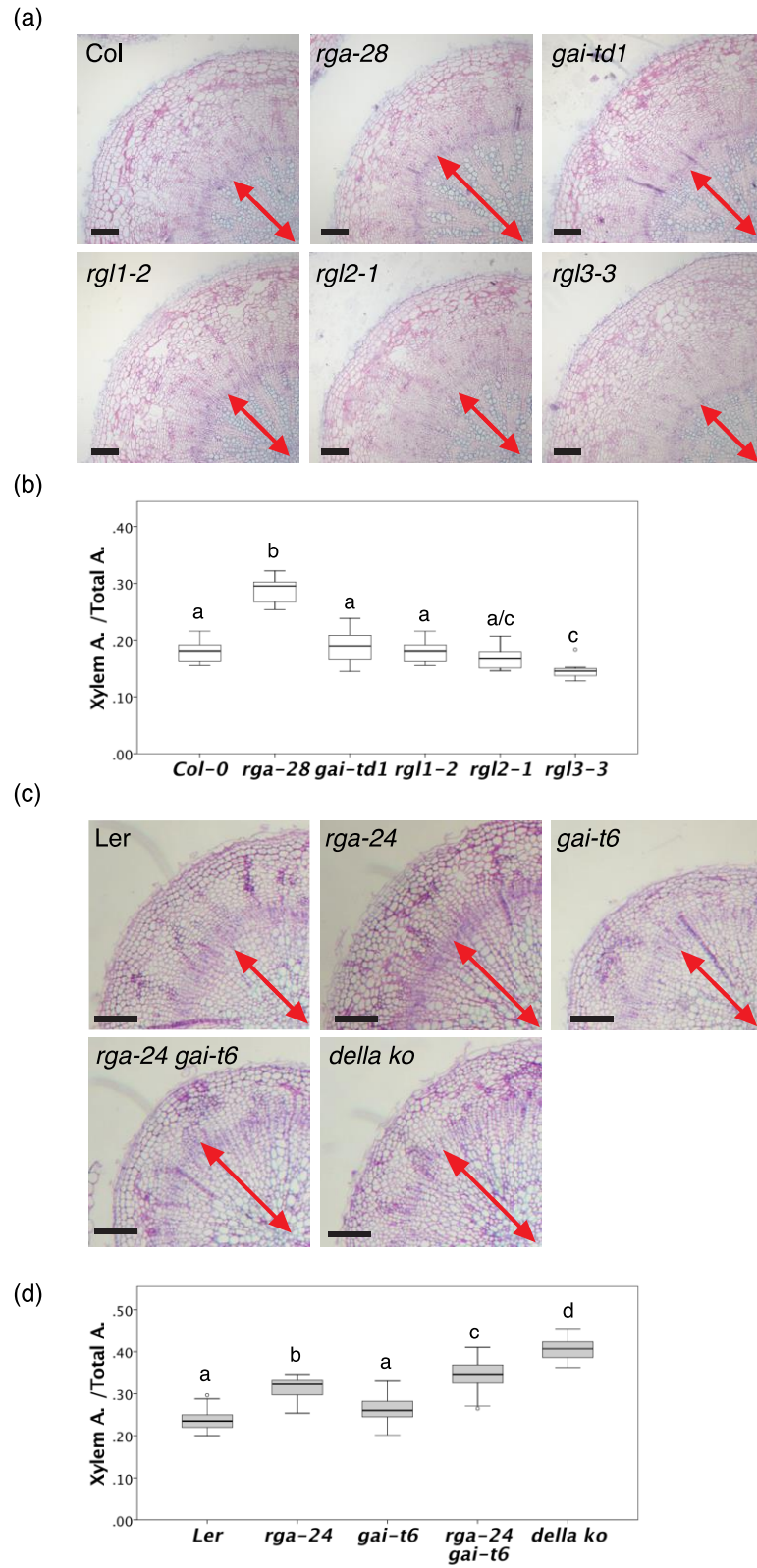


Fig. S1 RGA and GAI are the main DELLA regulators of secondary growth.

(a) Plastic hypocotyl cross-sections stained with toluidine blue of 10 day-after-flowering, showing xylem in *della* single mutants: *rga-28*, *gai-td1*, *rgl1-2*, *rgl2-1* and *rgl3-3*. (b) Quantification of the Xylem Area /Total area ratio in the experiment illustrated by representative pictures in (a). (c) Plastic cross-sections stained with toluidine blue of 8 day-after-flowering, showing xylem expansion in different combination of *della* mutants: *rga-24*, *gai-t6*, *rga-24 gai-t6* and *della ko*. (d) Quantification of the Xylem Area /Total area ratio in the experiment illustrated by representative pictures in (c). (e) Plastic cross-sections stained with toluidine blue of 15 day-after-flowering, showing xylem expansion in Mock and Dex treated transgenic plants of *rga:rga^D-GR* and *gai:gai^D-GR* (in Ler background). (b,d) Box plots: the dark line in the middle of the boxes represents the median, the T-bars that extend from the boxes (whiskers) include 95% of the data. Letters in the boxplots indicate statistical groups (One way ANOVA, post hoc Bonferroni for (b) n = 10–12 and post hoc Bonferroni for (d) n=20). Black bar =100µm, double head red arrow: xylem.

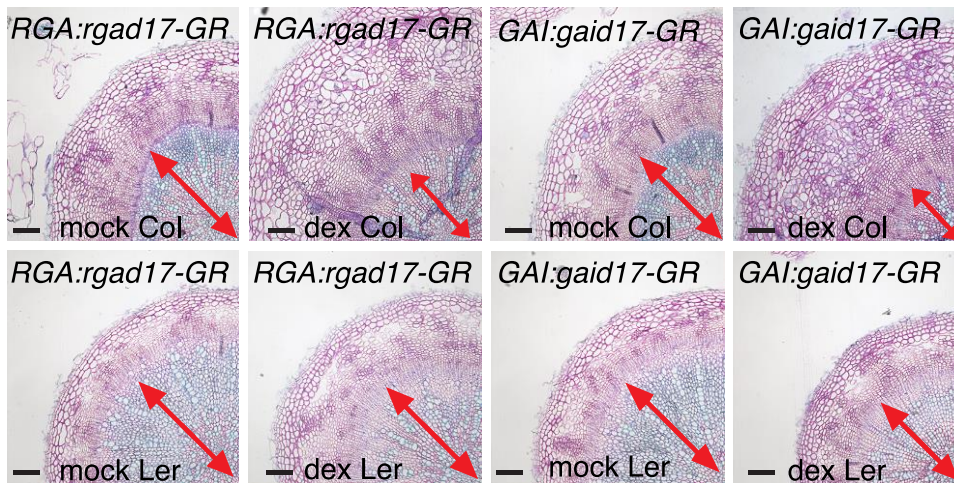


Fig S2 RGA and GAI dominant negative lines repress xylem expansion in both Col and Ler ecotypes.

Plastic hypocotyl cross-sections stained with toluidine blue of 15 day-after-flowering, showing xylem expansion in Mock and Dexamethasone (dex) treated transgenic plants of *rga:rga^D-GR* and *gai:gai^D-GR* (in Ler and Col background). Black bar =100µm, double head red arrow: xylem.

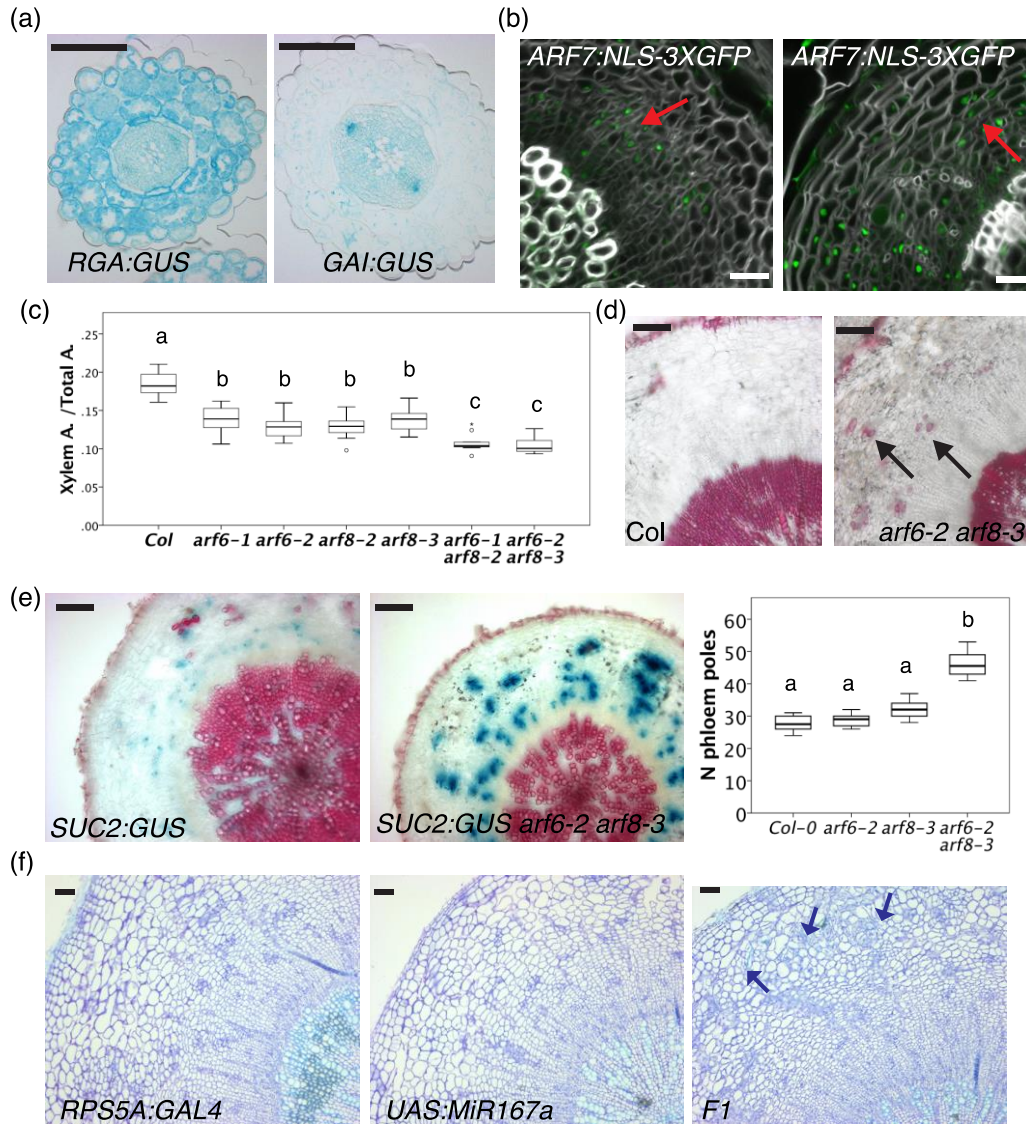


Fig S3 The phloem poles are the sites of DELLA and ARF expression and ectopic cell division in *arf6 arf8* mutant.

(a) Plastic hypocotyl cross-sections of *RGA:GUS* and *GAI:GUS* at 16 days after germination. (b) Vibratome hypocotyl cross-sections of *ARF7:NLS-GFP-GUS* respectively at 0 and 8 day-after-flowering (daf). (c) Quantification of Xylem/Total area ratio in *Col*, *arf6-1*, *arf6-2*, *arf8-2*, *arf8-3*, *arf6-1 arf8-2* and *arf6-2 arf8-3*. (d) Hypocotyl vibratome sections stained with phloroglucinol showing phloem fibers in *arf6 arf8* double mutants (black arrows; 60daf). (e) Plastic hypocotyl cross-section of *SUC2:GUS* and *arf6-2 arf8-3 SUC2:GUS* at 20 daf. Quantification of the number of phloem poles in *Col*, *arf6*, *arf8* and *arf6 arf8* at 10 daf. (f) Toluidine blue stained hypocotyl sections of 10 daf *RPS5A:GAL4*, *UAS:MIR167a* and F1 (*RPS5A:GAL4 x UAS:MIR167a*). Box

plot: the dark line in the middle of the boxes represents the median, the T-bars that extend from the boxes (whiskers) include 95% of the data. Letters in the boxplots indicate statistical groups (One way ANOVA, post hoc Bonferroni for (c) n = 8-16 and post hoc Bonferroni for (e) n=6) White bars = 20 μ m, black bar =100 μ m. Red arrow: GFP signal in the phloem. Blue arrow: ectopic divisions in the phloem.

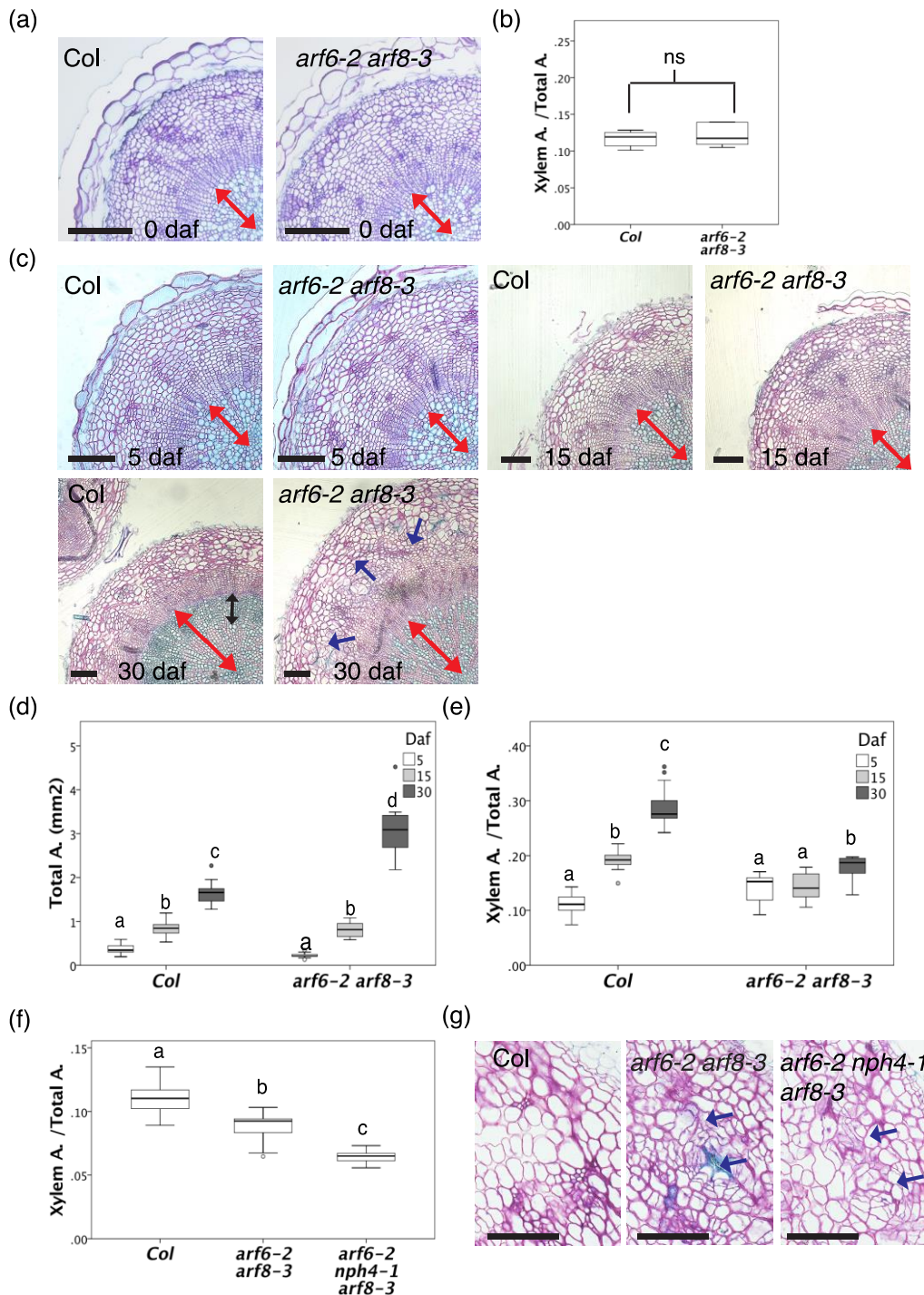


Fig. S4 Secondary growth dynamics in *arf* mutants.

(a) Plastic hypocotyl cross-sections stained with toluidine blue of flowering plants showing xylem expansion in Col-0 and *arf6-2 arf8-3*. (b) Quantification of the Xylem Area /Total area ratio in the experiment illustrated by representative pictures in (a), Student's Test (n=6-8). (c) Plastic hypocotyl cross-sections stained with toluidine blue showing xylem expansion in Col and *arf6-2 arf8-3* at 5, 15, 30 day-after-flowering (daf). (d) Quantification of the Total area in the experiment illustrated by representative examples in (c). (e) Quantification of Xylem/Total area ratio in the experiment illustrated by representative pictures in (c). Quantification of Xylem/Total area ratio in the experiment illustrated by representative pictures in (g). (d-f) Box plots: the dark line in the middle of the boxes represents the median, the T-bars that extend from the boxes (whiskers) include 95% of the data. Letters in the boxplots indicate statistical groups (One way ANOVA, post hoc Tamhane for (d) n=10-14, post hoc Bonferroni for (e) n =10-14 and post hoc Tamhane for (f) n=8-11). (g) Plastic hypocotyl cross-sections stained with toluidine blue showing the ectopic phloem cell division phenotype in *arf6-2 arf8-3* and *arf6-2 nph4-1 arf8-3* at 10 daf. Black bar =100µm, double head red arrow: xylem, double head black arrow: fibers. Blue arrow: ectopic divisions in the phloem.

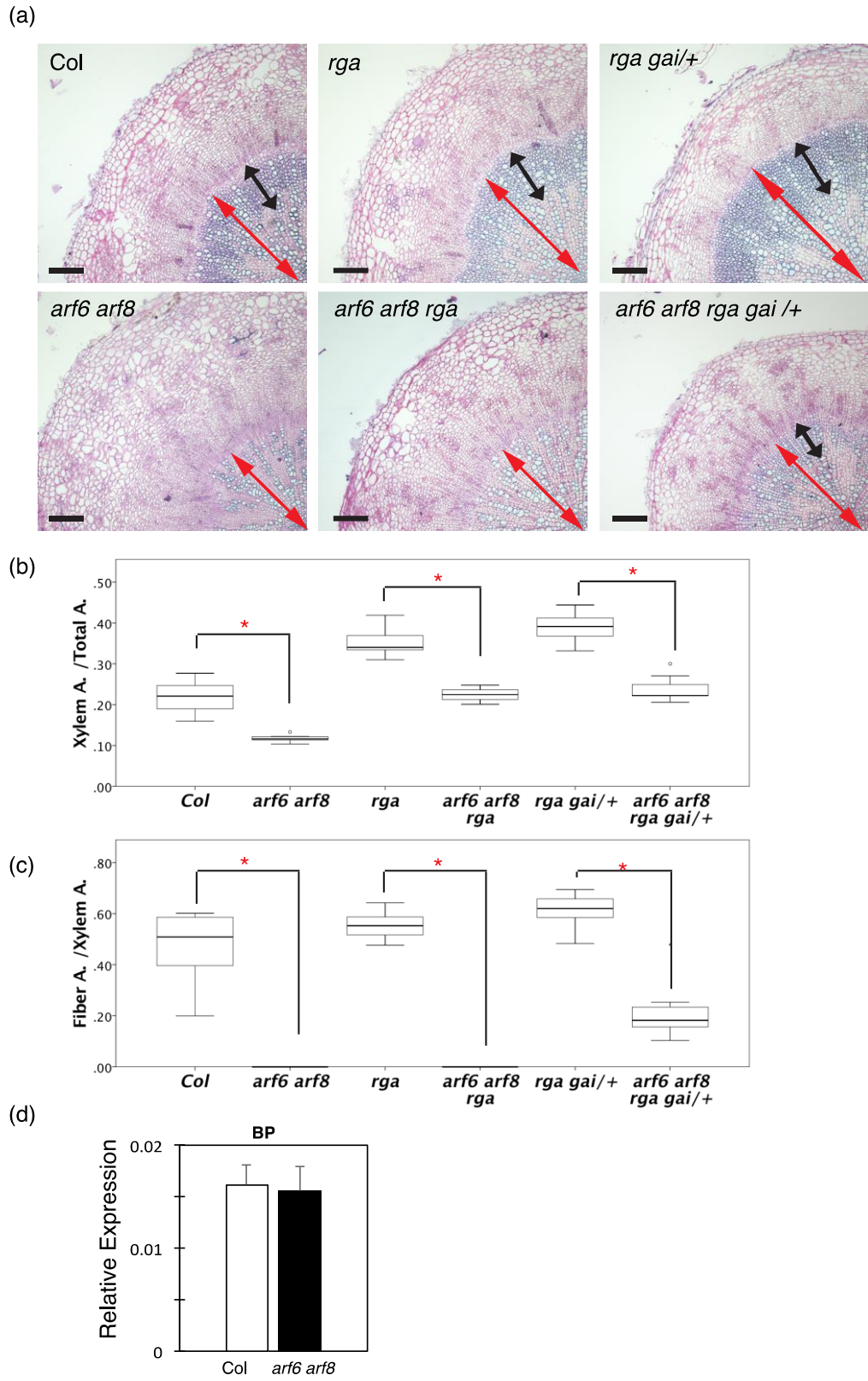


Fig. S5 Genetic interaction between ARFs and DELLA in the regulation of secondary growth.

(a) Plastic hypocotyl cross-sections stained with toluidine blue showing xylem expansion in Col *arf6 arf8*, *rga gai/+ arf6 arf8 rga* and *arf6 arf8 rga gai/+* at day-after-flowering ((b) Quantification of Xylem/Total area ratio in the experiment illustrated by representative pictures in (a). (c) Quantification of Fiber area/Xylem area ratio in the experiment illustrated by representative examples in (a). Box plots: the dark line in the middle of the boxes represents the median, the T-bars that extend from the boxes (whiskers) include 95% of the data. Student's or Welch t-test (red asterisk: $P < 0.05$, $n=3-12$). Black bar =100 μ m, double head red arrow: xylem, double head black arrow: fibers.

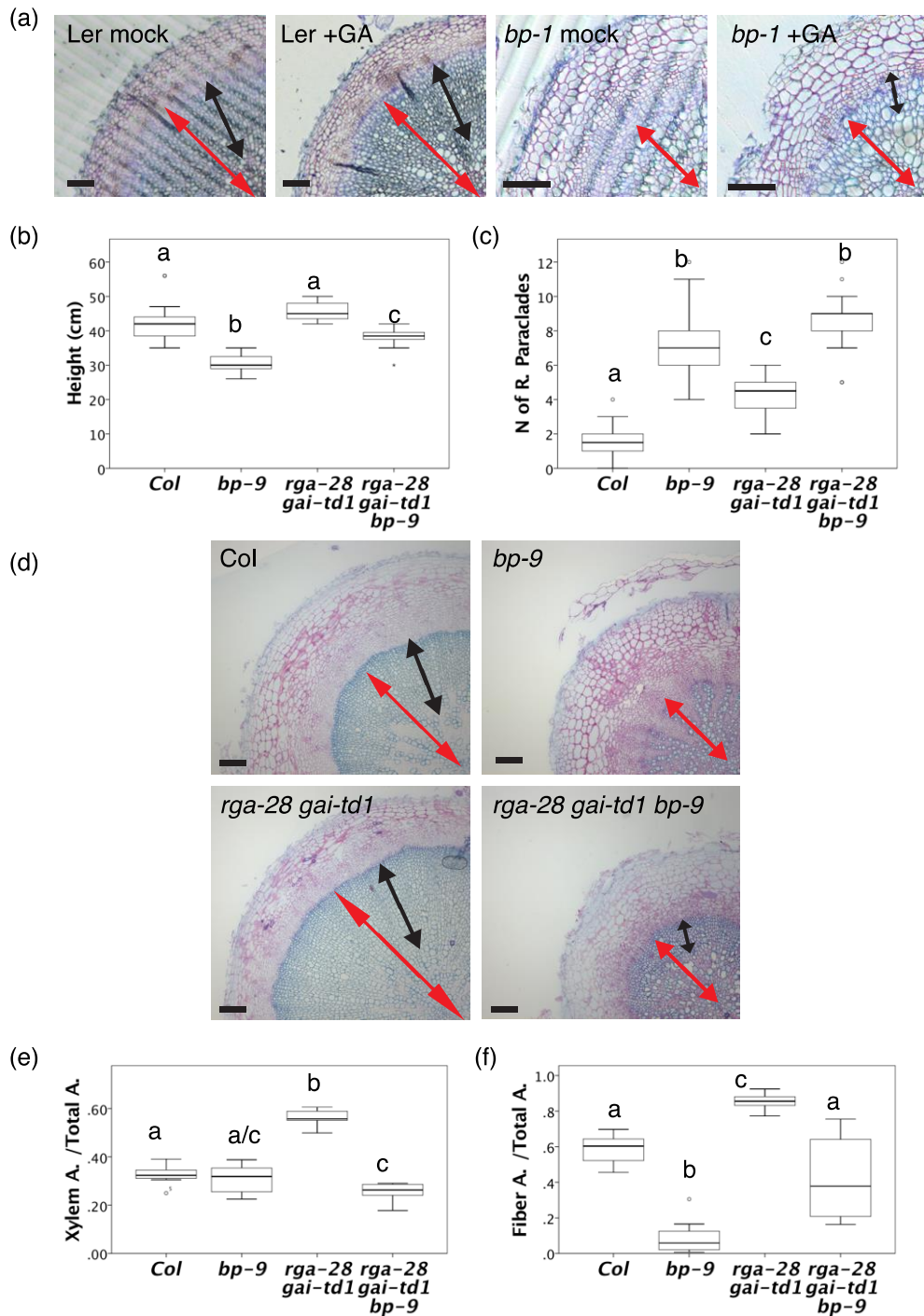


Fig. S6 Genetic interaction between DELLAs and BP.

a) Plastic hypocotyl cross-sections stained with toluidine blue showing xylem expansion in Ler and *Bp-1* mutants treated with mock or GA at 8 day-after-flowering (daf). (b,c) Quantification of stem height, rosette paraclades in Col, *bp-9*, *rga-28 gai-td1*, *rga-28 gai-td1 bp-9* at plant senescence. (d)

Plastic hypocotyl cross-sections stained with toluidine blue showing xylem expansion in in Col, *bp-9*, *rga-28 gai-td1*, *rga-28 gai-td1 bp-9* at plant senescence. (e) Quantification of Xylem/Total area ratio in the experiment illustrated by representative pictures in (d). (f) Quantification of Fiber area/Xylem area ratio in the experiment illustrated by representative examples in (d). (g) q-PCR showing relative expression of BP (normalized to EF1) in Col and *arf6 arf8* double mutants at 20daf. Box plots: the dark line in the middle of the boxes represents the median, the T-bars that extend from the boxes (whiskers) include 95% of the data. Letters in the boxplots indicate statistical groups (One way ANOVA, post hoc Bonferroni for (b) n=20, post hoc Tamhane for (c) n=20, post hoc Bonferroni for (e) n = 7-9 and post hoc Tamhane for (f), n = 7-9). Black bar =100µm, double head red arrow: xylem, double head black arrow: fibers.

Table S1 Primers used for genotyping.

Allele	WT/mut	primer name	sequence
<i>rga-28</i>	WT	RGA genoF	CGATTGTCCAACCACGGG
		RGAR_201	CAGCTAAGCATCCGATTTGC
	mut	rga28-244	ATGGCGGAGGTTGCTTTGAAACTCGAACA
		Ds3-2	CCGGTATATCCCGTTT TCG
<i>gai-td1</i>	WT	GAI_TDNA_LP3	CGGTAACGGCATGGATGAG
		GAI_TDNA_RP	AGCTTCGGCGAAGTAAGTAGC
	mut	GAI_TDNA_RP	AGCTTCGGCGAAGTAAGTAGC
		LB3	TAGCATCTGAATTTATAACCAATCTCGATACAC
<i>rgl1-1</i>	WT	RGL1 1670F	AAGCTAGCTCGAAACCCCAAAT
		RGL1 2295R	CCACAGAGCGCGTAGAGGATAAC
	mut	RGL1 1670F	AAGCTAGCTCGAAACCCCAAAT
		DS5-P1	CATGGGCTGGGCCTCAGTG
<i>rgl2-1</i>	WT	RGL2 856F	GCTGGTGAAACGCGTGGAACA
		RGL2 1883R	ACGCCGAGGTTGTGATGAGTG
	mut	RGL2 856F	GCTGGTGAAACGCGTGGAACA
		DS5-3	CGGTCGGTACGGGATTTTCC
<i>arf6-1</i>	WT	arf6-2 R	CCAAGGGTCATCGCCGAGGAGAAGAACGTC
		arf6-2 F	GACGAATCTACTGCAGGAG
	mut	arf6-2 F	GACGAATCTACTGCAGGAG
		LBb1.3	ATTTTGCCGATTTTCGGAAC
<i>arf6-2</i>	WT	arf6-2 R	CCAAGGGTCATCGCCGAGGAGAAGAACGTC
		arf6-2 F	GACGAATCTACTGCAGGAG
	mut	arf6-2 F	GACGAATCTACTGCAGGAG
		JMLB	GGCAATCAGCTGTTGCCCGTCTCACTGGTG
<i>arf8-2</i>	WT	arf8-3 R	CCATGGGTCATCACCAAGGAGAAGAATATC
		arf8-7 F	CAGGGCTAGCCAATCTGAGTTTGTGATACA
	mut	arf8-7 F	CAGGGCTAGCCAATCTGAGTTTGTGATACA
		LB3	TAGCATCTGAATTTATAACCAATCTCGATACAC
<i>arf8-3</i>	WT	arf8-7 F	CAGGGCTAGCCAATCTGAGTTTGTGATACA
		arf8-7 R	GACCACTTCCCAAATCACCCCTTCCATCTG
	mut	arf8-7 R	GACCACTTCCCAAATCACCCCTTCCATCTG
		JMLB	GGCAATCAGCTGTTGCCCGTCTCACTGGTG
<i>arf8-7</i>	WT	ARF8-7genoF	TAAACTTCCATTCAACATCATGGA
		ARF8-7genoR	AGTCGAGTTGTTTACTTTCCACAG
	mut	ARF8-7genoR	AGTCGAGTTGTTTACTTTCCACAG
		8474	ATAATAACGCTGCGGACATCTACATTTT
<i>nph4-1</i>	WT	nph4-1geno_F	TCCTGCTGAGTTTGTGGTTCCTT

		nph4-1geno_R	GGGGCTTGCTGATTCTGTTTGTTA
	mut	nph4-1geno_R	GGGGCTTGCTGATTCTGTTTGTTA
<i>bp-9</i>	WT	BP-14	TGTTAAGGGTTAGAACACCATG
		BP-3	GACAACAGCACCCTCCTCAAA
	mut	BP-3	GACAACAGCACCCTCCTCAAA
		dspm1	CTTATTTAGTAAGAGTGTGGGGTTTTGG

Table S2 Primers used for qPCR.

Genes	Primer	Sequence
EF1	EF1a.F	TGGTGACGCTGGTATGGTTA
	EF1a.R	TCCTTCTTGCCACGCTCTT
KNAT1/BP	KNAT1qPCR_F	TCCCATTACATCCTCAACA
	KNAT1qPCR_R	CCCCTCCGCTGTTATTCTCT
NST3	NST3 F qPCR	TGCATGAGTATCGCCTCGAC
	NST3 R qPCR	CCCTTCTTCTCCTCCGTGTC
NST1	NST1 F qPCR	GCTCCTCACGGCCAAAATC
	NST1 R qPCR	CTCCGACGGGACTGTTTAGG

References:

- Achard, P., Baghour, M., Chapple, A., Hedden, P., Van Der Straeten, D., Genschik, P., Moritz, T. and Harberd, N.P. (2007) The plant stress hormone ethylene controls floral transition via DELLA-dependent regulation of floral meristem-identity genes. *Proceedings of the National Academy of Sciences of the United States of America*, **104**, 6484-6489.
- Behr, M., Lutts, S., Hausman, J.F. and Guerriero, G. (2018) Jasmonic acid to boost secondary growth in hemp hypocotyl. *Planta*, **248**, 1029-1036.
- Beisson, F., Li, Y., Bonaventure, G., Pollard, M. and Ohlrogge, J.B. (2007) The Acyltransferase GPAT5 Is Required for the Synthesis of Suberin in Seed Coat and Root of Arabidopsis. *The Plant Cell* **19**, 351-368.
- Björklund, S., Antti, H., Uddestrand, I., Moritz, T. and Sundberg, B. (2007) Cross-talk between gibberellin and auxin in development of Populus wood: gibberellin stimulates polar auxin transport and has a common transcriptome with auxin. *Plant J*, **52**, 499-511.
- Carlsbecker, A., Lee, J.-Y., Roberts, C.J., Dettmer, J., Lehesranta, S., Zhou, J., Lindgren, O., Moreno-Risueno, M.A., Vatén, A., Thitamadee, S., Campilho, A., Sebastian, J., Bowman, J.L., Helariutta, Y. and Benfey, P.N. (2010) Cell signalling by microRNA165/6 directs gene dose-dependent root cell fate. *Nature*, **465**, 316-321.
- Chaffey, N., Cholewa, E., Regan, S. and Sundberg, B. (2002) Secondary xylem development in Arabidopsis: a model for wood formation. *Physiologia Plantarum*, **114**, 594-600.
- Cheng, H., Qin, L., Lee, S., Fu, X., Richards, D.E., Cao, D., Luo, D., Harberd, N.P. and Peng, J. (2004) Gibberellin regulates Arabidopsis floral development via suppression of DELLA protein function. *Development*, **131**, 1055-1064.
- Claeys, H., De Bodt, S. and Inze, D. (2014) Gibberellins and DELLAs: central nodes in growth regulatory networks. *Trends Plant Sci*, **19**, 231-239.
- Colebrook, E.H., Thomas, S.G., Phillips, A.L. and Hedden, P. (2014) The role of gibberellin signalling in plant responses to abiotic stress. *The Journal of experimental biology*, **217**, 67-75.
- Davière, J.-M. and Achard, P. (2016) A Pivotal Role of DELLAs in Regulating Multiple Hormone Signals. *Molecular Plant*, **9**, 10-20.
- de Reuille, P.B. and Ragni, L. (2017) Vascular Morphodynamics During Secondary Growth. *Methods in molecular biology (Clifton, N.J.)*, **1544**, 103-125.
- Demura, T. and Ye, Z.-H. (2010) Regulation of plant biomass production. *Current Opinion in Plant Biology*, **13**, 298-303.
- Dill, A. and Sun, T. (2001) Synergistic derepression of gibberellin signaling by removing RGA and GAI function in Arabidopsis thaliana. *Genetics*, **159**, 777-785.
- Du, J., Miura, E., Robischon, M., Martinez, C. and Groover, A. (2011) The Populus Class III HD ZIP Transcription Factor POPCORONA Affects Cell Differentiation during Secondary Growth of Woody Stems. *PLoS ONE*, **6**, e17458.
- Eriksson, M.E., Israelsson, M., Olsson, O. and Moritz, T. (2000) Increased gibberellin biosynthesis in transgenic trees promotes growth, biomass production and xylem fiber length. *Nature biotechnology*, **18**, 784-788.
- Feng, S., Martinez, C., Gusmaroli, G., Wang, Y., Zhou, J., Wang, F., Chen, L., Yu, L., Iglesias-Pedraz, J.M., Kircher, S., Schafer, E., Fu, X., Fan, L.M. and Deng, X.W. (2008) Coordinated regulation of Arabidopsis thaliana development by light and gibberellins. *Nature*, **451**, 475-479.
- Frigerio, M., Alabadi, D., Perez-Gomez, J., Garcia-Carcel, L., Phillips, A.L., Hedden, P. and Blazquez, M.A. (2006) Transcriptional regulation of gibberellin metabolism genes by auxin signaling in Arabidopsis. *Plant Physiol*, **142**, 553-563.
- Gutierrez, L., Bussell, J.D., Pacurar, D.I., Schwambach, J., Pacurar, M. and Bellini, C. (2009) Phenotypic plasticity of adventitious rooting in Arabidopsis is controlled by complex regulation of AUXIN RESPONSE FACTOR transcripts and microRNA abundance. *Plant Cell*, **21**, 3119-3132.

- Gutierrez, L., Mongelard, G., Flokova, K., Pacurar, D.I., Novak, O., Staswick, P., Kowalczyk, M., Pacurar, M., Demailly, H., Geiss, G. and Bellini, C.** (2012) Auxin controls Arabidopsis adventitious root initiation by regulating jasmonic acid homeostasis. *Plant Cell*, **24**, 2515-2527.
- Ikematsu, S., Tasaka, M., Torii, K.U. and Uchida, N.** (2017) ERECTA-family receptor kinase genes redundantly prevent premature progression of secondary growth in the Arabidopsis hypocotyl. *New Phytol*, **213**, 1697-1709.
- Jasinski, S., Piazza, P., Craft, J., Hay, A., Woolley, L., Rieu, I., Phillips, A., Hedden, P. and Tsiantis, M.** (2005) KNOX action in Arabidopsis is mediated by coordinate regulation of cytokinin and gibberellin activities. *Curr Biol*, **15**, 1560-1565.
- Kubo, M., Udagawa, M., Nishikubo, N., Horiguchi, G., Yamaguchi, M., Ito, J., Mimura, T., Fukuda, H. and Demura, T.** (2005) Transcription switches for protoxylem and metaxylem vessel formation. *Genes & Development*, **19**, 1855-1860.
- Kurihara, D., Mizuta, Y., Sato, Y. and Higashiyama, T.** (2015) ClearSee: a rapid optical clearing reagent for whole-plant fluorescence imaging. *Development*, **142**, 4168-4179.
- Lampropoulos, A., Sutikovic, Z., Wenzl, C., Maegele, I., Lohmann, J.U. and Forner, J.** (2013) GreenGate - A Novel, Versatile, and Efficient Cloning System for Plant Transgenesis. *PLoS ONE*, **8**, e83043.
- Liao, Y., Smyth, G.K. and Shi, W.** (2013) The Subread aligner: fast, accurate and scalable read mapping by seed-and-vote. *Nucleic acids research*, **41**, e108.
- Liebsch, D., Sunaryo, W., Holmlund, M., Norberg, M., Zhang, J., Hall, H.C., Helizon, H., Jin, X., Helariutta, Y., Nilsson, O., Polle, A. and Fischer, U.** (2014) Class I KNOX transcription factors promote differentiation of cambial derivatives into xylem fibers in the Arabidopsis hypocotyl. *Development*, **141**, 4311-4319.
- Locascio, A., Blázquez, M.A. and Alabadí, D.** (2013) Genomic Analysis of DELLA Protein Activity. *Plant and Cell Physiology*, **54**, 1229-1237.
- Love, M.I., Huber, W. and Anders, S.** (2014) Moderated estimation of fold change and dispersion for RNA-seq data with DESeq2. *Genome biology*, **15**, 550.
- Marin-de la Rosa, N., Sotillo, B., Miskolczi, P., Gibbs, D.J., Vicente, J., Carbonero, P., Onate-Sanchez, L., Holdsworth, M.J., Bhalerao, R., Alabadi, D. and Blazquez, M.A.** (2014) Large-scale identification of gibberellin-related transcription factors defines group VII ETHYLENE RESPONSE FACTORS as functional DELLA partners. *Plant Physiol*, **166**, 1022-1032.
- Mele, G., Ori, N., Sato, Y. and Hake, S.** (2003) The knotted1-like homeobox gene BREVIPEDICELLUS regulates cell differentiation by modulating metabolic pathways. *Genes Dev*, **17**, 2088-2093.
- Mitsuda, N., Iwase, A., Yamamoto, H., Yoshida, M., Seki, M., Shinozaki, K. and Ohme-Takagi, M.** (2007) NAC Transcription Factors, NST1 and NST3, Are Key Regulators of the Formation of Secondary Walls in Woody Tissues of Arabidopsis. *The Plant Cell Online*, **19**, 270-280.
- Nagpal, P., Ellis, C.M., Weber, H., Ploense, S.E., Barkawi, L.S., Guilfoyle, T.J., Hagen, G., Alonso, J.M., Cohen, J.D., Farmer, E.E., Ecker, J.R. and Reed, J.W.** (2005) Auxin response factors ARF6 and ARF8 promote jasmonic acid production and flower maturation. *Development*, **132**, 4107-4118.
- Oh, E., Zhu, J.Y., Bai, M.Y., Arenhart, R.A., Sun, Y. and Wang, Z.Y.** (2014) Cell elongation is regulated through a central circuit of interacting transcription factors in the Arabidopsis hypocotyl. *Elife*, **3**.
- Okushima, Y., Overvoorde, P.J., Arima, K., Alonso, J.M., Chan, A., Chang, C., Ecker, J.R., Hughes, B., Lui, A., Nguyen, D., Onodera, C., Quach, H., Smith, A., Yu, G. and Theologis, A.** (2005) Functional genomic analysis of the AUXIN RESPONSE FACTOR gene family members in Arabidopsis thaliana: unique and overlapping functions of ARF7 and ARF19. *Plant Cell*, **17**, 444-463.
- Pautot, V., Dockx, J., Hamant, O., Kronenberger, J., Grandjean, O., Jublot, D. and Traas, J.** (2001) KNAT2: evidence for a link between knotted-like genes and carpel development. *Plant Cell*, **13**, 1719-1734.

- Plackett, A.R.G., Ferguson, A.C., Powers, S.J., Wanchoo-Kohli, A., Phillips, A.L., Wilson, Z.A., Hedden, P. and Thomas, S.G.** (2014) DELLA activity is required for successful pollen development in the Columbia ecotype of Arabidopsis. *New Phytologist*, **201**, 825-836.
- Ragni, L. and Greb, T.** (2018) Secondary growth as a determinant of plant shape and form. *Seminars in Cell and Developmental Biology*.
- Ragni, L. and Hardtke, C.S.** (2014) Small but thick enough – the Arabidopsis hypocotyl as a model to study secondary growth. *Physiologia Plantarum*, **151**, 164-171.
- Ragni, L., Nieminen, K., Pacheco-Villalobos, D., Sibout, R., Schwechheimer, C. and Hardtke, C.S.** (2011) Mobile gibberellin directly stimulates Arabidopsis hypocotyl xylem expansion. *Plant Cell*, **23**, 1322-1336.
- Robischon, M., Du, J., Miura, E. and Groover, A.** (2011) The Populus Class III HD ZIP, popREVOLUTA, Influences Cambium Initiation and Patterning of Woody Stems. *Plant Physiology*, **155**, 1214-1225.
- Sankar, M., Nieminen, K., Ragni, L., Xenarios, I. and Hardtke, C.S.** (2014) Automated quantitative histology reveals vascular morphodynamics during Arabidopsis hypocotyl secondary growth. *Elife*, **3**, e01567.
- Schulze, W., Reinders, A., Ward, J., Lalonde, S. and Frommer, W.** (2003) Interactions between co-expressed Arabidopsis sucrose transporters in the split-ubiquitin system.
- Sibout, R., Plantegenet, S. and Hardtke, C.S.** (2008a) Flowering as a condition for xylem expansion in Arabidopsis hypocotyl and root. *Current Biology*, **18**, 458-463.
- Sibout, R., Plantegenet, S. and Hardtke, C.S.** (2008b) Flowering as a condition for xylem expansion in Arabidopsis hypocotyl and root. *Curr Biol*, **18**, 458-463.
- Spicer, R. and Groover, A.** (2010) Evolution of development of vascular cambia and secondary growth. *New Phytologist*, **186**, 577-592.
- Stowe-Evans, E.L., Harper, R.M., Motchoulski, A.V. and Liscum, E.** (1998) NPH4, a Conditional Modulator of Auxin-Dependent Differential Growth Responses in Arabidopsis. *Plant Physiology*, **118**, 1265-1275.
- Tabata, R., Ikezaki, M., Fujibe, T., Aida, M., Tian, C.E., Ueno, Y., Yamamoto, K.T., Machida, Y., Nakamura, K. and Ishiguro, S.** (2010) Arabidopsis auxin response factor6 and 8 regulate jasmonic acid biosynthesis and floral organ development via repression of class 1 KNOX genes. *Plant & cell physiology*, **51**, 164-175.
- Talon, M., Zeevaert, J.A. and Gage, D.A.** (1991) Identification of Gibberellins in Spinach and Effects of Light and Darkness on their Levels. *Plant Physiol*, **97**, 1521-1526.
- Torii, K.U., Mitsukawa, N., Oosumi, T., Matsuura, Y., Yokoyama, R., Whittier, R.F. and Komeda, Y.** (1996) The Arabidopsis ERECTA gene encodes a putative receptor protein kinase with extracellular leucine-rich repeats. *Plant Cell*, **8**, 735-746.
- Ursache, R., Andersen, T.G., Marhavy, P. and Geldner, N.** (2018) A protocol for combining fluorescent proteins with histological stains for diverse cell wall components. *Plant J*, **93**, 399-412.
- Weiss, D. and Ori, N.** (2007) Mechanisms of Cross Talk between Gibberellin and Other Hormones. *Plant Physiology*, **144**, 1240-1246.
- Woerlen, N., Allam, G., Popescu, A., Corrigan, L., Pautot, V. and Hepworth, S.R.** (2017) Repression of BLADE-ON-PETIOLE genes by KNOX homeodomain protein BREVIPEDICELLUS is essential for differentiation of secondary xylem in Arabidopsis root. *Planta*, 1-12.
- Wu, M.F., Tian, Q. and Reed, J.W.** (2006) Arabidopsis microRNA167 controls patterns of ARF6 and ARF8 expression, and regulates both female and male reproduction. *Development*, **133**, 4211-4218.
- Yang, J.H. and Wang, H.** (2016) Molecular Mechanisms for Vascular Development and Secondary Cell Wall Formation. *Front Plant Sci*, **7**, 356.
- Zhao, S. and Fernald, R.D.** (2005) Comprehensive algorithm for quantitative real-time polymerase chain reaction. *Journal of computational biology : a journal of computational molecular cell biology*, **12**, 1047-1064.

5.2 Draft manuscript 2:

***ARR1* and *ARR2* positively regulate phloem proliferation during hypocotyl xylem expansion**

Contribution:

All experiments were performed by MBT except:

MB generated the library for sequencing and LR analyzed the sequencing data

The interpretation of the results as well as the writing of the manuscript were done By MBT and LR.

Author	Author position	Scientific ideas %	Data generation %	Analysis & interpretation %	Paper writing %
Mehdi Ben Targem (MBT)	1	50	85	80	80
Martin Bayer (MB)	2		5	5	
Laura Ragni (LR)	3	50	10	15	20
Titel of paper: <i>ARR1</i> and <i>ARR2</i> positively regulate phloem proliferation during hypocotyl xylem expansion					
Status in publication process: Draft					

***ARR1* and *ARR2* positively regulate phloem proliferation during hypocotyl xylem expansion**

Authors: Mehdi Ben-Targem¹, Martin Bayer² and Laura Ragni^{1*}

Affiliations:

¹ZMBP- Center for Plant Molecular Biology, University of Tübingen, Auf der Morgenstelle 32, D-72076 Tübingen, Germany

²Max Planck Institute for Developmental Biology, Max-Planck-Ring 5, 72076 Tübingen

* Corresponding author: laura.ragni@zmbp.uni-tuebingen.de +49 (0)7071 - 29 76677

Summary

Secondary growth occurs throughout the development of seed plants. It results in the increase in girth of plant structures accompanied by the formation of wood: The most important natural source of renewable energy and major sink for excess atmospheric CO₂. Secondary growth in *Arabidopsis thaliana* hypocotyls is marked by two phases: A first phase characterized by the same production rate for xylem versus phloem and a second phase or xylem expansion phase characterized by accelerated xylem expansion. The shift between the two phases is triggered upon flowering by GA, which moves from the shoot to the hypocotyl where it locally induces DELLA degradation. It is surprising that the molecular mechanisms underlying such a developmental process are still poorly investigated.

In this study, we identified DELLA interacting factors controlling xylem expansion by analyzing the transcriptome related to REPRESSOR OF *ga1-3* (RGA) upon flowering. We identified a novel role for *type-B ARABIDOPSIS RESPONSE REGULATORS (ARR1)* and *ARR2* as negative regulators of fiber differentiation. We also identified a positive role in regulating phloem proliferation for *CORONATINE INSENSITIVE 1 COI1* and *TRANSCRIPTION FACTOR MYC2 (MYC2)* as well as *ARR1* and *ARR2*. Our results also indicate a specific role for JA on secondary growth as it only promotes xylem fiber and phloem fiber formation and does not alter the X/A ratio or the total area. Overall, our results suggest a central hormone cross-talk coordinated by DELLA between GA, Cytokinin and Jasmonate in the context of plant secondary growth.

Keywords: Phloem Xylem secondary growth, Cytokinin Jasmonate Gibberellin.

Introduction:

Vascular expansion is achieved via secondary growth, it is an important factor limiting plant growth as water and solute are constantly transported through vascular tissues, it also confers mechanical strength to the plant. In dicotyledons, secondary growth results in the thickening of plant organs and the continuous production of xylem tissue (wood), the principal form of biomass (Demura and Ye, 2010, Spicer and Groover, 2010). Secondary growth is achieved via the vascular cambium, a meristematic tissue that lies between the xylem and phloem. In a thickening stem both radial and periclinal divisions occur within the cambium. Cells produced by periclinal divisions mature into phloem on the outside and xylem (wood) on the inside (Murmanis, 1971, Elo *et al.*, 2009).

Arabidopsis is a valid model to study secondary growth, with several key advantages (Chaffey *et al.*, 2002, Sibout *et al.*, 2008b), in fact the main players affecting secondary growth remain the same between herbaceous and woody plants. For instance, *VASCULAR-RELATED NAC-DOMAIN6 (VND6)* and *VND7* work as transcription switches for metaxylem and protoxylem vessel formation, both in *Arabidopsis* and *Populus* (Kubo *et al.*, 2005), Additionally *WUSCHEL HOMEODOMAIN RELATED 4 (WOX4)* a conserved transcription factor among seed plants acting downstream of the *CLE41/PXY* signaling pathway and controlling the procambium cells formation (Hirakawa *et al.*, 2010, Suer *et al.*, 2011), has most likely a conserved role in vascular meristems maintenance among seed plants (Nardmann and Werr, 2013).

Another key advantage rendering the hypocotyl a suitable model for studying secondary growth, is the possibility to study and observe radial growth separately from elongation, as hypocotyl primary growth stops few days after germination, but most importantly the hypocotyl produces fibers and vessels with the same structural characteristics as an angiosperm tree.

Secondary growth in the hypocotyl is characterized by two major phases: the first phase, before flowering, where phloem and xylem are generated in the same rate resulting in a xylem to total area ratio close to one. The second phase starts upon flowering, it is called the xylem expansion phase, resulting in a much higher xylem to total area ratio (Sibout *et al.*, 2008b). This developmental transition is mediated by Gibberellins. In fact, upon flowering, GA signaling acts locally in the hypocotyl via DELLA protein degradation to trigger xylem expansion (Ragni *et al.*, 2011).

The positive role of GA seems to be conserved across species as it promotes secondary growth both in trees and Arabidopsis, for instance, GA treated trees and mutants overproducing GA, exhibited increased overall secondary growth as well as fiber elongation (Digby and Wareing, 1966, Eriksson *et al.*, 2000b). In poplar stem, GA promotes wood formation through increasing auxin polar transport and enhancing fiber elongation in the developing xylem (Björklund *et al.*, 2007, Mauriat and Moritz, 2009). Whereas in Arabidopsis, GA predominantly promote secondary growth through DELLA degradation, there are five members in Arabidopsis: *REPRESSOR OF gal-3 (RGA)*, *GA-INSENSITIVE (GAI)*, *RGA-LIKE1 (RGL1)*, *RGL2*, and *RGL3*, in fact in *della* quadruple mutant, xylem expansion was significantly increased as compared with the wild type Ler at flowering, consistently ectopic expression of dominant DELLA dramatically suppressed xylem expansion (Ragni *et al.*, 2011). Nevertheless, the mechanism through which DELLA regulate secondary growth and its interacting partners is yet to be identified.

Cytokinins (CK) also largely contribute to the control of secondary growth; promoting it through regulating cambial activity, in fact, secondary growth is severely reduced in Arabidopsis CK deficient mutants as illustrated by the lack of cambium accompanied by a drastic reduction in radial growth in *ipt1;3;5;7* biosynthesis mutant (Matsumoto-Kitano *et al.*, 2008). Accordingly, enhancing CK biosynthesis in poplar resulted in the increase of the number of cambial cells and the total biomass (Immanen *et al.*, 2016). Additionally, two transcription factors promoting secondary growth and increasing cambium cell number: the Arabidopsis regulatory gene *AINTEGUMENTATA (ANT)* and the cell cycle regulator *CYCLIN D3 (CYCD3)*, are downregulated in plants overexpressing CK catabolic enzyme genes. Whereas exogenous CK application increase their expression (Randall *et al.*, 2015).

Type B response regulators are transcription factors that act as positive regulators in the two-component cytokinin signaling pathway, they play key roles in Cytokinin signaling and development in Arabidopsis (Argyros *et al.*, 2008). Cytokinin regulates a broad spectrum of downstream responses through the phosphorelay cascade culminating in the transcriptional regulation by type-B ARABIDOPSIS RESPONSE REGULATORS (type-B ARR's). Notably, ARR1 among other type B regulators, has been identified as a central regulator of Cytokinin signaling and development in Arabidopsis. It has been shown that ARR1 and DELLA act as transcriptional co-regulators in Arabidopsis, in a larger perspective, type-B ARRs and DELLAs

are known to jointly promote transcription of a wide array of target genes (Marin-de la Rosa *et al.*, 2015).

Jasmonate, is another positive regulator of cambium proliferation and secondary growth, in fact, *Coronatine-insensitive 1 (COI1)* and *Transcription factor MYC2 (MYC2)*, two positive mediators of JA signaling were identified as promoting secondary growth in the Arabidopsis stem whereas *JASMONATE ZIM-DOMAIN (JAZ10)* and *JAZ7* function as repressors of secondary growth in the stem (Sehr *et al.*, 2010). Furthermore, transcriptome analysis revealed upregulation of jasmonate biosynthesis/signaling genes in the perennial and woody *soc1 ful* double mutant (Melzer *et al.*, 2008, Davin *et al.*, 2016).

Importantly, MYC2-JAZ1 interaction is prevented by DELLA competitive binding to JAZ1, thus enabling MYC2 to regulate its target set of genes (Hou *et al.*, 2010). But most importantly MYC2 is able to directly interact with DELLA Proteins in the context of Sesquiterpene Synthase Gene Expression Regulation (Hong *et al.*, 2012)

DELLA proteins are known to be repressors of secondary growth. But, what are the downstream factors affected by DELLA, and how does GA cross-talk with other hormones to orchestrate secondary growth is still largely unknown. To answer this question we analyzed the transcriptome of *RGA::rgad-GR* line conditionally expressing a dominant version of DELLA that cannot be degraded in the presence of GA. Our results suggest a cross-talk between GA, Cytokinin and Jasmonate in the context of secondary growth regulation. We revealed that *ARR1* and *ARR2* repress fiber differentiation and promote phloem proliferation whereas *COI1* and *MYC2* are only involved in promoting phloem proliferation in Arabidopsis hypocotyl.

Results:

Transcriptome analysis revealed a cross-talking hub tuned by DELLA, controlling secondary growth.

The central role of DELLA in xylem expansion and fiber accumulation has been previously documented; DELLA proteins are regarded as repressors of secondary growth, in fact *della* quadruple mutants where GA signaling is constitutively on, showed enhanced xylem expansion and fiber production in Arabidopsis (Ragni *et al.*, 2011). Consistently, upon Dexamethasone activation of *RGA::rgad-GR* and *GAI::gaid-GR* lines, a severe decrease in hypocotyl xylem

expansion and total absence of fiber was observed, with a larger effect on the *RGA::rgad-GR* line (Ragni *et al.*, 2011).

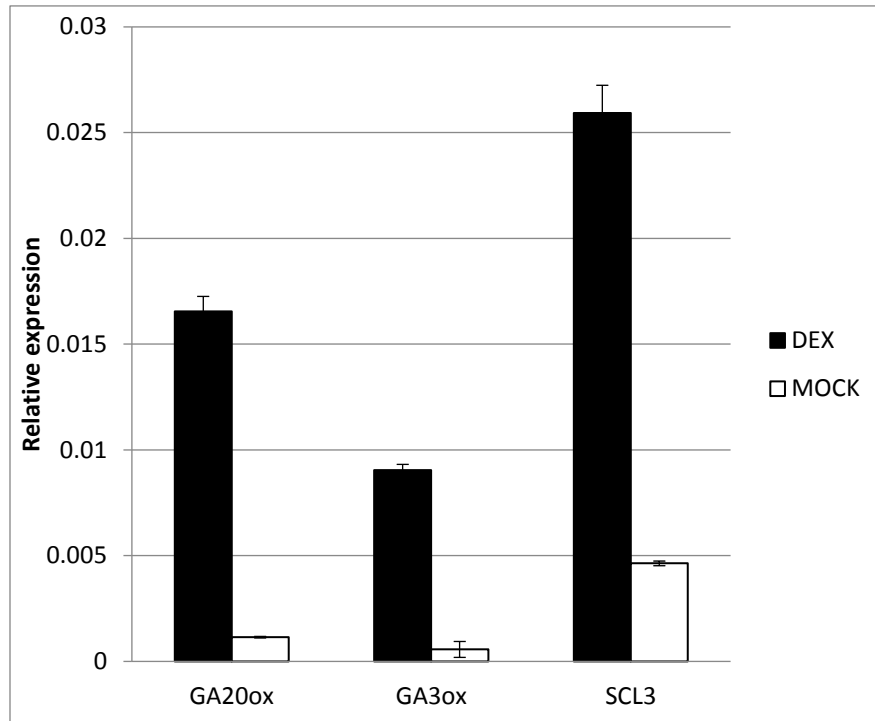
As DELLA is known to work in transcriptional complexes affecting gene expression, we wondered about DELLA downstream targets responsible about such a phenotype, to this end, we used DEX inducible *RGA:rgaD-GR* line (in Ler) to perform RNA sequencing.

We optimized DEX treatment as it can not be classically performed by immersing the plant in 1/2MS liquid due to the age of the plant but only 2/3 of the root were submerged by 1/2 MS liquid. We opted for time points shortly upon flowering as we are interested in factors directly affected by DELLA at the beginning of xylem expansion phase. We found that 3h is sufficient to induce differential expression of the DELLA known target genes *SCL3*, *GA20ox* and *GA3ox*, thus we opted for this time point (Figure 1a).

Stringent statistical analysis of the transcriptome data revealed major differential expression of genes classified in (Figure 1b) with the upregulation of 146 genes comprising CK related genes. Among which, *CYTOKININ RESPONSE FACTOR 1 (CRF1)*, some MYB transcription factors as well as genes involved in GA biosynthesis. Whereas 209 genes were downregulated, among them, Jasmonate related genes such as *JASMONATE ZIM-DOMAIN (JAZ7)* and *JAZ10*, genes belonging to BHLH family and several NAC transcription factors such as *NAC SECONDARY WALL THICKENING PROMOTING FACTOR1 (NST1)*. This is consistent with the phenotype caused by DELLA insensitive mutations as *NST1* acts as a key regulator of secondary wall thickenings in interfascicular fibers and secondary xylem, except for vascular vessels, affecting formation of cells destined to be woody tissues. (Mitsuda *et al.*, 2007), *NST1* downregulation upon 3 hours of Dexamethasone treatment suggest that it might be a direct target of DELLA. We confirmed the RNA sequencing results by qPCR in another independent experiment, the same differential expression was observed for the set of genes we tested (Figure S1a,b)

We assayed knock out mutants at 10 days after flowering of the most prominent genes comparing to Col-0. We didn't observe any secondary growth alteration via inactivation of *METACASPASE 7 (MC7)*, *CRF1*, *ETHYLENE RESPONSE FACTOR (ERF10)*, *JAZ7* and *JAZ10* (Figure S1d). This is probably due to redundancy among members of the gene family each of them belong to.

a)



b)

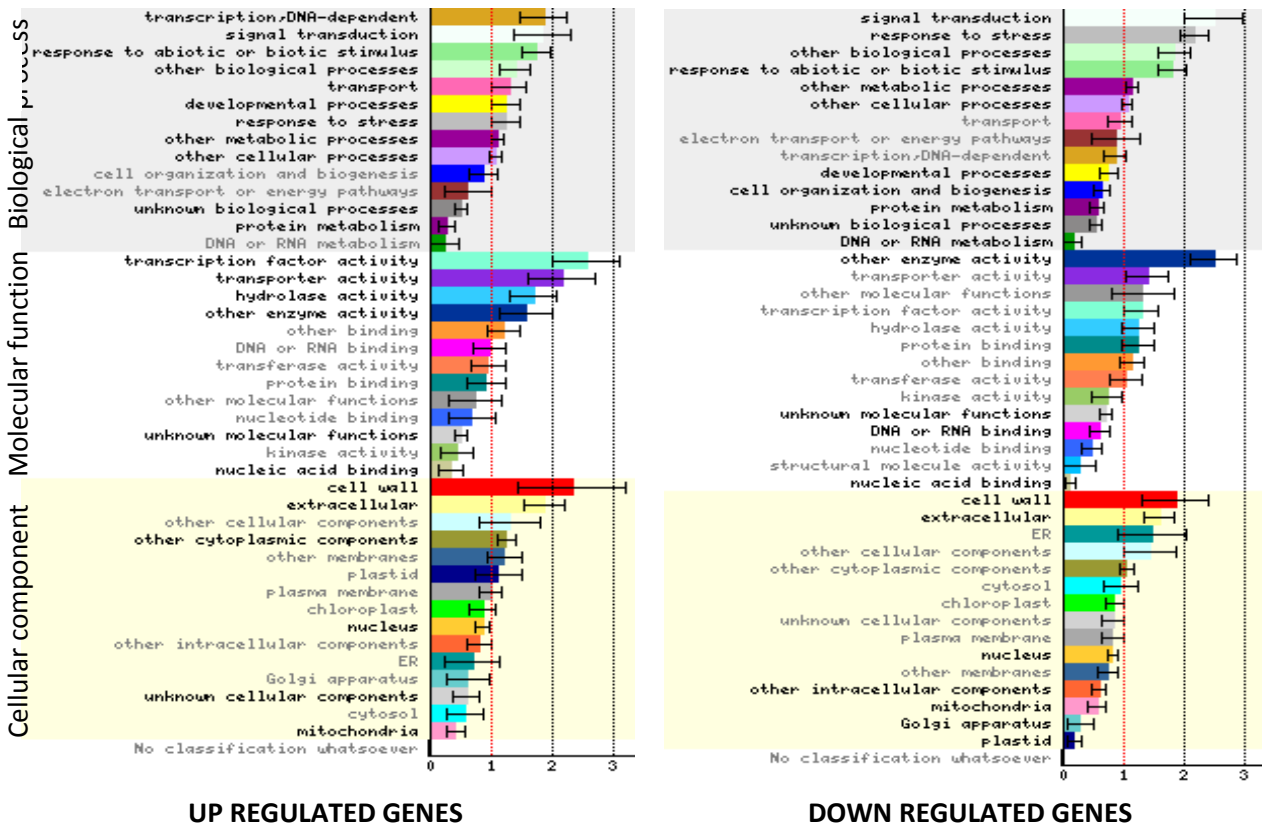


Fig. 1 RGA transcriptome reveals a hormonal cross-talk upon xylem expansion.

(a) Q-PCR showing relative expressions, confirming that *GA20ox*, *GA3ox* and *SCL3* are up-regulated in the hypocotyls of RGA:rgaD-GR transgenic plants upon 3 hours Dexamethasone treatment. (b) Classification of the up-regulated vs down-regulated genes according to Cellular component, molecular function and biological process. The red line represents +/-1 log₂-fold change threshold.

***ARR1* and *ARR2* repress fiber differentiation and promote phloem proliferation in *Arabidopsis* hypocotyl.**

RNA seq revealed altered expression of cytokinin related genes upon Dexamethasone treatment. Notably, CRF's, which are known to affect the development of both the root and the shoot, functioning as positive regulators of root growth and partially acting by the regulation of the RAM size. *CRF1* was remarkably up-regulated upon DEX treatment suggesting its link with DELLA signaling in regulating secondary growth. *crf1* mutants have been reported to function as negative regulator of rosette size, as illustrated by the phenotype of its over-expressor line (Raines et al., 2016). Subsequently, we analyzed *crf1* mutant plants, they showed no difference comparing to Col-0 in terms of secondary growth, this is not surprising since CRFs play redundant roles as positive regulators of root growth (Raines et al., 2016). We then decided to analyze mutants in typeB ARR's since they control the expression of CRFs, as illustrated by the compromise in CRF genes expression in *arr1arr12* mutant indicating that the type-B ARR's control their cytokinin related regulation (Rashotte et al., 2006). We chose to further analyze *ARR1* and *ARR2* as they belong to the sub-family 1 mediating most of Cytokinin responses (Hill et al., 2013), but most of all because they have been reported to jointly promote the transcription of a wide range of target genes together with DELLA proteins, hence mediating the cross-talk between the two major hormones.

As a result, *ARR1* doesn't seem to alter the xylem occupancy (X/A ratio), instead it has a positive effect on the overall hypocotyl total area as provided by our data on *arr1* mutant, *ARR2* has a mild positive effect on xylem occupancy as shown by *arr2* mutant (Figure 2a,c). The increase in X/A ratio in *arr1 arr2* seem to be due to attenuated phloem proliferation in the double mutant rather than enhanced xylem production (Figure S2a,b), *ARR1* and *ARR2* seem to act redundantly as negative regulators of fiber differentiation and positive regulators of phloem proliferation. This is supported by the phenotype of the double mutant *arr1 arr2* as it showed significantly higher X/A and F/X ratio comparing to Col-0 (Figure 2b,d).

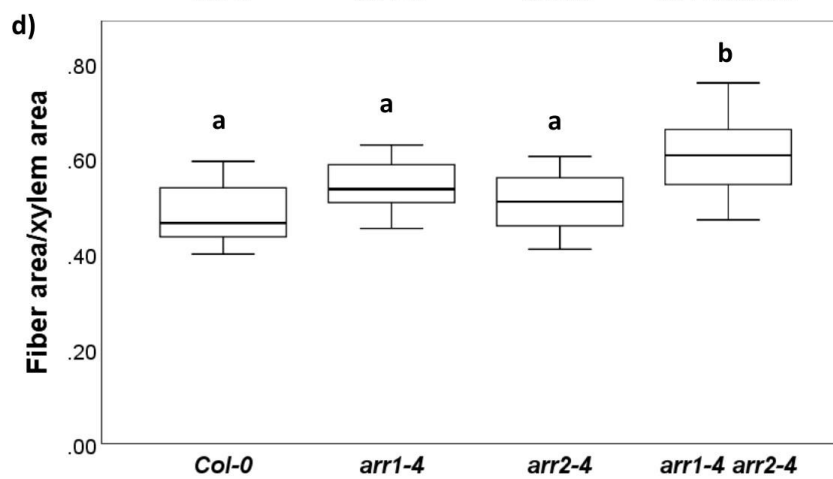
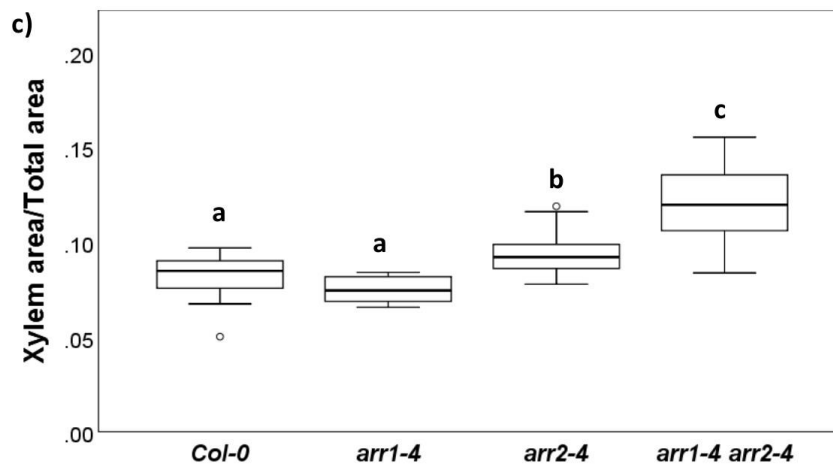
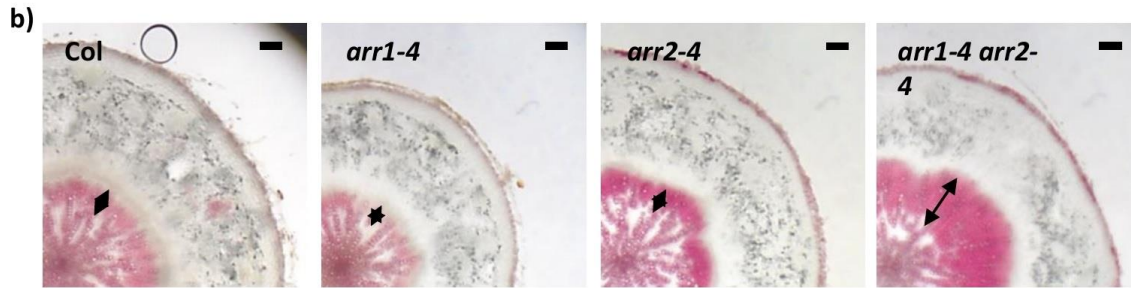
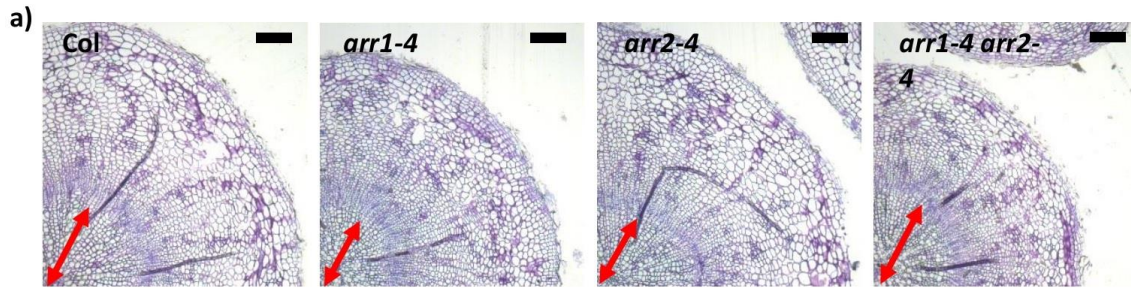


Fig. 2 ARR1 and ARR2 promote phloem proliferation and repress fiber differentiation.

(a) Plastic hypocotyl cross-sections stained with 0.1 % toluidine blue of 10 day-after-flowering (daf), showing reduced phloem proliferation in *arr1*, *arr2* and *arr1 arr2* double mutant. (b) Phloroglucinol stained vibratome sections of 20 daf hypocotyl, showing enhanced fiber formation in *arr1 arr2* double mutant (c) Quantification of the Xylem Area /Total area ratio in the experiment illustrated by representative pictures in (a). (d) Quantification of Fiber Area/Xylem Area ratio in the experiment illustrated by representative pictures in (b). (c-d) Box plots: the dark line in the middle of the boxes is the median, the T-bars that extend from the boxes (whiskers) include 95% of the data. Letters in the boxplots indicate statistical groups, one-way ANOVA (post hoc Tamhane was used determine the groups in (c) sample size n =13-20, post hoc Bonferroni for (d) n=11-19). Black bars= 100 μ m. Double head black arrows=Fiber.

***COII* and *MYC2* positively regulate phloem proliferation in the Arabidopsis hypocotyl.**

The role of jasmonate in regulating secondary growth has been described previously in Arabidopsis (Sehr et al., 2010). In fact, JA application has a positive effect on cambium activity and JA signaling contributes to stem cambium regulation. In more details, *JAZ10*, *MYC2*, *COII*, and less effectively *JAZ7*, have been identified as cambium regulators in Arabidopsis stem: analysis of IC interfascicular cambium dynamics revealed that acropetal progression is enhanced in *jaz10-1*, *jaz10-2* and *jaz7-1* whereas *coil-1* and *myc2-3* mutants showed the opposite phenotype (Sehr et al., 2010). Our sequencing results revealed several jasmonate related genes, the most prominent among them are *JAZ7* and *JAZ10*, both of them were downregulated upon dexamethasone treatment. By analyzing *JAZ7* and *JAZ10* single mutants no secondary growth phenotype was observed comparing to the wild type Col-0 in the hypocotyl, unlike their previously described role in the stem, this can be explained by the spatial specificity of these JAZ factors (Chini et al., 2007, Browse, 2009). Thus, we decided to check the *coil-1* and *myc2-3* mutants where JA signaling is impaired (no JA response genes are activated). We observed a reduction in the total area of *coil-1* and *myc2-3* at 10 daf, resulting in a higher xylem occupancy (X/A ratio), but less overall secondary growth (Figure 3a,b,d). The reduction in xylem occupancy is rather attributed to attenuated phloem proliferation as the xylem area was unchanged in *coil*, *myc2* mutants comparing to the WT (Figure 3b,c,d). Our observations in the hypocotyl are consistent with the positive role attributed to *COII* and *MYC2* regulating secondary growth in the stem (Sehr et al., 2010). As a conclusion, *COII* and *MYC2* positively regulate overall secondary growth in the hypocotyl.

To further understand JA mediated secondary growth, we opted for JA treatment for 20 days upon flowering, our preliminary results showed that the total area and the xylem expansion were not altered whereas significant amounts of fiber was accumulated in the xylem of treated plants comparing to mock (Figure S3a,b,c). Additionally, all treated plants (including Col-0, *arf6*

arf8 and *rga gai*) showed ectopic phloem fiber formation (Figure S3a). (For details about *arf6 arf8* see previous chapter).

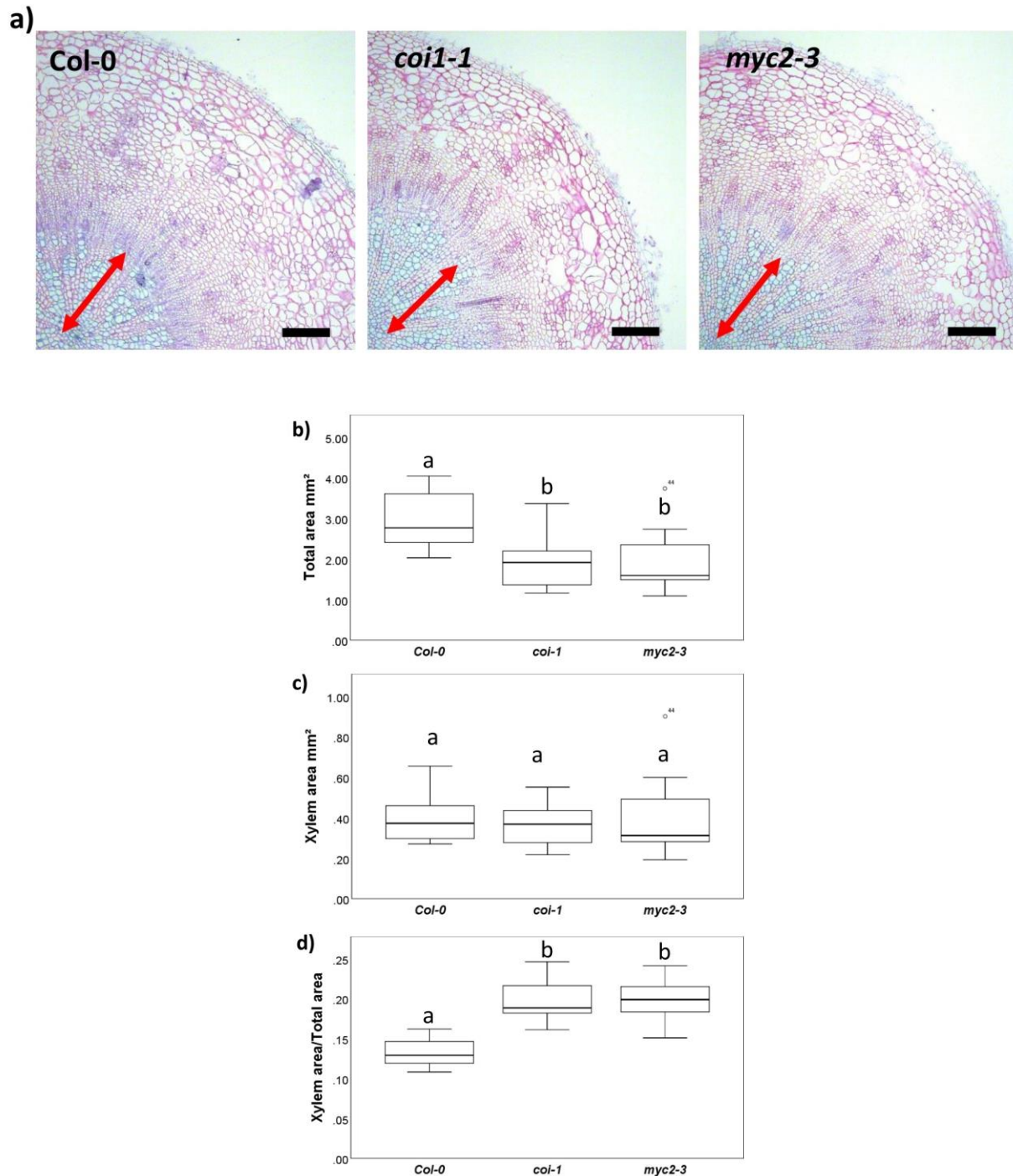


Fig. 3 COI1 and MYC2 promote phloem proliferation.

(a) Plastic hypocotyl cross-sections stained with 0.1 % toluidine blue of 10 day-after-flowering (daf), showing reduced phloem proliferation in *coi1-1*, *myc2-3*. (b) Quantification of the Xylem

Total area in the experiment illustrated by representative pictures in (a). (c) Quantification of the Xylem area in the experiment illustrated by representative pictures in (a). (d) Quantification of the Xylem Area /Total area ratio in the experiment illustrated by representative pictures in (a). (b-c-d) Box plots: the dark line in the middle of the boxes is the median, the T-bars that extend from the boxes (whiskers) include 95% of the data. Letters in the boxplots indicate statistical groups, one-way ANOVA (post hoc Bonferroni was used to determine the groups in (b,c and d) sample size n =15-20). Black bars= 100µm.

Discussion:

GA regulates various aspects of plant growth and development, it mediates its response through the degradation of DELLAs. The DELLA proteins can interact with many TFs belonging to a wide array of families, they function mainly in protein complexes repressing or activating downstream responses (Locascio *et al.*, 2013), thus playing the role of central signaling hubs connecting different signaling cascades (Claeys *et al.*, 2014, Marin-de la Rosa *et al.*, 2014). In addition, other hormones such as auxins, cytokinins and ethylene can modulate the GA pathway (Jasinski *et al.*, 2005, Frigerio *et al.*, 2006, Achard *et al.*, 2007, Claeys *et al.*, 2014, Marin-de la Rosa *et al.*, 2014).

GA also controls secondary growth in trees and Arabidopsis, in fact, recent findings revealed a central role of DELLA proteins in controlling xylem expansion and fiber differentiation in Arabidopsis hypocotyl. GA moves from the shoot apex to the hypocotyl where it triggers DELLA degradation upon flowering which leads to the shift from the first phase to the second phase of secondary growth also called xylem expansion phase. The latter phase is characterized by higher production of xylem comparing to phloem leading to the increase of xylem occupancy and fiber differentiation in the hypocotyl (Ragni *et al.*, 2011). DELLA proteins have highly redundant functions (Cao *et al.*, 2005), but RGA seems to have a greater impact on secondary growth comparing to GAI. In fact, impairing GA signaling in transgenic plants carrying a functional truncated version of DELLA (insensitive to GA mediated degradation) resulted in a dramatic decrease in hypocotyl xylem expansion and total lack of fiber, with a larger effect for the RGA comparing to GAI lines (Ragni *et al.*, 2011).

In this study we revealed transcriptome changes related to DELLA at the beginning of the xylem expansion phase. For this purpose we used the line conditionally expressing the dominant RGA form. Analysis of the transcriptome data revealed up-regulation of Cytokinin signaling related genes coupled by the down-regulation of Jasmonate signaling genes. These data suggest a

complex cross-talk between GA, Cytokinin and Jasmonate, in controlling early stages of the xylem expansion phase.

Among the Cytokinin signaling related genes *CRF1* was remarkably up regulated. *CRF1* functions as negative regulator of rosette size and belongs to *CRF* gene family known to affect meristem size (Raines et al., 2016). By analyzing *crf1* mutant plants, no difference in secondary growth was observed comparing to the WT, this can be explained by redundancy among CRFs (Raines et al., 2016). This prompted us to study their up-stream regulators, the type-B ARR1s which control cytokinin related regulation of the *CRF* gene family (Rashotte et al., 2006). We chose to further investigate *ARR1* and *ARR2* as they belong to the sub-family 1 of type B-ARRs mediating most of Cytokinin responses (Hill et al., 2013), but mostly because *ARR1* is known to mediate the presence of DELLA at target promoters and jointly promote the transcription of a wide range of target genes together with DELLA proteins (Marin-de la Rosa et al., 2015). Our results, indicate that *ARR1* has a positive effect on the overall hypocotyl total area whereas *ARR2* has a mild negative effect on xylem occupancy due to attenuated phloem proliferation. *ARR1* and *ARR2* seem to act redundantly as positive regulators of phloem proliferation and negatively regulate fiber differentiation.

We also revealed another crosstalk between GA and JA, several jasmonate related signaling genes were downregulated among which *JAZ7* and *JAZ10*. These two genes have been previously assigned negative roles in controlling secondary growth in the Arabidopsis stem (Sehr et al., 2010). We wondered about their role in regulating secondary growth in the hypocotyl. Our results indicated that *jaz7-1* and *jaz10-1* are indistinguishable from the WT at 10 daf. The fact that *JAZ7* and *JAZ10* do not affect secondary growth the way it does in stem can be explained by the spatial specificity of JAZ factors (Chini et al., 2007, Browse, 2009). We then decided to investigate mutants impaired in JA signaling perception. Our results pointed out a positive role in controlling overall hypocotyl secondary growth for both *CO11* and *MYC2* precisely in phloem proliferation, consistently with the positive role attributed to them in controlling secondary growth in Arabidopsis stem (Sehr et al., 2010).

We then investigated the effect of constitutive JA response by applying JA for 20 days upon flowering. Our results suggest a specific role for Jasmonate on secondary growth, since it only promotes xylem fiber and phloem fiber formation and does not alter the X/A ratio or the total area

in Col-0, *rga gai* and *arf6 arf8* (mentioned earlier in draft manuscript 1). The specific role of JA in phloem fiber formation is probably mediated through JAZ protein degradation. However which *JAZ(s)* are responsible for the fiber phenotype in the hypocotyl remains unraveled. DELLA can sequester JAZ1 enabling MYC2 to regulate its target set of genes (Hou et al., 2010). Conversely, DELLA can also sequester MYC2 allowing regulation of gene expression in the context of Sesquiterpene Synthase (Hong *et al.*, 2012). Our results are in the favor of a scenario in which DELLA interact with JAZ protein before flowering resulting in xylem expansion and fiber formation repression, as JA application enhances fiber formation probably through JAZ protein degradation. However, what are the JAZ(s) interactors? Whether DELLA interacts with MYC2 to activate phloem proliferation before flowering in the hypocotyl is yet to be determined.

To conclude, we propose a model (Figure 4) that could partially explain the shift to xylem expansion phase during secondary growth in Arabidopsis hypocotyl. Before flowering, *ARR1*, *ARR2* and probably other phloem proliferation activators and fiber formation repressors interact with DELLA proteins resulting in phloem proliferation and repression of fiber formation since DELLA proteins accumulate in the hypocotyl due to low concentration of bio-active GA before flowering. Whereas after flowering, it is possible that *ARR1*, *ARR2* and DELLA are no longer interacting to maintain phloem proliferation in the hypocotyl. This can be due to higher bio-active GA concentrations leading to DELLA degradation (Talon *et al.*, 1991), particularly in the Arabidopsis hypocotyl where GA can move through the plant from the shoot apex to the hypocotyl triggering the shift to the xylem expansion phase (Ragni *et al.*, 2011).

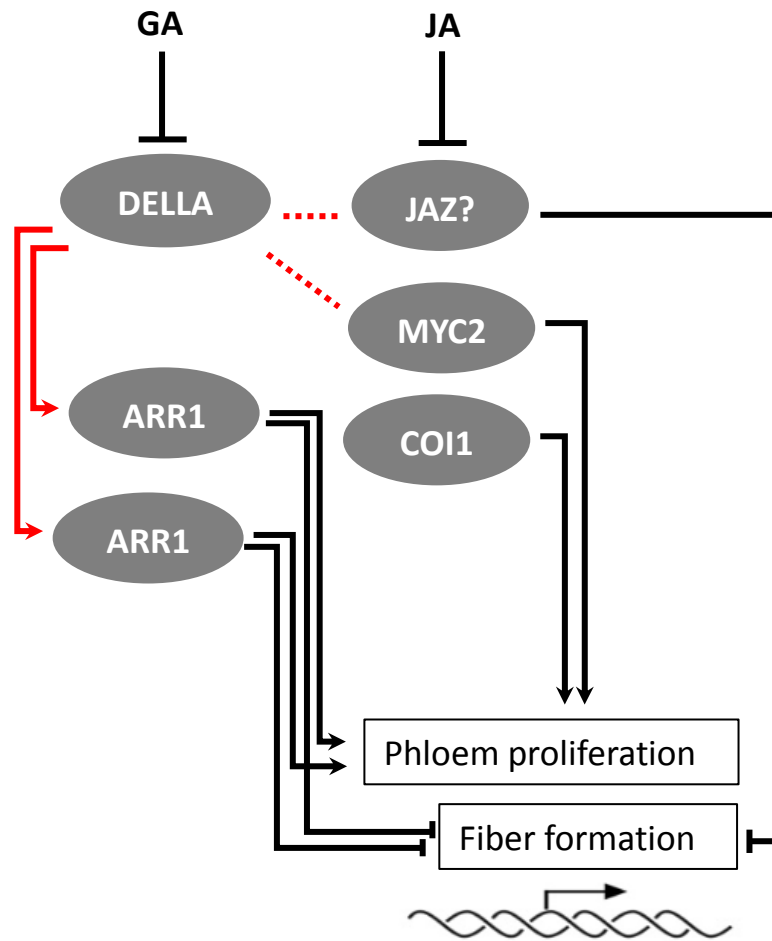


Fig.4 Proposed model on GA mediated secondary growth control and crosstalk with Cytokinin and Jasmonate. Hypothesized links are illustrated with dashed lines. Red arrows represent protein-protein interactions. The lines and arrows illustrate interactions. Compare text for details.

Experimental procedure:

Plant material and growth

The majority of the lines used are in Col-0 background unless otherwise specified in the text/figure. Plants used for RNAseq experiment were grown in vitro in continuous light until sampling. For all the other experiments, plants were grown in soil in long day conditions (16 hours light versus 8 hours dark) and the sampling time is stated in the text/figure. *arr1-4*, *arr2-4* and the double mutant *arr1-4 arr2-4* were kindly provided by Klaus Harter (ZMBP), *RGA:rgaD-GR* was previously described in (Ragni et al., 2011), *coil-1* was described in (Xie et al., 1998). *myc2-3* (salk_061267), *jaz10-1* (sail_92_D08), *jaz7-1* (WixcDsLox7M11) and the following lines were ordered from NASC: *crf1* (N686553), *mc7* (N506679), *erf10* (N799828). Primers for genotyping are listed in table S1.

Dexamethasone and JA Treatment

Induction of in-vitro grown *RGA:rga^D-GR* plants was achieved by submerging square plates vertically in liquid 10 μ M dexamethasone (dex) $\frac{1}{2}$ Murashige and Skoog solution with $\frac{2}{3}$ of the root covered with $\frac{1}{2}$ MS solution, for 3 hours upon flowering. For JA on soil treatments, plants were watered from flowering on, with a 100 μ M JA or mock solution at similar frequency three times per week until hypocotyl sampling according to the experiment.

qPCR and RNA seq.

RNA extraction was performed using the Universal RNA Purification Kit (Roboklon) according to the manufacturer protocol. C-DNA was synthesized using AMV Reverse Transcriptases (Roboklon) according to manufacturer protocol. qPCR was performed using MESA blue (Eurogentec) in a CFX96 Real-TimeSystem machine (BIO-RAD). Primers used for qPCR are listed in table S2. The relative expression was calculated using qPCR miner (<http://ewindup.info/miner/>) (Zhao and Fernald, 2005) normalizing the sample against the expression of EF1. qPCR experiment were repeated at least 2 times. RNA was extracted from 120 hypocotyls at flowering from plants grown in-vitro for each treatment (Mock/DEX). 3 biological replicates were used for RNA-seq, quality was checked at the Bioanalyzer. Libraries were prepared using the TruSeq RNA Library Prep Kit (Illumina) according to manufacturer protocol. Sequencing was performed pair ended using an Illumina HiSeq3000. Reads were aligned against the Arabidopsis genome (version

TAIR10) using Tophat v2 (<http://ccb.jhu.edu/software/tophat>). Read counting was done using the R package: Rsubread (Liao *et al.*, 2013) and differentially expressed gene were calculated using R package: DESeq2 (Love *et al.*, 2014). Gene ontology was performed using GOrilla (<http://cbl-gorilla.cs.technion.ac.il/>).

Histology and stainings

Vibratome sections (50–80 μm) were obtained via a Leica VT-1000 vibratome, from hypocotyls embedded in 6% agarose block, slices were collected in water in microscope slides, stained and/or imaged. For Phloroglucinol staining, a ready solution (VWR, 26337.180) was applied directly to the section. Images were taken with a Zeiss Axio M2 imager microscope. Plastic hypocotyl cross-sections (5 μm) were obtained as described in (Barbier de Reuille & Ragni, 2017) and stained with 0.1 % toluidine blue.

Images acquisition

A Zeiss Axio M2 imager microscope or a Zeiss Axiophot microscope was used to take images at different magnifications of vibratome sections (50–80 μm) as well as 5 μm sections obtained from plastic embedded hypocotyls as previously described by (de Reuille and Ragni, 2017) and stained with 0.1% toluidine blue solution.

Image analyses and statistical analyses

The total hypocotyl cross section area, the xylem area and the fiber area were analyzed using ImageJ software as previously described (Sibout *et al.*, 2008b). Statistical analyses were performed using IBM SPSS Statistics version 24-25 (IBM). We first tested all datasets for homogeneity of variances using Levene's Test of Equality of Variances. For multiple comparison, we calculated the significant differences between each dataset using One way ANOVA with Tamhane's post hoc (equal variance not assumed) or a Bonferroni correction (equal variance assumed). For comparing two groups we used Welch's t-test (not homogenous variance) or a Student's t-test (homogeneous variance). The significance threshold was set to p-value < 0.05.

Supporting Information

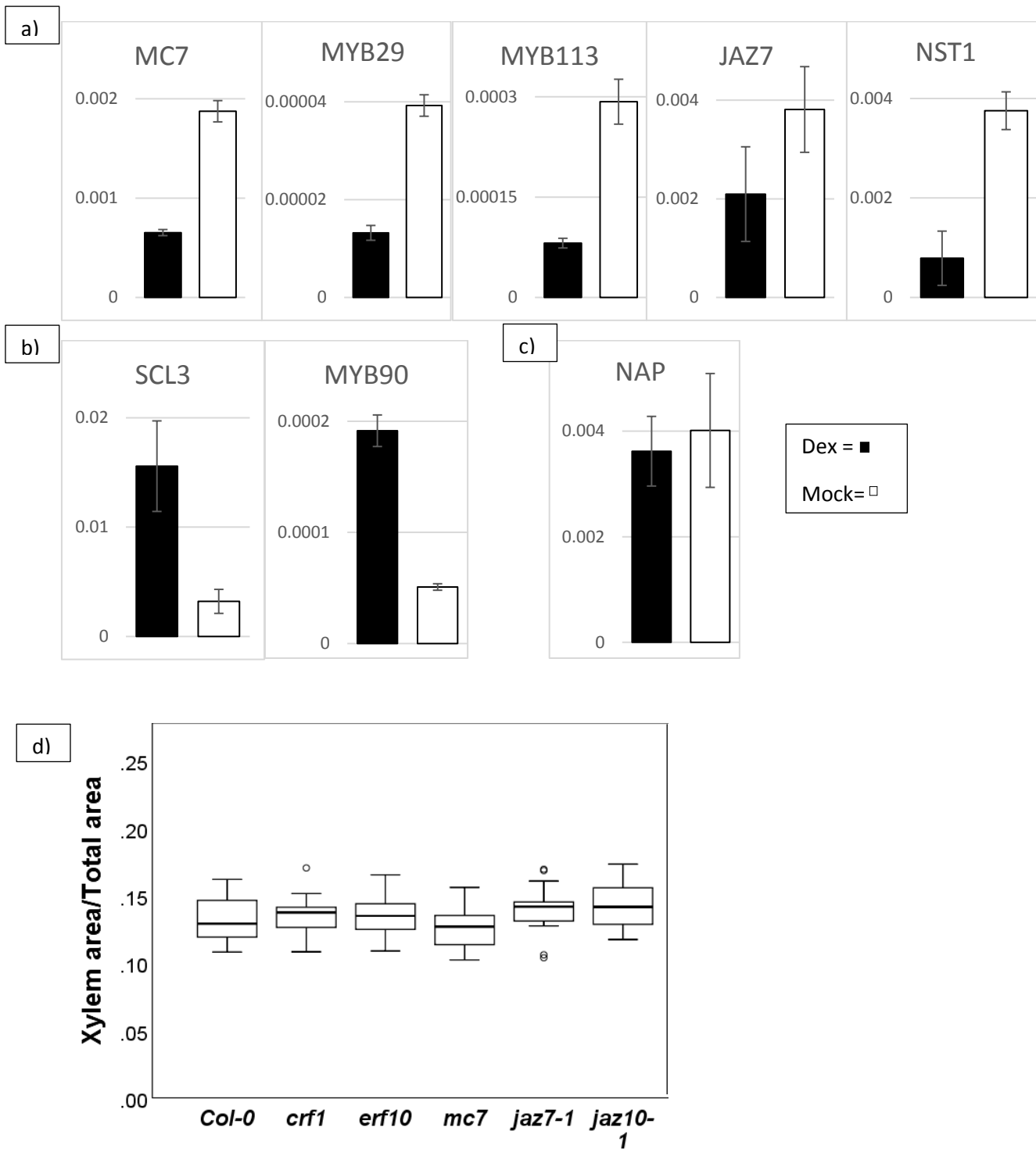


Fig. S1 qPCR confirmation of genes differentially expressed in RNAseq and phenotypic characterization.

(a,b,c) Q-PCR showing relative expressions, confirming that MC7 (AT1G79310), MYB29 (AT5G07690), MYB113 (AT1G66370), JAZ7 (AT2G34600) and NST1 (AT2G46770) are downregulated (a) whereas SCL3 (AT1G50420) and MYB90 (AT1G66390) are upregulated (b) in the hypocotyls of RGA:rgaD-GR transgenic plants upon 3 hours Dexamethasone treatment, confirming the RNAseq data but not for NAP (AT1G69490) (c) as it remained unchanged. (d) Quantification of the Xylem Total area of 10 day-after-flowering (daf) hypocotyls, showing no significant difference between Col-0, *erf10*, *crf1*, *mc7*, *jaz7-1* and *jaz10-1*. Box plots: the dark line in the middle of the boxes is the median, the T-bars that extend from the boxes (whiskers) include 95% of the data. Letters in the boxplots indicate statistical groups, one-way ANOVA (post hoc Bonferroni was used) sample size n =15-20).

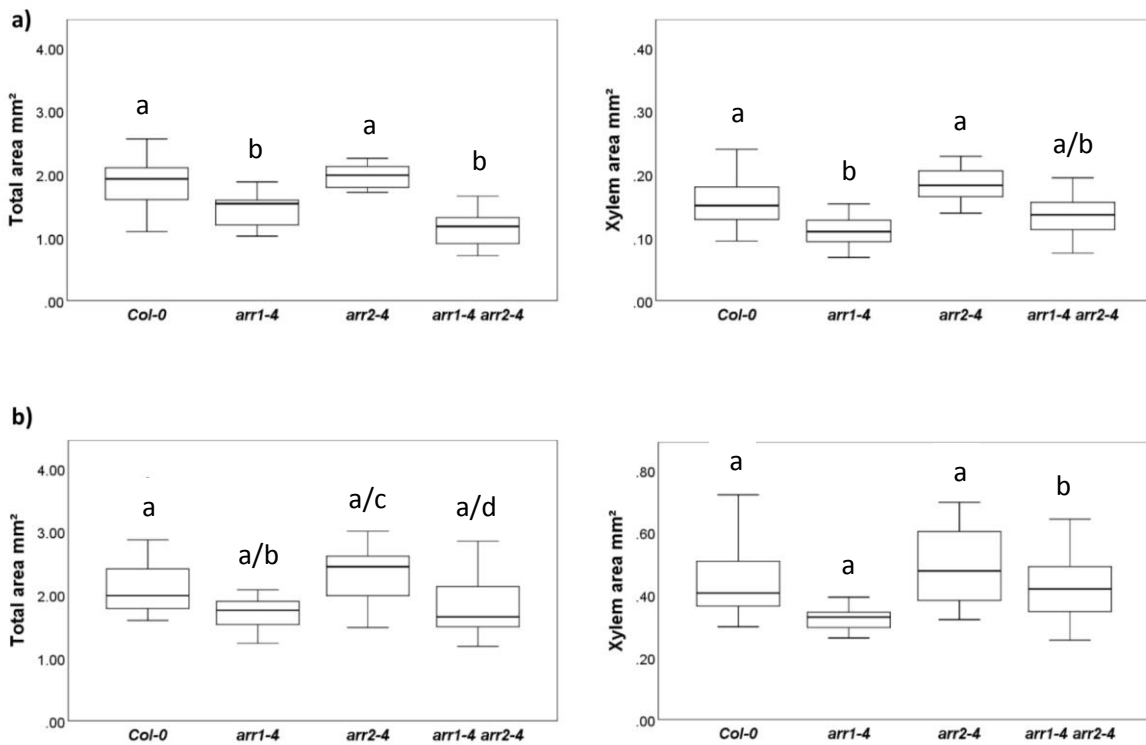


Fig. S2 Quantification of total and xylem area in *arr1*, *arr2* and *arr1 arr2* mutants.

(a,b) Quantification of the Xylem and Total area in the experiment illustrated by representative pictures in (Figure 2a,b). Box plots: the dark line in the middle of the boxes is the median, the T-bars that extend from the boxes (whiskers) include 95% of the data. Letters in the boxplots indicate statistical groups, one-way ANOVA (post hoc Bonferroni was used determine the groups in (a)

sample size n =13-20, post hoc Bonferroni for for the total area and Tamhane for the xylem area were used to determine the groups in (b) n=11-19). Black bars= 100 μ m.

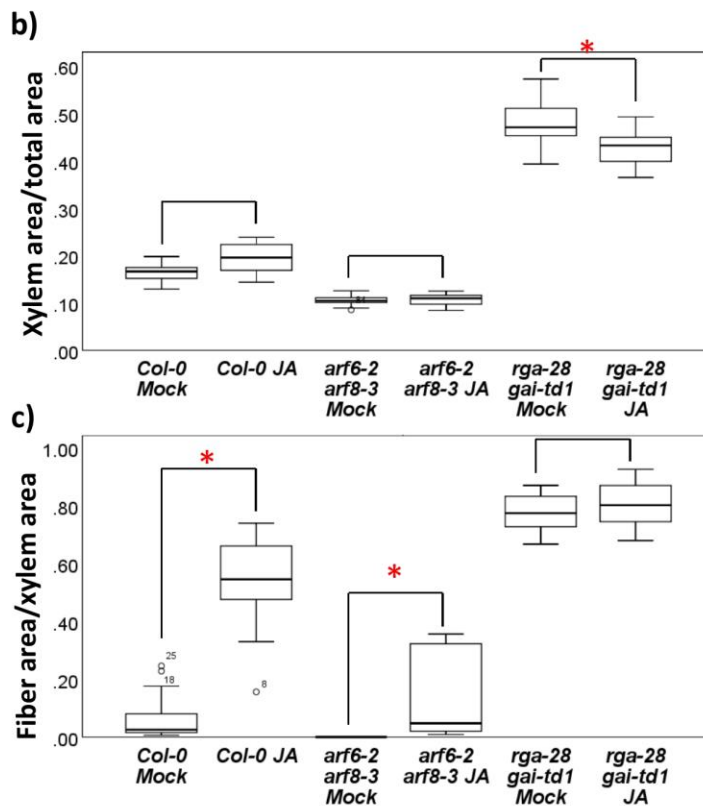
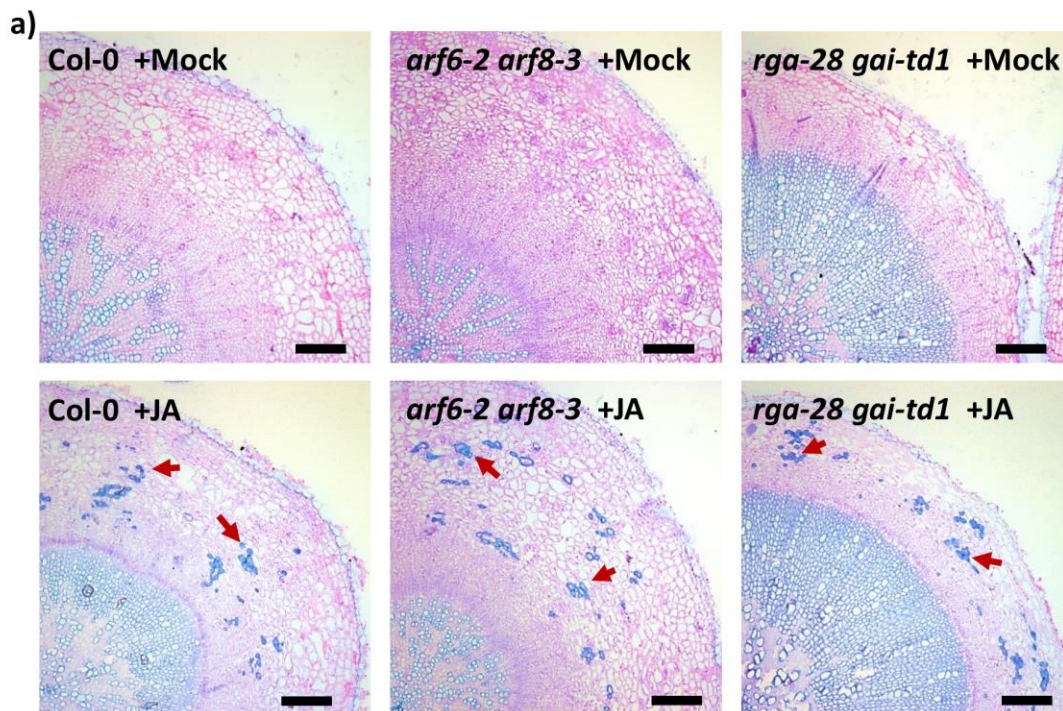


Fig. S3 JA promotes phloem fiber formation without altering X/A ratio.

(a) Plastic hypocotyl cross-sections stained with 0.1 % toluidine blue of *col-0*, *arf6-2 arf8-3* and *rga-28 gai-td1* mutants treated with mock or JA at 20 day-after- flowering (daf), showing ectopic fiber formation in the phloem of JA treated plants (Red arrows). (b) Quantification of the Xylem/Total area in the experiment illustrated by representative pictures in (a). (c) Quantification of the Fiber/Xylem area in the experiment illustrated by representative pictures in (a). (b,c) Box plots: the dark line in the middle of the boxes is the median, the T-bars that extend from the boxes (whiskers) include 95% of the data. Student's or Welch t-test (red asterisk: $P < 0.05$, sample size $n > 10$). Black bars = 100 μ m. (Preliminary data = Experiment done only ones)

Table S1 Primers used for genotyping.

arr1 F geno	GAAGAACAAACATGGATTCGATATAGTA
arr1 R geno	CCGTCATAAACGAGTTGTTAAGATTG
ARR2-4 geno RP	TTGCTGATGTTCTTGTTGTGC
ARR2-4 geno LP	TCTGTTGAATTGCATCAGCAG
jaz10-1 LP	CTTCTCGAGAAAACGTTGCAG
jaz10-1 RP	TCACATGAGAAATCAGAATCCG
Jaz7-1 LP	GGTACACCGCGGATTAATAATC
Jaz7-1 RP	ACCCATTTTAGGAGACCGTTG
myc2-3 LP	CTCGAGCTGGTTCTTGATTG
myc2-3 RP	TGGTTTTCTTGTTTTGATG
ERF10 LPgeno	CGCAATAACTTCAGGCAGATC
ERF10 RPgeno	GGTATACATTTTATTGGCGCG
MC7 LPgeno	GGTAAAGTGAACCTGCTGTCCG
MC7 RPgeno	AATTGGATTCAAGTCGGAAGG

Table S2 Primers used for qPCR.

EF1a.F	TGGTGACGCTGGTATGGTTA
EF1a.R	TCCTTCTTGCCACGCTCTT
AtGA3ox1 F2 qPCR	AAGGTTTCACCATCACTGGC
AtGA3ox1 R2 q PCR	CGGGTAGTGATTTAGCTGGAG
GA20ox2F qPCR	TCCAACGATAATAGTGGCT
GA20ox2R qPCR	TTGGCATGGAGGATAATGA
SCL3-5RQ	ATTATGCGATGTTGCAGG
SCL3-3RQ	ATTACACCCACACCAGAC
MYB29 F qPCR	AGAAAGGAGCATGGACTGCC
MYB29 R qPCR	GCGAGAAGCGTGTAGCATGA
MYB90 qPCR F	AGCCATCTCAATGGTCTGCC
MYB90 qPCR R	GTCGCTTCAGGAACAATCGC
MYB113 F qPCR	GGTCTCAATCGGTGCCGAAA
MYB113 R qPCR	TCCGACCAGGCAATCTACCA
NAP F qPCR	AAACCATGCCCTGTCTCCAT
NAP R qPCR	TTGAACCGCTGTGAATGGCT
ERF10 F qPCR	AGGAAGTGAGTGACAAGGGC
ERF10 R qPCR	TTATGGCAGCGGAGTCGTAG
MC7 F qPCR	CGGAAACAGGGGAAGAGGAT
MC7 R qPCR	CTCGATTTGGCTTCGTCGTG
JAZ7 F qPCR	CGACTTGGAACTTCGCCTTC
JAZ7 R qPCR	GCGTTAGCCTCAAGATGGGT
NST3 F qPCR	TGCATGAGTATCGCCTCGAC
NST3 R qPCR	CCCTTCTTCTCCTCCGTGTC
NST1 F qPCR	GCTCCTCACGGCCAAAATC
NST1 R qPCR	CTCCGACGGGACTGTTTAGG

References:

- Achard, P., Baghour, M., Chapple, A., Hedden, P., Van Der Straeten, D., Genschik, P., Moritz, T. and Harberd, N.P.** (2007) The plant stress hormone ethylene controls floral transition via DELLA-dependent regulation of floral meristem-identity genes. *Proceedings of the National Academy of Sciences of the United States of America*, **104**, 6484-6489.
- Argyros, R.D., Mathews, D.E., Chiang, Y.H., Palmer, C.M., Thibault, D.M., Etheridge, N., Argyros, D.A., Mason, M.G., Kieber, J.J. and Schaller, G.E.** (2008) Type B response regulators of Arabidopsis play key roles in cytokinin signaling and plant development. *Plant Cell*, **20**, 2102-2116.
- Björklund, S., Antti, H., Uddestrand, I., Moritz, T. and Sundberg, B.** (2007) Cross-talk between gibberellin and auxin in development of Populus wood: gibberellin stimulates polar auxin transport and has a common transcriptome with auxin. *Plant J*, **52**, 499-511.
- Browse, J.** (2009) Jasmonate passes muster: a receptor and targets for the defense hormone. *Annual review of plant biology*, **60**, 183-205.
- Cao, D., Hussain, A., Cheng, H. and Peng, J.** (2005) Loss of function of four DELLA genes leads to light- and gibberellin-independent seed germination in Arabidopsis. *Planta*, **223**, 105-113.
- Chaffey, N., Cholewa, E., Regan, S. and Sundberg, B.** (2002) Secondary xylem development in Arabidopsis: a model for wood formation. *Physiologia Plantarum*, **114**, 594-600.
- Chini, A., Fonseca, S., Fernandez, G., Adie, B., Chico, J.M., Lorenzo, O., Garcia-Casado, G., Lopez-Vidriero, I., Lozano, F.M., Ponce, M.R., Micol, J.L. and Solano, R.** (2007) The JAZ family of repressors is the missing link in jasmonate signalling. *Nature*, **448**, 666-671.
- Claeys, H., De Bodt, S. and Inze, D.** (2014) Gibberellins and DELLAs: central nodes in growth regulatory networks. *Trends Plant Sci*, **19**, 231-239.
- Davin, N., Edger, P.P., Hefer, C.A., Mizrachi, E., Schuetz, M., Smets, E., Myburg, A.A., Douglas, C.J., Schranz, M.E. and Lens, F.** (2016) Functional network analysis of genes differentially expressed during xylogenesis in social woody Arabidopsis plants. *The Plant journal*, **86**, 376-390.
- de Reuille, P.B. and Ragni, L.** (2017) Vascular Morphodynamics During Secondary Growth. *Methods in molecular biology (Clifton, N.J.)*, **1544**, 103-125.
- Demura, T. and Ye, Z.-H.** (2010) Regulation of plant biomass production. *Current Opinion in Plant Biology*, **13**, 298-303.
- Digby, J. and Wareing, P.F.** (1966) The Effect of Applied Growth Hormones on Cambial Division and the Differentiation of the Cambial Derivatives *Annals of Botany*, **30**, 539-548.
- Elo, A., Immanen, J., Nieminen, K. and Helariutta, Y.** (2009) Stem cell function during plant vascular development. *Semin Cell Dev Biol*, **20**, 1097-1106.
- Eriksson, M.E., Israelsson, M., Olsson, O. and Moritz, T.** (2000) Increased gibberellin biosynthesis in transgenic trees promotes growth, biomass production and xylem fiber length. *Nat Biotech*, **18**, 784-788.
- Frigerio, M., Alabadi, D., Perez-Gomez, J., Garcia-Carcel, L., Phillips, A.L., Hedden, P. and Blazquez, M.A.** (2006) Transcriptional regulation of gibberellin metabolism genes by auxin signaling in Arabidopsis. *Plant Physiol*, **142**, 553-563.
- Hill, K., Mathews, D.E., Kim, H.J., Street, I.H., Wildes, S.L., Chiang, Y.-H., Mason, M.G., Alonso, J.M., Ecker, J.R., Kieber, J.J. and Schaller, G.E.** (2013) Functional Characterization of Type-B Response Regulators in the Arabidopsis Cytokinin Response. *Plant Physiology*, **162**, 212-224.

- Hirakawa, Y., Kondo, Y. and Fukuda, H.** (2010) TDIF Peptide Signaling Regulates Vascular Stem Cell Proliferation via the *WOX4* Homeobox Gene in *Arabidopsis*. *The Plant Cell*, **22**, 2618-2629.
- Hong, G.J., Xue, X.Y., Mao, Y.B., Wang, L.J. and Chen, X.Y.** (2012) *Arabidopsis* MYC2 interacts with DELLA proteins in regulating sesquiterpene synthase gene expression. *Plant Cell*, **24**, 2635-2648.
- Hou, X., Lee, L.Y., Xia, K., Yan, Y. and Yu, H.** (2010) DELLAs modulate jasmonate signaling via competitive binding to JAZs. *Dev Cell*, **19**, 884-894.
- Immanen, J., Nieminen, K., Smolander, O.P., Kojima, M., Alonso Serra, J., Koskinen, P., Zhang, J., Elo, A., Mahonen, A.P., Street, N., Bhalerao, R.P., Paulin, L., Auvinen, P., Sakakibara, H. and Helariutta, Y.** (2016) Cytokinin and Auxin Display Distinct but Interconnected Distribution and Signaling Profiles to Stimulate Cambial Activity. *Curr Biol*, **26**, 1990-1997.
- Jasinski, S., Piazza, P., Craft, J., Hay, A., Woolley, L., Rieu, I., Phillips, A., Hedden, P. and Tsiantis, M.** (2005) KNOX action in *Arabidopsis* is mediated by coordinate regulation of cytokinin and gibberellin activities. *Curr Biol*, **15**, 1560-1565.
- Kubo, M., Udagawa, M., Nishikubo, N., Horiguchi, G., Yamaguchi, M., Ito, J., Mimura, T., Fukuda, H. and Demura, T.** (2005) Transcription switches for protoxylem and metaxylem vessel formation. *Genes & Development*, **19**, 1855-1860.
- Liao, Y., Smyth, G.K. and Shi, W.** (2013) The Subread aligner: fast, accurate and scalable read mapping by seed-and-vote. *Nucleic acids research*, **41**, e108.
- Locascio, A., Blázquez, M.A. and Alabadí, D.** (2013) Genomic Analysis of DELLA Protein Activity. *Plant and Cell Physiology*, **54**, 1229-1237.
- Love, M.I., Huber, W. and Anders, S.** (2014) Moderated estimation of fold change and dispersion for RNA-seq data with DESeq2. *Genome biology*, **15**, 550.
- Marin-de la Rosa, N., Pfeiffer, A., Hill, K., Locascio, A., Bhalerao, R.P., Miskolczi, P., Gronlund, A.L., Wanchoo-Kohli, A., Thomas, S.G., Bennett, M.J., Lohmann, J.U., Blázquez, M.A. and Alabadi, D.** (2015) Genome Wide Binding Site Analysis Reveals Transcriptional Coactivation of Cytokinin-Responsive Genes by DELLA Proteins. *PLoS Genet*, **11**, e1005337.
- Marin-de la Rosa, N., Sotillo, B., Miskolczi, P., Gibbs, D.J., Vicente, J., Carbonero, P., Onate-Sanchez, L., Holdsworth, M.J., Bhalerao, R., Alabadi, D. and Blázquez, M.A.** (2014) Large-scale identification of gibberellin-related transcription factors defines group VII ETHYLENE RESPONSE FACTORS as functional DELLA partners. *Plant Physiol*, **166**, 1022-1032.
- Matsumoto-Kitano, M., Kusumoto, T., Tarkowski, P., Kinoshita-Tsujimura, K., Václavíková, K., Miyawaki, K. and Kakimoto, T.** (2008) Cytokinins are central regulators of cambial activity. *Proceedings of the National Academy of Sciences*, **105**, 20027-20031.
- Mauriat, M. and Moritz, T.** (2009) Analyses of GA20ox- and GID1-over-expressing aspen suggest that gibberellins play two distinct roles in wood formation. *The Plant Journal*, **58**, 989-1003.
- Melzer, S., Lens, F., Gennen, J., Vanneste, S., Rohde, A. and Beeckman, T.** (2008) Flowering-time genes modulate meristem determinacy and growth form in *Arabidopsis thaliana*. *Nature Genetics*, **40**, 1489-1492.
- Mitsuda, N., Iwase, A., Yamamoto, H., Yoshida, M., Seki, M., Shinozaki, K. and Ohme-Takagi, M.** (2007) NAC Transcription Factors, NST1 and NST3, Are Key Regulators of the Formation of Secondary Walls in Woody Tissues of *Arabidopsis*. *The Plant Cell Online*, **19**, 270-280.
- Murmanis, L.** (1971) Structural Changes in the Vascular Cambium of *Pinus strobus* L. during an Annual Cycle. *Annals of Botany*, **35**, 133-141.
- Nardmann, J. and Werr, W.** (2013) Symplesiomorphies in the WUSCHEL clade suggest that the last common ancestor of seed plants contained at least four independent stem cell niches. *New Phytologist*, n/a-n/a.
- Ragni, L., Nieminen, K., Pacheco-Villalobos, D., Sibout, R., Schwechheimer, C. and Hardtke, C.S.** (2011) Mobile gibberellin directly stimulates *Arabidopsis* hypocotyl xylem expansion. *Plant Cell*, **23**, 1322-1336.

- Raines, T., Shanks, C., Cheng, C.Y., McPherson, D., Argueso, C.T., Kim, H.J., Franco-Zorrilla, J.M., Lopez-Vidriero, I., Solano, R., Vankova, R., Schaller, G.E. and Kieber, J.J.** (2016) The cytokinin response factors modulate root and shoot growth and promote leaf senescence in *Arabidopsis*. *Plant J*, **85**, 134-147.
- Randall, R.S., Miyashima, S., Blomster, T., Zhang, J., Elo, A., Karlberg, A., Immanen, J., Nieminen, K., Lee, J.Y., Kakimoto, T., Blajicka, K., Melnyk, C.W., Alcasabas, A., Forzani, C., Matsumoto-Kitano, M., Mahonen, A.P., Bhalerao, R., Dewitte, W., Helariutta, Y. and Murray, J.A.** (2015) AINTEGUMENTA and the D-type cyclin CYCD3;1 regulate root secondary growth and respond to cytokinins. *Biology open*, **4**, 1229-1236.
- Rashotte, A.M., Mason, M.G., Hutchison, C.E., Ferreira, F.J., Schaller, G.E. and Kieber, J.J.** (2006) A subset of *Arabidopsis* AP2 transcription factors mediates cytokinin responses in concert with a two-component pathway. *Proceedings of the National Academy of Sciences of the United States of America*, **103**, 11081-11085.
- Sehr, E.M., Agusti, J., Lehner, R., Farmer, E.E., Schwarz, M. and Greb, T.** (2010) Analysis of secondary growth in the *Arabidopsis* shoot reveals a positive role of jasmonate signalling in cambium formation. *The Plant Journal*, **63**, 811-822.
- Sibout, R., Plantegenet, S. and Hardtke, C.S.** (2008) Flowering as a condition for xylem expansion in *Arabidopsis* hypocotyl and root. *Curr Biol*, **18**, 458-463.
- Spicer, R. and Groover, A.** (2010) Evolution of development of vascular cambia and secondary growth. *New Phytologist*, **186**, 577-592.
- Suer, S., Agusti, J., Sanchez, P., Schwarz, M. and Greb, T.** (2011) WOX4 Imparts Auxin Responsiveness to Cambium Cells in *Arabidopsis*. *The Plant Cell Online*, **23**, 3247-3259.
- Talon, M., Zeevaart, J.A. and Gage, D.A.** (1991) Identification of Gibberellins in Spinach and Effects of Light and Darkness on their Levels. *Plant Physiol*, **97**, 1521-1526.
- Xie, D.X., Feys, B.F., James, S., Nieto-Rostro, M. and Turner, J.G.** (1998) COI1: an *Arabidopsis* gene required for jasmonate-regulated defense and fertility. *Science*, **280**, 1091-1094.
- Zhao, S. and Fernald, R.D.** (2005) Comprehensive algorithm for quantitative real-time polymerase chain reaction. *Journal of computational biology : a journal of computational molecular cell biology*, **12**, 1047-1064.

6 Discussion

Bioactive gibberellins (GAs) control a wide range of processes during plant development, including seed germination, leaf expansion, stem and root elongation, flowering time, flower and fruit development (Fleet and Sun, 2005). GA signaling is mainly perceived through DELLA induced degradation. DELLAs regulate gene expression through various mechanisms, among which: Sequestration of DNA-binding transcription factors that induce or repress the target genes, interaction with negative regulators thereby relieving the repression of certain genes, DELLA can also be present in transcriptional complexes. Additionally, other interactors can modulate the ability of DELLAs to interact with DNA-binding transcription factors (Locascio *et al.*, 2013). DELLAs can also function as transcriptional coactivator by jointly promoting transcription of target genes (Marin-de la Rosa *et al.*, 2015). Most recently, it has been suggested that DELLAs may act as co-repressors to suppress gene transcription by interacting with a negative transcription factor (Li *et al.*, 2016). As detailed above, DELLA proteins can interact with many TFs belonging to diverse families, regulating various transcriptional networks suggesting their role as central signaling hubs connecting different signaling cascades. (Claeys *et al.*, 2014, Marin-de la Rosa *et al.*, 2014). In addition, other hormones such as auxins, cytokinins or ethylene can modulate the GA signaling pathway (Jasinski *et al.*, 2005, Frigerio *et al.*, 2006, Achard *et al.*, 2007), placing it as major regulator in plant growth and development (Claeys *et al.*, 2014).

GA positively regulate secondary growth by promoting wood formation and cambial activity in trees (Digby and Wareing, 1966, Eriksson *et al.*, 2000b). Secondary growth involves the vascular cambium, a meristematic tissue that produces xylem inwards and phloem outwards (Murmanis, 1970, Elo *et al.*, 2009). In Arabidopsis, secondary growth can be divided into two major phases based on morphology studies and growth rates of vascular tissues. The shift from the first phase to the second phase of secondary growth or xylem expansion phase is predominantly mediated through GA signaling. Upon flowering, secondary growth in the hypocotyl is accompanied by a major transcriptional reprogramming following GA mediated DELLA degradation. The xylem is produced in a higher proportion whereas the phloem proliferation is attenuated leading to higher xylem occupancy (xylem/total area). Xylem fiber also differentiate in the hypocotyl during the xylem expansion phase following DELLA signaling, this is illustrated by GA treatment and mutants in which GA signaling is constitutively on. Conversely, the induction of dominant DELLA (insensitive to GA mediated degradation) resulted in a dramatic decrease in hypocotyl xylem

expansion and total lack of fiber (Ragni *et al.*, 2011) (this study). Secondary growth parameters such as the overall hypocotyl total area and the xylem occupancy also depend on the ecotype, for example xylem occupancy is much higher in Ler comparing to Col-0 or Kz accessions (Ragni *et al.*, 2011).

In this study, we aimed at getting more insights on the role of DELLA dependent GA signaling during secondary growth. We demonstrated that among the five *DELLA* gene members, secondary growth is mostly affected by *RGA* and *GAI* with a higher impact for *RGA*. Despite the huge difference in secondary growth that exist between col and Ler, with Ler having a higher X/A ratio comparing to Col (Ragni *et al.*, 2011). The role of *RGA* and *GAI* in secondary growth seems to be conserved across ecotypes, as the double inactivation of *RGA* and *GAI* confer the same increase in xylem occupancy in Col and Ler ecotypes. Interestingly, the difference between Col and Ler in secondary growth is not due to *ERECTA* gene inactivation in Ler background (Ikematsu *et al.*, 2017) (This study). *ERECTA* doesn't seem neither to act in a GA dependent manner as suggested by the fact that *rga gai* and the *rga gai er* were undistinguishable in Col background.

In order to understand the molecular mechanisms of DELLA action and its specificity during secondary growth, we aimed at finding DELLA interacting factors accompanying the shift to the xylem expansion phase. To this end, we first characterized published DELLA interacting partners that are known to be expressed in the hypocotyl and involved in hypocotyl growth regulation, such as *ARF6*, *ARF7* and *ARF8* (Oh *et al.*, 2014). Consistently, we showed that expression of *ARF6*, *ARF7* and *ARF8* in the hypocotyl during secondary growth overlaps with that of *RGA* and *GAI*. We also discovered a novel role for *ARF6*, *ARF7* and *ARF8* as xylem expansion promoting factors. The identified ARF's seem to act redundantly on regulating xylem expansion and fiber formation, in fact *arf7* mutants are characterized by decreased overall secondary growth, whereas *arf6* and *arf8* single mutants showed a slight but significant reduction in X/A ratio. These ARF's are more luckily promoting xylem expansion after flowering as we first showed that the double mutant *arf6 arf8* is identical to the WT before the shift to the xylem expansion phase, also *arf6 arf8* keeps a low xylem/total area ratio after flowering coupled by absence of fiber in the xylem. In fact, knocking out *ARF6* and *ARF8*, prevents the shift to the xylem expansion phase, as a result, hypocotyls of *arf6 arf8* develop a bigger total area (starting from 5 days after flowering) due to continued phloem proliferation, which usually decrease in favor of xylem expansion in the WT. Another interesting feature is that the double mutant *arf6 arf8* has twice the number of phloem poles than wild-type counterparts at 10 days after flowering. It is possible that *ARF6* and *ARF8*

regulate the vascular cambium activity and program it to produce less phloem, as it has been reported that other ARFs are capable of regulating the vascular cambium activity (Brackmann *et al.*, 2018). In addition to the aberrant phloem production, the phloem tissue of *arf6 arf8* hypocotyls is characterized by ectopic cell division in the phloem poles. Interestingly the sites of ectopic cell division can differentiate fiber at very late stages after flowering (40 daf in our conditions). This could be explained by the fact that *arf6 arf8* accumulate more bioactive JA compared to the WT. As it has been shown that *ARF6* and *ARF8* genes positively regulate the expression of the auxin responsive genes *GH3.3*, *GH3.5* and *GH3.6* which increases JA conjugation, consequently reducing free JA levels (Gutierrez *et al.*, 2012). Consistently, the positive role of JA in promoting the differentiation of phloem fiber has been most recently revealed in Hemp (Behr *et al.*, 2018) but also in Arabidopsis (This study). The transcriptome profile of *arf6 arf8* explains its phenotype, in fact several key factors regulating xylem differentiation such as *NST1*, *NST3*, *SND2*, *SND3*, *MYB46* and *MYB83* as well as the same *GH3* genes conjugating JA were down-regulated.

To better understand the nature of interaction between DELLA and ARFs during secondary growth, we checked if enhancing GA response in *arf6 arf8* background has any effect after flowering where supposedly the plant shifts to xylem expansion. To this end, we checked the effect of total inactivation of DELLA in *arf6 arf8* background. Either by GA treatment upon flowering or by mutating *RGA* and/or *GAI* in *arf6 arf8* mutant background. In both cases, the plants seem to be less responsive to GA by slightly expanding the xylem and differentiating fiber. Which is not the case for the WT, that exhibited full response to GA enhancement. Both GA treated WT plants and the double mutants *rga gai* are characterized by tremendous xylem expansion and fiber differentiation after flowering. The fact that *arf6 arf8* is partially responding to GA imply the presence of other downstream secondary growth activators that may be released in the total absence of DELLA. ARF7 is another ARF activator that is phylogenetically closer to ARF6 and ARF8 than ARF5/MP, it is also known to interact with DELLA (Oh *et al.*, 2014). To check if ARF7 is another GA downstream activator of secondary growth we first investigated the triple mutant *arf6 nph4/arf7 ar8* which showed and even lower X/A ratio comparing to *arf6 arf8*, but also lack of fiber differentiation and ectopic phloem cell division. We then investigated the GA responsiveness of the triple mutant *arf6 arf7 arf8*, comparing to *arf6 arf8* and the WT by treating the plants with GA for 20 days upon flowering. As we expected, the triple mutant was even less responsive to GA treatment in terms of xylem expansion and fiber differentiation comparing to the double.

Given the previous findings, one possible explanation of *arf6 arf8* phenotype (absence of fiber and reduced xylem occupancy) is that from flowering on, ARF7 and probably other positive regulator(s) of xylem expansion and fiber accumulation are sequestered by the remaining undegraded DELLA proteins in the hypocotyl of the double mutant *arf6 arf8*.

As discussed above, our results suggest the existence of downstream activator(s) other than ARF6 ARF7 and ARF8 since the triple *arf6 arf7 arf8* is still capable to confer a very mild response to GA. We explored BP/KNAT1 as it acts as xylem expansion and fiber differentiation activator downstream of the GA signaling pathway, as illustrated by the decrease in xylem expansion and absence of fiber in *bp* mutant hypocotyls at 21 dag upon GA treatment (Ikematsu *et al.*, 2017).

We then wondered if enhancing GA response in *bp* mutant render it capable to differentiate xylem fiber in the hypocotyls at very late stages after flowering. To this end, we generated the triple mutant *rga gai bp* in Col-0 background. At senescence, the hypocotyls of *rga gai bp* showed mild fiber differentiation, which is not the case for *bp*. Our results suggest that fiber differentiation is not exclusively mediated through BP, We generated the triple mutant *arf6 arf8 bp*, as we wanted to investigate the effect of mutating three major xylem expansion and fiber formation activators.

The phenotype of the triple *arf6 arf8 bp* is characterized by absolute cambium defect resulting in a dramatically tiny plant with a hypocotyl total area 1/tenth of the WT after flowering. We also demonstrated that BP expression does not change in *arf6 arf8* hypocotyls after flowering. Additionally, expression levels of the key regulators of secondary walls or fiber formation in woody tissues of *Arabidopsis thaliana*, *NST1* and *NST3*, are decreased both in *bp* and *arf6 arf8* mutants explaining absence of fiber in their hypocotyls until very late developmental stages. Taking into account the previous findings, we suppose that ARF6, ARF8 and BP are capable to jointly co-regulate cambium activity.

In the other hand, we analyzed the transcriptome data related to RGA upon flowering as we demonstrated that RGA has a greater impact comparing to other DELLAs, RNA sequencing revealed many genes with significantly altered expression patterns. Notably, Cytokinin related genes were up-regulated, Jasmonate related genes were downregulated and GA biosynthesis genes such as *GA3ox* and *GA20ox* were up-regulated as a response to trigger the degradation of the induced dominant RGA.

Among the Cytokinin signaling related genes, *CRF1* which belong to CYTOKININ RESPONSE FACTOR (CRF) gene family involved in regulating meristem size (Raines *et al.*, 2016), is known to negatively regulate *Arabidopsis* rosette size. By analyzing *crf1* mutant plants no difference with

the WT was detected in secondary growth. Redundancy among members of the CRF gene family (Raines et al., 2016) can explain the *crf1* result. This led us to investigate the upstream regulators of CRF gene family which are type-B ARR_s (Rashotte et al., 2006). *ARR1* and *ARR2* caught our interest as they are known to physically interact with DELLA and jointly promote transcription of a wide set of target genes (Marin-de la Rosa et al., 2015), but also because they belong to the type B-ARR_s sub-family 1 mediating most of Cytokinin responses (Hill et al., 2013).

Our results suggest a novel role for *ARR1* as positive regulator of overall hypocotyl secondary growth as shown by reduced total area of *arr1* mutants, we also identified a positive role for *ARR2* in promoting phloem proliferation. Overall, *ARR1* and *ARR2* seem to act redundantly as positive regulators of phloem proliferation and negatively regulate fiber differentiation.

Our RNA sequencing data highlighted another crosstalk between GA and JA, among the Jasmonate related signaling genes *JAZ7* and *JAZ10* were remarkably downregulated. This is not consistent with the fact that *JAZ10* and to a lesser extent *JAZ7* have negative effects on secondary growth in the Arabidopsis stem (Sehr et al., 2010). As DELLA has been reported to interact with JAZ (Hou et al., 2010), a possible speculation is that upon DELLA dominant induction, JAZ proteins are somehow stabilized leading to downregulation of their own expression as a feedback loop.

Unlike the stem, *JAZ7* and *JAZ10* do not seem to affect secondary growth in the hypocotyl as suggested by our results, *jaz7-1* as well as *jaz10-1* are indistinguishable from the WT at 10 daf. This can be explained by spatial specificity among JAZ proteins (Chini et al., 2007, Browse, 2009). We then wondered about the effect of impairing JA perception on hypocotyl secondary growth by analyzing *coi1-1* and *myc2-3* mutants. Our results indicated that both *COI1* and *MYC2* have positive roles in phloem proliferation in the hypocotyl thus positively regulating overall secondary growth, consistently with the positive role attributed to *COI1* and *MYC2* in controlling secondary growth in Arabidopsis stem (Sehr et al., 2010).

To complete the picture, we investigated the effect of constitutive JA response by applying JA for 20 days upon flowering on WT, *arf6 arf8* and *rga gai* mutants. Our preliminary results suggest a specific role for Jasmonate on secondary growth, since it only promotes xylem fiber and phloem fiber formation and does not alter the X/A ratio or the total area of the treated plants. The ectopic formation of fiber in the phloem tissue resulting from JA application has been previously observed in other species such as conifers (Hudgins et al., 2004) and cannabis (Behr et al., 2018), suggesting that this role is preserved among plant species. The specific role of JA in Arabidopsis phloem fiber

formation is probably mediated through JAZ protein degradation. Therefore, it is worth to check the phenotype of JAZ single and multiple mutants to reveal which JAZ(s) are responsible for the fiber phenotype in the hypocotyl.

DELLA protein was reported to regulate JA signaling via competitive binding to JAZ(s) enabling MYC2 to regulate its target set of genes (Hou *et al.*, 2010). Conversely, DELLA regulate expression of Sesquiterpene Synthase genes through interacting with MYC2 (Hong *et al.*, 2012). Our results suggest a scenario in which DELLA and JAZ proteins interact before flowering resulting in fiber formation repression. However, what are the JAZ(s) interactors? Whether DELLA interacts with MYC2 to activate phloem proliferation before flowering in the hypocotyl is yet to be determined.

To conclude, we propose a model that could explain the shift to xylem expansion phase during secondary growth (Figure 2).

Before flowering, DELLA proteins sequester ARF6, ARF7, ARF8 and probably other xylem expansion activators such as BP. Additionally, DELLA might interact with ARR1 and ARR2 to maintain phloem proliferation and repress fiber formation. This can explain the secondary growth phenotype before flowering as DELLA accumulates in the hypocotyl due to low concentration of bio-active GA. After flowering, ARF6, ARF7, ARF8 and probably other xylem expansion activators such as BP are released from DELLA repression in the hypocotyl triggering xylem expansion and fiber differentiation. whereas ARR1 and ARR2 are unable to interact with DELLA due to higher bio-active GA concentrations leading to DELLA degradation (Talon *et al.*, 1991). Particularly in the hypocotyl where GA can move through the plant from the shoot apex to the hypocotyl upon flowering to locally trigger DELLA degradation (Ragni *et al.*, 2011).

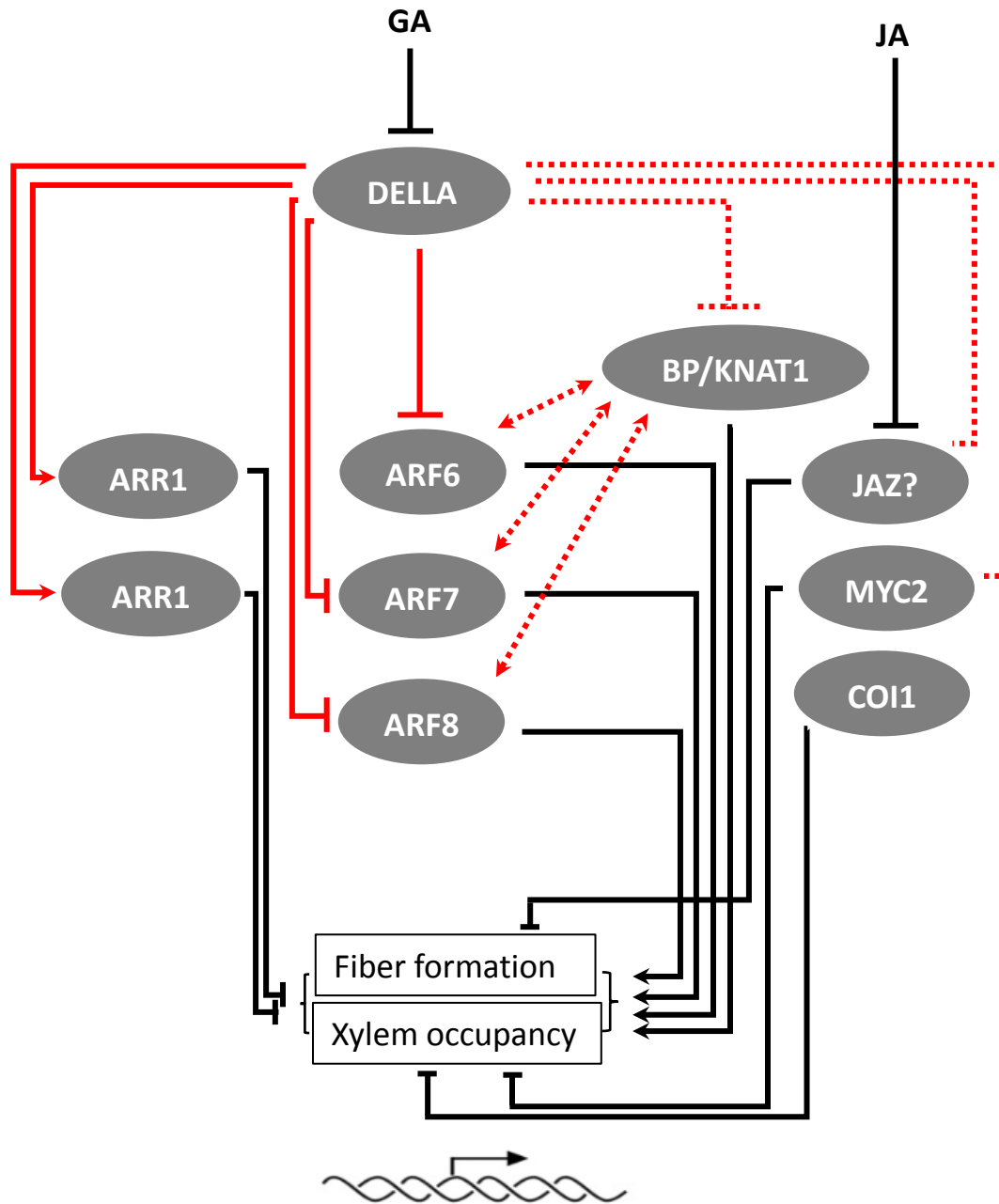


Fig. 2 Proposed model on GA mediated secondary growth control and crosstalk with Auxin, Cytokinin and Jasmonate. Hypothesized links are illustrated with dashed lines. Red arrows represent protein-protein interactions. The lines and arrows illustrate interactions. Compare text for details.

7 References

- Achard, P., Baghour, M., Chapple, A., Hedden, P., Van Der Straeten, D., Genschik, P., Moritz, T. and Harberd, N.P. (2007) The plant stress hormone ethylene controls floral transition via DELLA-dependent regulation of floral meristem-identity genes. *Proceedings of the National Academy of Sciences of the United States of America*, **104**, 6484-6489.
- Agusti, J., Herold, S., Schwarz, M., Sanchez, P., Ljung, K., Dun, E.A., Brewer, P.B., Beveridge, C.A., Sieberer, T., Sehr, E.M. and Greb, T. (2011a) Strigolactone signaling is required for auxin-dependent stimulation of secondary growth in plants. *Proceedings of the National Academy of Sciences*, **108**, 20242-20247.
- Agusti, J., Lichtenberger, R., Schwarz, M., Nehlin, L. and Greb, T. (2011b) Characterization of Transcriptome Remodeling during Cambium Formation Identifies MOL1 and RUL1 As Opposing Regulators of Secondary Growth. *PLoS Genetics*, **7**, e1001312.
- Argyros, R.D., Mathews, D.E., Chiang, Y.H., Palmer, C.M., Thibault, D.M., Etheridge, N., Argyros, D.A., Mason, M.G., Kieber, J.J. and Schaller, G.E. (2008) Type B response regulators of Arabidopsis play key roles in cytokinin signaling and plant development. *Plant Cell*, **20**, 2102-2116.
- Baima, S., Forte, V., Possenti, M., Peñalosa, A., Leoni, G., Salvi, S., Felici, B., Ruberti, I. and Morelli, G. (2014) Negative feedback regulation of auxin signaling by ATHB8/ACL5-BUD2 transcription module. *Molecular Plant*, **7**, 1006-1025.
- Behr, M., Lutts, S., Hausman, J.F. and Guerriero, G. (2018) Jasmonic acid to boost secondary growth in hemp hypocotyl. *Planta*, **248**, 1029-1036.
- Beisson, F., Li, Y., Bonaventure, G., Pollard, M. and Ohlrogge, J.B. (2007) The Acyltransferase GPAT5 Is Required for the Synthesis of Suberin in Seed Coat and Root of Arabidopsis. *The Plant Cell* **19**, 351-368.
- Bennett, T., Hines, G., van Rongen, M., Waldie, T., Sawchuk, M.G., Scarpella, E., Ljung, K. and Leyser, O. (2016) Connective Auxin Transport in the Shoot Facilitates Communication between Shoot Apices. *PLoS biology*, **14**, e1002446.
- Björklund, S., Antti, H., Uddestrand, I., Moritz, T. and Sundberg, B. (2007) Cross-talk between gibberellin and auxin in development of Populus wood: gibberellin stimulates polar auxin transport and has a common transcriptome with auxin. *Plant J*, **52**, 499-511.
- Brackmann, K., Qi, J., Gebert, M., Jouannet, V., Schlamp, T., Gruenwald, K., Wallner, E.S., D.D., N., Letvitsky, V., Agusti, J., Sanchez, P., Lohmann, J.U. and Greb, T. (2018) Spatial specificity of auxin responses coordinates wood formation. *Nature communications*.
- Browse, J. (2009) Jasmonate passes muster: a receptor and targets for the defense hormone. *Annual review of plant biology*, **60**, 183-205.
- Cano-Delgado, A., Yin, Y., Yu, C., Vafeados, D., Mora-Garcia, S., Cheng, J.C., Nam, K.H., Li, J. and Chory, J. (2004) BRL1 and BRL3 are novel brassinosteroid receptors that function in vascular differentiation in Arabidopsis. *Development*, **131**, 5341-5351.
- Cao, D., Hussain, A., Cheng, H. and Peng, J. (2005) Loss of function of four DELLA genes leads to light- and gibberellin-independent seed germination in Arabidopsis. *Planta*, **223**, 105-113.
- Carlsbecker, A., Lee, J.-Y., Roberts, C.J., Dettmer, J., Lehesranta, S., Zhou, J., Lindgren, O., Moreno-Risueno, M.A., Vatén, A., Thitamadee, S., Campilho, A., Sebastian, J., Bowman, J.L., Helariutta, Y. and Benfey, P.N. (2010a) Cell signalling by microRNA165/6 directs gene dose-dependent root cell fate. *Nature*, **465**, 316-321.
- Carlsbecker, A., Lee, J.Y., Roberts, C.J., Dettmer, J., Lehesranta, S., Zhou, J., Lindgren, O., Moreno-Risueno, M.A., Vatén, A., Thitamadee, S., Campilho, A., Sebastian, J., Bowman, J.L., Helariutta, Y. and Benfey, P.N. (2010b) Cell signalling by microRNA165/6 directs gene dose-dependent root cell fate. *Nature*, **465**, 316-321.
- Chaffey, N. (1999) Cambium: old challenges – new opportunities. *Trees*, **13**, 138-151.

- Chaffey, N., Cholewa, E., Regan, S. and Sundberg, B.** (2002) Secondary xylem development in Arabidopsis: a model for wood formation. *Physiologia Plantarum*, **114**, 594-600.
- Cheng, H., Qin, L., Lee, S., Fu, X., Richards, D.E., Cao, D., Luo, D., Harberd, N.P. and Peng, J.** (2004) Gibberellin regulates Arabidopsis floral development via suppression of DELLA protein function. *Development*, **131**, 1055-1064.
- Chini, A., Fonseca, S., Fernandez, G., Adie, B., Chico, J.M., Lorenzo, O., Garcia-Casado, G., Lopez-Vidriero, I., Lozano, F.M., Ponce, M.R., Micol, J.L. and Solano, R.** (2007) The JAZ family of repressors is the missing link in jasmonate signalling. *Nature*, **448**, 666-671.
- Claeys, H., De Bodt, S. and Inze, D.** (2014) Gibberellins and DELLAs: central nodes in growth regulatory networks. *Trends Plant Sci*, **19**, 231-239.
- Colebrook, E.H., Thomas, S.G., Phillips, A.L. and Hedden, P.** (2014) The role of gibberellin signalling in plant responses to abiotic stress. *The Journal of experimental biology*, **217**, 67-75.
- Davière, J.-M. and Achard, P.** (2016) A Pivotal Role of DELLAs in Regulating Multiple Hormone Signals. *Molecular Plant*, **9**, 10-20.
- Davin, N., Edger, P.P., Hefer, C.A., Mizrachi, E., Schuetz, M., Smets, E., Myburg, A.A., Douglas, C.J., Schranz, M.E. and Lens, F.** (2016) Functional network analysis of genes differentially expressed during xylogenesis in social woody Arabidopsis plants. *The Plant journal*, **86**, 376-390.
- de Reuille, P.B. and Ragni, L.** (2017) Vascular Morphodynamics During Secondary Growth. *Methods in molecular biology (Clifton, N.J.)*, **1544**, 103-125.
- Demura, T. and Ye, Z.-H.** (2010) Regulation of plant biomass production. *Current Opinion in Plant Biology*, **13**, 298-303.
- Digby, J. and Wareing, P.F.** (1966) The Effect of Applied Growth Hormones on Cambial Division and the Differentiation of the Cambial Derivatives *Annals of Botany*, **30**, 539-548.
- Dill, A. and Sun, T.** (2001) Synergistic derepression of gibberellin signaling by removing RGA and GAI function in Arabidopsis thaliana. *Genetics*, **159**, 777-785.
- Dinneny, J.R. and Yanofsky, M.F.** (2004) Vascular patterning: xylem or phloem? *Curr Biol*, **14**, R112-114.
- Du, J., Miura, E., Robischon, M., Martinez, C. and Groover, A.** (2011) The Populus Class III HD ZIP Transcription Factor POPCORONA Affects Cell Differentiation during Secondary Growth of Woody Stems. *PLoS ONE*, **6**, e17458.
- Elo, A., Immanen, J., Nieminen, K. and Helariutta, Y.** (2009) Stem cell function during plant vascular development. *Semin Cell Dev Biol*, **20**, 1097-1106.
- Eriksson, M.E., Israelsson, M., Olsson, O. and Moritz, T.** (2000a) Increased gibberellin biosynthesis in transgenic trees promotes growth, biomass production and xylem fiber length. *Nature biotechnology*, **18**, 784-788.
- Eriksson, M.E., Israelsson, M., Olsson, O. and Moritz, T.** (2000b) Increased gibberellin biosynthesis in transgenic trees promotes growth, biomass production and xylem fiber length. *Nat Biotech*, **18**, 784-788.
- Esau, K.** (1977) *Anatomy of Seed Plants*: Wiley.
- Etchells, J.P., Provost, C.M., Mishra, L. and Turner, S.R.** (2013) *WOX4* and *WOX14* act downstream of the PXY receptor kinase to regulate plant vascular proliferation independently of any role in vascular organisation. *Development*, **140**, 2224-2234.
- Feng, S., Martinez, C., Gusmaroli, G., Wang, Y., Zhou, J., Wang, F., Chen, L., Yu, L., Iglesias-Pedraz, J.M., Kircher, S., Schafer, E., Fu, X., Fan, L.M. and Deng, X.W.** (2008) Coordinated regulation of Arabidopsis thaliana development by light and gibberellins. *Nature*, **451**, 475-479.
- Fleet, C.M. and Sun, T.P.** (2005) A DELLAcate balance: the role of gibberellin in plant morphogenesis. *Curr Opin Plant Biol*, **8**, 77-85.
- Frigerio, M., Alabadi, D., Perez-Gomez, J., Garcia-Carcel, L., Phillips, A.L., Hedden, P. and Blazquez, M.A.** (2006) Transcriptional regulation of gibberellin metabolism genes by auxin signaling in Arabidopsis. *Plant Physiol*, **142**, 553-563.

- Fukazawa, J., Teramura, H., Murakoshi, S., Nasuno, K., Nishida, N., Ito, T., Yoshida, M., Kamiya, Y., Yamaguchi, S. and Takahashi, Y.** (2014) DELLAs function as coactivators of GAI-ASSOCIATED FACTOR1 in regulation of gibberellin homeostasis and signaling in Arabidopsis. *Plant Cell*, **26**, 2920-2938.
- Grieneisen, V.A., Xu, J., Marée, A.F.M., Hogeweg, P. and Scheres, B.** (2007) Auxin transport is sufficient to generate a maximum and gradient guiding root growth. *Nature*, **449**, 1008.
- Griffiths, J., Murase, K., Rieu, I., Zentella, R., Zhang, Z.L., Powers, S.J., Gong, F., Phillips, A.L., Hedden, P., Sun, T.P. and Thomas, S.G.** (2006) Genetic characterization and functional analysis of the GID1 gibberellin receptors in Arabidopsis. *Plant Cell*, **18**, 3399-3414.
- Groh, B., Hubner, C. and Lenzian, K.J.** (2002) Water and oxygen permeance of phellems isolated from trees: the role of waxes and lenticels. *Planta*, **215**, 794-801.
- Gutierrez, L., Bussell, J.D., Pacurar, D.I., Schwambach, J., Pacurar, M. and Bellini, C.** (2009) Phenotypic plasticity of adventitious rooting in Arabidopsis is controlled by complex regulation of AUXIN RESPONSE FACTOR transcripts and microRNA abundance. *Plant Cell*, **21**, 3119-3132.
- Gutierrez, L., Mongelard, G., Flokova, K., Pacurar, D.I., Novak, O., Staswick, P., Kowalczyk, M., Pacurar, M., Demailly, H., Geiss, G. and Bellini, C.** (2012) Auxin controls Arabidopsis adventitious root initiation by regulating jasmonic acid homeostasis. *Plant Cell*, **24**, 2515-2527.
- Han, S., Cho, H., Noh, J., Qi, J., Jung, H.J., Nam, H., Lee, S., Hwang, D., Greb, T. and Hwang, I.** (2018) BIL1-mediated MP phosphorylation integrates PXY and cytokinin signalling in secondary growth. *Nat Plants*, **4**, 605-614.
- Hill, K., Mathews, D.E., Kim, H.J., Street, I.H., Wildes, S.L., Chiang, Y.-H., Mason, M.G., Alonso, J.M., Ecker, J.R., Kieber, J.J. and Schaller, G.E.** (2013) Functional Characterization of Type-B Response Regulators in the Arabidopsis Cytokinin Response. *Plant Physiology*, **162**, 212-224.
- Hirakawa, Y., Kondo, Y. and Fukuda, H.** (2010) TDIF Peptide Signaling Regulates Vascular Stem Cell Proliferation via the *WOX4* Homeobox Gene in Arabidopsis. *The Plant Cell*, **22**, 2618-2629.
- Hohm, T., Zitzler, E. and Simon, R.** (2010) A dynamic model for stem cell homeostasis and patterning in Arabidopsis meristems. *PLoS One*, **5**, e9189.
- Hong, G.J., Xue, X.Y., Mao, Y.B., Wang, L.J. and Chen, X.Y.** (2012) Arabidopsis MYC2 interacts with DELLA proteins in regulating sesquiterpene synthase gene expression. *Plant Cell*, **24**, 2635-2648.
- Hou, X., Lee, L.Y., Xia, K., Yan, Y. and Yu, H.** (2010) DELLAs modulate jasmonate signaling via competitive binding to JAZs. *Dev Cell*, **19**, 884-894.
- Hudgins, J.W., Christiansen, E. and Franceschi, V.R.** (2004) Induction of anatomically based defense responses in stems of diverse conifers by methyl jasmonate: a phylogenetic perspective. *Tree physiology*, **24**, 251-264.
- Ikematsu, S., Tasaka, M., Torii, K.U. and Uchida, N.** (2017) ERECTA-family receptor kinase genes redundantly prevent premature progression of secondary growth in the Arabidopsis hypocotyl. *New Phytol*, **213**, 1697-1709.
- Immanen, J., Nieminen, K., Smolander, O.P., Kojima, M., Alonso Serra, J., Koskinen, P., Zhang, J., Elo, A., Mahonen, A.P., Street, N., Bhalerao, R.P., Paulin, L., Auvinen, P., Sakakibara, H. and Helariutta, Y.** (2016) Cytokinin and Auxin Display Distinct but Interconnected Distribution and Signaling Profiles to Stimulate Cambial Activity. *Curr Biol*, **26**, 1990-1997.
- Jasinski, S., Piazza, P., Craft, J., Hay, A., Woolley, L., Rieu, I., Phillips, A., Hedden, P. and Tsiantis, M.** (2005) KNOX action in Arabidopsis is mediated by coordinate regulation of cytokinin and gibberellin activities. *Curr Biol*, **15**, 1560-1565.
- Kaneda, M., Schuetz, M., Lin, B.S., Chanis, C., Hamberger, B., Western, T.L., Ehlting, J. and Samuels, A.L.** (2011) ABC transporters coordinately expressed during lignification of Arabidopsis stems include a set of ABCBs associated with auxin transport. *J Exp Bot*, **62**, 2063-2077.

- Kondo, Y., Ito, T., Nakagami, H., Hirakawa, Y., Saito, M., Tamaki, T., Shirasu, K. and Fukuda, H.** (2014) Plant GSK3 proteins regulate xylem cell differentiation downstream of TDIF-TDR signalling. *Nature communications*, **5**, 3504.
- Kubo, M., Udagawa, M., Nishikubo, N., Horiguchi, G., Yamaguchi, M., Ito, J., Mimura, T., Fukuda, H. and Demura, T.** (2005) Transcription switches for protoxylem and metaxylem vessel formation. *Genes & Development*, **19**, 1855-1860.
- Kurihara, D., Mizuta, Y., Sato, Y. and Higashiyama, T.** (2015) ClearSee: a rapid optical clearing reagent for whole-plant fluorescence imaging. *Development*, **142**, 4168-4179.
- Lampropoulos, A., Sutikovic, Z., Wenzl, C., Maegele, I., Lohmann, J.U. and Forner, J.** (2013) GreenGate - A Novel, Versatile, and Efficient Cloning System for Plant Transgenesis. *PLoS ONE*, **8**, e83043.
- Lendzian, K.J.** (2006) Survival strategies of plants during secondary growth: barrier properties of phellements and lenticels towards water, oxygen, and carbon dioxide. *Journal of Experimental Botany*, **57**, 2535-2546.
- Li, M., An, F., Li, W., Ma, M., Feng, Y., Zhang, X. and Guo, H.** (2016) DELLA proteins interact with FLC to repress flowering transition. *J Integr Plant Biol*, **58**, 642-655.
- Liao, Y., Smyth, G.K. and Shi, W.** (2013) The Subread aligner: fast, accurate and scalable read mapping by seed-and-vote. *Nucleic acids research*, **41**, e108.
- Liebsch, D., Sunaryo, W., Holmlund, M., Norberg, M., Zhang, J., Hall, H.C., Helizon, H., Jin, X., Helariutta, Y., Nilsson, O., Polle, A. and Fischer, U.** (2014) Class I KNOX transcription factors promote differentiation of cambial derivatives into xylem fibers in the Arabidopsis hypocotyl. *Development*, **141**, 4311-4319.
- Locascio, A., Blázquez, M.A. and Alabadí, D.** (2013) Genomic Analysis of DELLA Protein Activity. *Plant and Cell Physiology*, **54**, 1229-1237.
- Love, M.I., Huber, W. and Anders, S.** (2014) Moderated estimation of fold change and dispersion for RNA-seq data with DESeq2. *Genome biology*, **15**, 550.
- Lulai, E.C. and Freeman, T.P.** (2001) The Importance of Phellogen Cells and their Structural Characteristics in Susceptibility and Resistance to Excortiation in Immature and Mature Potato Tuber (*Solanum tuberosum* L.) Periderm. *Annals of Botany*, **88**, 555-561.
- Marin-de la Rosa, N., Pfeiffer, A., Hill, K., Locascio, A., Bhalerao, R.P., Miskolczi, P., Gronlund, A.L., Wanchoo-Kohli, A., Thomas, S.G., Bennett, M.J., Lohmann, J.U., Blázquez, M.A. and Alabadi, D.** (2015) Genome Wide Binding Site Analysis Reveals Transcriptional Coactivation of Cytokinin-Responsive Genes by DELLA Proteins. *PLoS Genet*, **11**, e1005337.
- Marin-de la Rosa, N., Sotillo, B., Miskolczi, P., Gibbs, D.J., Vicente, J., Carbonero, P., Onate-Sanchez, L., Holdsworth, M.J., Bhalerao, R., Alabadi, D. and Blázquez, M.A.** (2014) Large-scale identification of gibberellin-related transcription factors defines group VII ETHYLENE RESPONSE FACTORS as functional DELLA partners. *Plant Physiol*, **166**, 1022-1032.
- Matsumoto-Kitano, M., Kusumoto, T., Tarkowski, P., Kinoshita-Tsujimura, K., Václavíková, K., Miyawaki, K. and Kakimoto, T.** (2008) Cytokinins are central regulators of cambial activity. *Proceedings of the National Academy of Sciences*, **105**, 20027-20031.
- Mauriat, M. and Moritz, T.** (2009) Analyses of GA20ox- and GID1-over-expressing aspen suggest that gibberellins play two distinct roles in wood formation. *The Plant Journal*, **58**, 989-1003.
- Mazur, E. and Kurczynska, E.U.** (2012) Rays, intrusive growth, and storied cambium in the inflorescence stems of Arabidopsis thaliana (L.) Heynh. *Protoplasma*, **249**, 217-220.
- Mele, G., Ori, N., Sato, Y. and Hake, S.** (2003) The knotted1-like homeobox gene BREVIPEDICELLUS regulates cell differentiation by modulating metabolic pathways. *Genes Dev*, **17**, 2088-2093.
- Melzer, S., Lens, F., Gennen, J., Vanneste, S., Rohde, A. and Beeckman, T.** (2008) Flowering-time genes modulate meristem determinacy and growth form in Arabidopsis thaliana. *Nature Genetics*, **40**, 1489-1492.
- Milhinhos, A., Prestele, J., Bollhoner, B., Matos, A., Vera-Sirera, F., Rambla, J.L., Ljung, K., Carbonell, J., Blázquez, M.A., Tuominen, H. and Miguel, C.M.** (2013) Thermospermine levels

- are controlled by an auxin-dependent feedback loop mechanism in *Populus* xylem. *Plant J*, **75**, 685-698.
- Mitsuda, N., Iwase, A., Yamamoto, H., Yoshida, M., Seki, M., Shinozaki, K. and Ohme-Takagi, M.** (2007) NAC Transcription Factors, NST1 and NST3, Are Key Regulators of the Formation of Secondary Walls in Woody Tissues of Arabidopsis. *The Plant Cell Online*, **19**, 270-280.
- Morita, J., Kato, K., Nakane, T., Kondo, Y., Fukuda, H., Nishimasu, H., Ishitani, R. and Nureki, O.** (2016) Crystal structure of the plant receptor-like kinase TDR in complex with the TDIF peptide. *Nature communications*, **7**, 12383.
- Murmanis, L.** (1970) Locating the initial in the vascular cambium of *Pinus strobus* L. by electron microscopy. *Wood Science and Technology*, **4**, 1-14.
- Murmanis, L.** (1971) Structural Changes in the Vascular Cambium of *Pinus strobus* L. during an Annual Cycle. *Annals of Botany*, **35**, 133-141.
- Nagpal, P., Ellis, C.M., Weber, H., Ploense, S.E., Barkawi, L.S., Guilfoyle, T.J., Hagen, G., Alonso, J.M., Cohen, J.D., Farmer, E.E., Ecker, J.R. and Reed, J.W.** (2005) Auxin response factors ARF6 and ARF8 promote jasmonic acid production and flower maturation. *Development*, **132**, 4107-4118.
- Nakajima, M., Shimada, A., Takashi, Y., Kim, Y.C., Park, S.H., Ueguchi-Tanaka, M., Suzuki, H., Katoh, E., Iuchi, S., Kobayashi, M., Maeda, T., Matsuoka, M. and Yamaguchi, I.** (2006) Identification and characterization of Arabidopsis gibberellin receptors. *Plant J*, **46**, 880-889.
- Nardmann, J. and Werr, W.** (2013) Sympleiomorphies in the WUSCHEL clade suggest that the last common ancestor of seed plants contained at least four independent stem cell niches. *New Phytologist*, n/a-n/a.
- Oh, E., Zhu, J.Y., Bai, M.Y., Arenhart, R.A., Sun, Y. and Wang, Z.Y.** (2014) Cell elongation is regulated through a central circuit of interacting transcription factors in the Arabidopsis hypocotyl. *Elife*, **3**.
- Okushima, Y., Overvoorde, P.J., Arima, K., Alonso, J.M., Chan, A., Chang, C., Ecker, J.R., Hughes, B., Lui, A., Nguyen, D., Onodera, C., Quach, H., Smith, A., Yu, G. and Theologis, A.** (2005) Functional genomic analysis of the AUXIN RESPONSE FACTOR gene family members in Arabidopsis thaliana: unique and overlapping functions of ARF7 and ARF19. *Plant Cell*, **17**, 444-463.
- Pautot, V., Dockx, J., Hamant, O., Kronenberger, J., Grandjean, O., Jublot, D. and Traas, J.** (2001) KNAT2: evidence for a link between knotted-like genes and carpel development. *Plant Cell*, **13**, 1719-1734.
- Petersson, S.V., Johansson, A.I., Kowalczyk, M., Makoveychuk, A., Wang, J.Y., Moritz, T., Grebe, M., Benfey, P.N., Sandberg, G. and Ljung, K.** (2009) An auxin gradient and maximum in the Arabidopsis root apex shown by high-resolution cell-specific analysis of IAA distribution and synthesis. *Plant Cell*, **21**, 1659-1668.
- Plackett, A.R.G., Ferguson, A.C., Powers, S.J., Wanchoo-Kohli, A., Phillips, A.L., Wilson, Z.A., Hedden, P. and Thomas, S.G.** (2014) DELLA activity is required for successful pollen development in the Columbia ecotype of Arabidopsis. *New Phytologist*, **201**, 825-836.
- Plomion, C., Leprovost, G. and Stokes, A.** (2001) Wood formation in trees. *Plant Physiol*, **127**, 1513-1523.
- Ragni, L. and Greb, T.** (2017) Secondary growth as a determinant of plant shape and form. *Semin Cell Dev Biol*.
- Ragni, L. and Greb, T.** (2018) Secondary growth as a determinant of plant shape and form. *Seminars in Cell and Developmental Biology*.
- Ragni, L. and Hardtke, C.S.** (2014) Small but thick enough – the Arabidopsis hypocotyl as a model to study secondary growth. *Physiologia Plantarum*, **151**, 164-171.
- Ragni, L., Nieminen, K., Pacheco-Villalobos, D., Sibout, R., Schwechheimer, C. and Hardtke, C.S.** (2011) Mobile gibberellin directly stimulates Arabidopsis hypocotyl xylem expansion. *Plant Cell*, **23**, 1322-1336.

- Raines, T., Shanks, C., Cheng, C.Y., McPherson, D., Argueso, C.T., Kim, H.J., Franco-Zorrilla, J.M., Lopez-Vidriero, I., Solano, R., Vankova, R., Schaller, G.E. and Kieber, J.J.** (2016) The cytokinin response factors modulate root and shoot growth and promote leaf senescence in *Arabidopsis*. *Plant J*, **85**, 134-147.
- Randall, R.S., Miyashima, S., Blomster, T., Zhang, J., Elo, A., Karlberg, A., Immanen, J., Nieminen, K., Lee, J.Y., Kakimoto, T., Blajecka, K., Melnyk, C.W., Alcasabas, A., Forzani, C., Matsumoto-Kitano, M., Mahonen, A.P., Bhalerao, R., Dewitte, W., Helariutta, Y. and Murray, J.A.** (2015) AINTEGUMENTA and the D-type cyclin CYCD3;1 regulate root secondary growth and respond to cytokinins. *Biology open*, **4**, 1229-1236.
- Rashotte, A.M., Mason, M.G., Hutchison, C.E., Ferreira, F.J., Schaller, G.E. and Kieber, J.J.** (2006) A subset of *Arabidopsis* AP2 transcription factors mediates cytokinin responses in concert with a two-component pathway. *Proceedings of the National Academy of Sciences of the United States of America*, **103**, 11081-11085.
- Robischon, M., Du, J., Miura, E. and Groover, A.** (2011) The Populus Class III HD ZIP, popREVOLUTA, Influences Cambium Initiation and Patterning of Woody Stems. *Plant Physiology*, **155**, 1214-1225.
- Sankar, M., Nieminen, K., Ragni, L., Xenarios, I. and Hardtke, C.S.** (2014) Automated quantitative histology reveals vascular morphodynamics during *Arabidopsis* hypocotyl secondary growth. *Elife*, **3**, e01567.
- Savidge, R.A.** (1983) The role of plant hormones in higher plant cellular differentiation. II. Experiments with the vascular cambium, and sclereid and tracheid differentiation in the pine, *Pinus contorta*. *The Histochemical journal*, **15**, 447-466.
- Scheres, B.** (2007) Stem-cell niches: nursery rhymes across kingdoms. *Nat Rev Mol Cell Biol*, **8**, 345-354.
- Schulze, W., Reinders, A., Ward, J., Lalonde, S. and Frommer, W.** (2003) Interactions between co-expressed *Arabidopsis* sucrose transporters in the split-ubiquitin system.
- Sehr, E.M., Agusti, J., Lehner, R., Farmer, E.E., Schwarz, M. and Greb, T.** (2010) Analysis of secondary growth in the *Arabidopsis* shoot reveals a positive role of jasmonate signalling in cambium formation. *The Plant Journal*, **63**, 811-822.
- Sibout, R., Plantegenet, S. and Hardtke, C.S.** (2008a) Flowering as a condition for xylem expansion in *Arabidopsis* hypocotyl and root. *Current Biology*, **18**, 458-463.
- Sibout, R., Plantegenet, S. and Hardtke, C.S.** (2008b) Flowering as a condition for xylem expansion in *Arabidopsis* hypocotyl and root. *Curr Biol*, **18**, 458-463.
- Snow, R.** (1935) ACTIVATION OF CAMBIAL GROWTH BY PURE HORMONES. *New Phytologist*, **34**, 347-360.
- Spicer, R. and Groover, A.** (2010) Evolution of development of vascular cambia and secondary growth. *New Phytologist*, **186**, 577-592.
- Stowe-Evans, E.L., Harper, R.M., Motchoulski, A.V. and Liscum, E.** (1998) NPH4, a Conditional Modulator of Auxin-Dependent Differential Growth Responses in *Arabidopsis*. *Plant Physiology*, **118**, 1265-1275.
- Suer, S., Agusti, J., Sanchez, P., Schwarz, M. and Greb, T.** (2011) WOX4 Imparts Auxin Responsiveness to Cambium Cells in *Arabidopsis*. *The Plant Cell Online*, **23**, 3247-3259.
- Tabata, R., Ikezaki, M., Fujibe, T., Aida, M., Tian, C.E., Ueno, Y., Yamamoto, K.T., Machida, Y., Nakamura, K. and Ishiguro, S.** (2010) *Arabidopsis* auxin response factor6 and 8 regulate jasmonic acid biosynthesis and floral organ development via repression of class 1 KNOX genes. *Plant & cell physiology*, **51**, 164-175.
- Talon, M., Zeevaert, J.A. and Gage, D.A.** (1991) Identification of Gibberellins in Spinach and Effects of Light and Darkness on their Levels. *Plant Physiol*, **97**, 1521-1526.
- Thomas, S.G. and Sun, T.P.** (2004) Update on gibberellin signaling. A tale of the tall and the short. *Plant Physiol*, **135**, 668-676.
- Tian, C.E., Muto, H., Higuchi, K., Matamura, T., Tatematsu, K., Koshiba, T. and Yamamoto, K.T.** (2004) Disruption and overexpression of auxin response factor 8 gene of *Arabidopsis* affect

- hypocotyl elongation and root growth habit, indicating its possible involvement in auxin homeostasis in light condition. *Plant J*, **40**, 333-343.
- Torii, K.U., Mitsukawa, N., Oosumi, T., Matsuura, Y., Yokoyama, R., Whittier, R.F. and Komeda, Y.** (1996) The Arabidopsis ERECTA gene encodes a putative receptor protein kinase with extracellular leucine-rich repeats. *Plant Cell*, **8**, 735-746.
- Ursache, R., Andersen, T.G., Marhavy, P. and Geldner, N.** (2018) A protocol for combining fluorescent proteins with histological stains for diverse cell wall components. *Plant J*, **93**, 399-412.
- Uyttewaal, M., Traas, J. and Hamant, O.** (2010) Integrating physical stress, growth, and development. *Curr Opin Plant Biol*, **13**, 46-52.
- Wang, J., Kucukoglu, M., Zhang, L., Chen, P., Decker, D., Nilsson, O., Jones, B., Sandberg, G. and Zheng, B.** (2013) The Arabidopsis LRR-RLK, PXC1, is a regulator of secondary wall formation correlated with the TDIF-PXY/TDR-WOX4 signaling pathway. *BMC plant biology*, **13**, 94.
- Weiss, D. and Ori, N.** (2007) Mechanisms of Cross Talk between Gibberellin and Other Hormones. *Plant Physiology*, **144**, 1240-1246.
- Woerlen, N., Allam, G., Popescu, A., Corrigan, L., Pautot, V. and Hepworth, S.R.** (2017) Repression of BLADE-ON-PETIOLE genes by KNOX homeodomain protein BREVIPEDICELLUS is essential for differentiation of secondary xylem in Arabidopsis root. *Planta*, 1-12.
- Wu, M.F., Tian, Q. and Reed, J.W.** (2006) Arabidopsis microRNA167 controls patterns of ARF6 and ARF8 expression, and regulates both female and male reproduction. *Development*, **133**, 4211-4218.
- Xie, D.X., Feys, B.F., James, S., Nieto-Rostro, M. and Turner, J.G.** (1998) COI1: an Arabidopsis gene required for jasmonate-regulated defense and fertility. *Science*, **280**, 1091-1094.
- Yamamoto, R., Demura, T. and Fukuda, H.** (1997) Brassinosteroids induce entry into the final stage of tracheary element differentiation in cultured Zinnia cells. *Plant & cell physiology*, **38**, 980-983.
- Yamamoto, R., Fujioka, S., Iwamoto, K., Demura, T., Takatsuto, S., Yoshida, S. and Fukuda, H.** (2007) Co-regulation of brassinosteroid biosynthesis-related genes during xylem cell differentiation. *Plant & cell physiology*, **48**, 74-83.
- Yang, J.H. and Wang, H.** (2016) Molecular Mechanisms for Vascular Development and Secondary Cell Wall Formation. *Front Plant Sci*, **7**, 356.
- Ye, Z.H.** (2002) Vascular tissue differentiation and pattern formation in plants. *Annual review of plant biology*, **53**, 183-202.
- Yoshida, H., Hirano, K., Sato, T., Mitsuda, N., Nomoto, M., Maeo, K., Koketsu, E., Mitani, R., Kawamura, M., Ishiguro, S., Tada, Y., Ohme-Takagi, M., Matsuoka, M. and Ueguchi-Tanaka, M.** (2014) DELLA protein functions as a transcriptional activator through the DNA binding of the indeterminate domain family proteins. *Proceedings of the National Academy of Sciences of the United States of America*, **111**, 7861-7866.
- Zhang, J., Elo, A. and Helariutta, Y.** (2011) Arabidopsis as a model for wood formation. *Current Opinion in Biotechnology*, **22**, 293-299.
- Zhang, Q., Xie, Z., Zhang, R., Xu, P., Liu, H., Yang, H.Q., Doblin, M.S., Bacic, A. and Li, L.** (2018) Blue light regulates secondary cell wall thickening via MYC2/MYC4 activation of the NST1-directed transcriptional network in Arabidopsis. *Plant Cell*.
- Zhao, S. and Fernald, R.D.** (2005) Comprehensive algorithm for quantitative real-time polymerase chain reaction. *Journal of computational biology : a journal of computational molecular cell biology*, **12**, 1047-1064.
- Zhao, Z., Andersen, S.U., Ljung, K., Dolezal, K., Miotk, A., Schultheiss, S.J. and Lohmann, J.U.** (2010) Hormonal control of the shoot stem-cell niche. *Nature*, **465**, 1089-1092.
- Zhong, R. and Ye, Z.H.** (1999) IFL1, a gene regulating interfascicular fiber differentiation in Arabidopsis, encodes a homeodomain-leucine zipper protein. *Plant Cell*, **11**, 2139-2152.
- Zhou, Y., Liu, X., Engstrom, E.M., Nimchuk, Z.L., Pruneda-Paz, J.L., Tarr, P.T., Yan, A., Kay, S.A. and Meyerowitz, E.M.** (2014) Control of plant stem cell function by conserved interacting transcriptional regulators. *Nature*, **517**, 377.

8 Appendices

8.1 Published article 1:

Novel tools for quantifying secondary growth.

This is a review based on the current literature. LR wrote the review together with AW, MBT and PBR. MBT contributes with the pictures used in figure 1.

Author	Author position	Scientific ideas %	Data generation %	Analysis & interpretation %	Paper writing %
Anna Wunderling (AW)	1	20	Not applicable	Not applicable	20
Mehdi Ben Targem (MBT)	2	10	Not applicable	Not applicable	10
Pierre Barbier de Reuille (PBR)	3	20	Not applicable	Not applicable	20
Laura Ragni (LR)	4	50	Not applicable	Not applicable	50
Titel of paper: Novel tools for quantifying secondary growth					
Status in publication process: Accepted					



REVIEW PAPER

Novel tools for quantifying secondary growth

Anna Wunderling¹, Mehdi Ben Targem¹, Pierre Barbier de Reuille² and Laura Ragni^{1,*}

¹ ZMBP, University of Tübingen, Auf der Morgenstelle 32, D-72076 Tübingen, Germany

² University of Bern, Altenbergrain 21, CH-3013 Bern, Switzerland

* Correspondence: laura.ragni@zmbp.uni-tuebingen.de

Received 20 July 2016; Editorial decision 9 November 2016; Accepted 9 November 2016

Editor: Simon Turner, University of Manchester

Abstract

Secondary growth occurs in dicotyledons and gymnosperms, and results in an increased girth of plant organs. It is driven primarily by the vascular cambium, which produces thousands of cells throughout the life of several plant species. For instance, even in the small herbaceous model plant *Arabidopsis*, manual quantification of this massive process is impractical. Here, we provide a comprehensive overview of current methods used to measure radial growth. We discuss the issues and problematics related to its quantification. We highlight recent advances and tools developed for automated cellular phenotyping and its future applications.

Key words: *Arabidopsis*, automated cellular phenotyping, machine learning, quantitative histology, secondary growth.

Introduction

Secondary growth, the radial thickening of plant organs, is a large-scale process: thousands of cells are produced by the vascular cambium throughout the life of most woody dicotyledonous plants and gymnosperms (Spicer and Groover, 2010; Ragni and Hardtke, 2014; Zhang *et al.*, 2014). It occurs in the root, hypocotyl and stem of the herbaceous model species *Arabidopsis thaliana* (*Arabidopsis*). However, even in this relatively small model plant, soon after secondary growth begins, cell abundance is too large to perform manual quantifications effectively (Sankar *et al.*, 2014).

Vascular anatomical disposition differs throughout the plant kingdom, depending on the species, the organ considered, and even the developmental stage. For instance, during secondary growth in *Arabidopsis*, the root and hypocotyl rearrange their vasculature from a diarch symmetry (with two opposite initial phloem and xylem poles) to a fully radial symmetry (with a ring of cambial cells that produces inward daughter cells, which will differentiate into xylem and outward daughter cells that will develop into phloem) (Esau,

1977; Dolan and Roberts, 1995; Chaffey *et al.*, 2002; Ragni and Hardtke, 2014). In contrast, in the stem, secondary growth arises with the formation of the fascicular cambia in the 7–8 collateral bundles and later with the formation of an interfascicular cambium, which connects the bundles (Esau, 1977; Altamura *et al.*, 2001; Ragni and Hardtke, 2014).

Another lateral meristem that contributes to the increase in girth of plant organs is the cork cambium or phellogen. It produces the phelloderm on the inner side and the cork or phellem tissues on the outer side. In many plant species, cork cells develop into suberized dead cells at maturity. Together with the phellogen, the phelloderm and phellem form the periderm (Esau, 1977). The periderm replaces the epidermis in stems, branches, and roots of most dicotyledons, and gymnosperms once the latter can no longer accommodate radial growth. The periderm acts as a protective barrier against biotic and abiotic stress (Pereira, 2011). Furthermore, the parenchymatic components of the phelloderm fulfill a function in storing starch (Esau, 1977).

The periderm can be studied in the root and hypocotyl of *Arabidopsis* (Dolan and Roberts, 1995; Chaffey *et al.*, 2002). Working with the *Arabidopsis* hypocotyl offers several advantages because radial growth progression can be easily followed over time (as elongation and secondary growth are uncoupled) and the disposition of the vasculature is reminiscent of trees. Together these features make the *Arabidopsis* hypocotyl a good model to study secondary growth (Chaffey *et al.*, 2002; Ragni and Hardtke, 2014). Briefly, hypocotyl secondary growth can be divided into two phases based on cell morphology and proliferation rate: an early phase in which xylem mainly comprises water-conducting cells and parenchyma, and a later phase of so-called xylem expansion in which xylem occupancy is increased and fibers differentiate (Chaffey *et al.*, 2002; Sibout *et al.*, 2008).

Many factors controlling vascular secondary growth have been identified (see the following reviews for more detail: Furuta *et al.*, 2014; Zhang *et al.*, 2014; Jouannet *et al.*, 2015; De Rybel *et al.*, 2016). However, not all the players are known, and the spatio-temporal regulation of radial growth is far from being understood. In this review, we will provide an overview of the issues posed by secondary growth quantification. Moreover, we will present approaches and tools that have the potential to advance the field.

Current approaches for the quantification of secondary growth

In tree species, overall secondary growth is traditionally quantified as stem diameter at reference internode positions, while more accurate analyses are achieved by measuring tissue widths, number of cells per tissue files, distances between tissues (i.e. distance from the outer bark to the pith), or a combination of these measurements (such as the ratio between the width of the wood and the stem radius) (Nieminen *et al.*, 2008; Etchells *et al.*, 2015; Miguel *et al.*, 2016). Similarly, in the model plant *Arabidopsis*, overall secondary growth is quantified as diameter or the area of the different organs (the stem, the root, and the hypocotyl) (Altamura *et al.*, 2001; Chaffey *et al.*, 2002).

More specific parameters can be used to quantify *Arabidopsis* stem radial growth as the number of cells per vascular bundle, the tangential over radial ratio of vascular bundles, the lateral extension of the tissue produced by the interfascicular cambium, and the acropetal progression of interfascicular cambium initiation along the stem (Sehr *et al.*, 2010; Agusti *et al.*, 2011a, b; Etchells *et al.*, 2012, 2013) (Fig. 1A). For the *Arabidopsis* hypocotyl and root, valid alternatives to diameter length are the xylem over total area ratio (xylem occupancy) (Fig. 1B) or the xylem over phloem area ratio (Sibout *et al.*, 2008). More insights on xylem composition can be obtained by macerating woody samples to estimate the relative number of different cell types and their characteristics, such as shape and size (Franklin, 1945; Chaffey *et al.*, 2002; Muñiz *et al.*, 2008; Ragni *et al.*, 2011) or by measuring the so-called ‘xylem 1’ (vessels and parenchyma) and ‘xylem 2’ (fibers and vessels) (Fig. 1C) (Chaffey *et al.*, 2002; Liebsch *et al.*, 2014).

Challenges of secondary growth quantification

Many of the previously mentioned approaches only coarsely describe radial growth and do not capture its complexity at the morphological and temporal level. For instance, a reduction of hypocotyl area does not always reflect an overall reduction in cell proliferation. It could be due to small changes in cell sizes that cannot be easily detected by eye, or by an increased/decreased proliferation rate in one specific tissue. Along the same lines, both the presence of larger xylem vessels and more cell divisions could account for higher xylem occupancy in the hypocotyl radial section (Sankar *et al.*, 2014; Lehmann and Hardtke, 2016). To be able to account for these growth patterns, it is necessary to track and quantify growth at a cellular level (Sankar *et al.*, 2014).

However, manual quantification of secondary growth morphodynamics is impractical even in the tiny *Arabidopsis* plant, as there are >15 000 cell files in a mature hypocotyl. Moreover, the quantification of vascular morphodynamics is hampered not only by the scale of the process but also by the inaccessibility of certain tissues due to their deep location

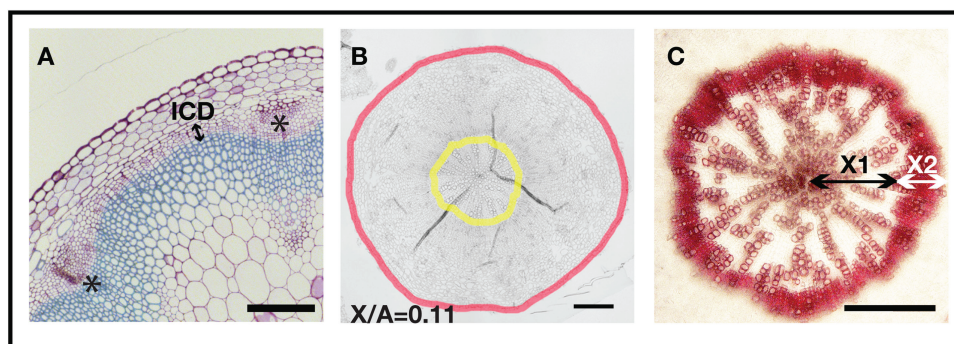


Fig. 1. Examples of secondary growth quantification. Cross-sections of plastic-embedded *Arabidopsis*: (A) Col-0 stem, 0.5 cm from the base of a 9-week-old plant; (B) Col-0 hypocotyl at 12 d after flowering. X/A, ratio between the xylem area and the total area; ICD, interfascicular cambium-derived tissue; * vascular bundle. (C) Vibratome section of *Arabidopsis* hypocotyl (Col-0, 15 d after flowering) stained with phluoroglucinol (in red) showing how ‘xylem 1’ (X1) and ‘xylem 2’ (X2) are measured. Scale bar=200 μ m.

such as the xylem. Consequently, live imaging is challenging, and the majority of the measurements are achieved on cross-sections of embedded fixed samples. Thus, temporal resolution is also limited by sample preparation.

A further aspect to consider is that severe defects in radial growth often coincide with decreased plant viability. This renders the isolation of such plants challenging and the interpretation of those results even more difficult, as it is arduous to distinguish the direct contribution to secondary growth from pleiotropic effects. Thus, many studies rely on weak alleles or partially redundant contexts, in which plant fitness is not affected and phenotypes are mild. Therefore, quantification of secondary growth will benefit from novel tools for automated cellular phenotyping (Sankar *et al.*, 2014; Lehmann and Hardtke, 2016).

Finally, it is important to emphasize that secondary growth studies in Arabidopsis should be normalized to the developmental stage rather than to absolute age, as flowering greatly influences secondary growth progression. For instance, it triggers xylem expansion and fiber formation in the root and in the hypocotyl (Sibout *et al.*, 2008; Ragni *et al.*, 2011; Ragni and Hardtke, 2014).

Quantitative histology

In the last few years, the increasing volume of genotyping data, generated using low-cost sequencing technology, has shifted attention from more efficient genotyping to more automated and precise phenotyping. However, while high-throughput plant phenotyping is well developed for laboratory and field experiments in model and crop plants, automated cellular phenotyping is still a novel field and it has only recently been applied to secondary growth (Sankar *et al.*, 2014; Hall *et al.*, 2016; Lehmann and Hardtke, 2016). Sankar *et al.* (2014) define ‘quantitative histology’ as an automated identification/quantification of cell types and cellular morphological descriptors in a tissue.

Several pipelines, such as RootScan, RootAnalyzer, PHIV-RootCell, and the method of Montenegro-Johnson and colleagues exist for the characterization and quantification of primary root growth (Burton *et al.*, 2012; Chopin *et al.*, 2015; Lartaud *et al.*, 2015; Montenegro-Johnson *et al.*, 2015). These tools were developed to classify rice, wheat, and Arabidopsis roots, respectively. To ensure a high quality classification, these methods exploit *a priori* knowledge of root architecture (Burton *et al.*, 2012; Chopin *et al.*, 2015; Lartaud *et al.*, 2015; Montenegro-Johnson *et al.*, 2015). This renders their usage

very specific and not easy to adapt to other species or organs. More recently, two methods for automating cell extraction, quantitative shape analysis and cell type classification (in any 2D tissue of interest), were developed independently (Sankar *et al.*, 2014; Hall *et al.*, 2016). Relying on generic machine learning (ML) methods, these protocols can be generalized and applied to tissues other than those used in the respective studies. For this reason, these methods can really form the basis of the so-called ‘quantitative histology’.

In more detail, both approaches rely on similar methodology, splitting the task into four steps: (i) image acquisition; (ii) image pre-processing; (iii) image segmentation and feature extraction; and (iv) cell type classification (Sankar *et al.*, 2014; Hall *et al.*, 2016) (Table 1; Fig. 2).

Image acquisition is one of the most critical steps, and its importance has often been underestimated. The quality and the nature of the pictures acquired greatly influence the ease with which the other steps in the pipeline can be performed (i.e. images that are suited for segmentation required less pre-processing). A related point is the standardization of the image acquisition process among experiments; parameters will not change if the images are acquired in the same way and in the same conditions, allowing large-scale samples. Due to the fact that live imaging of thick organs, such as the hypocotyl during secondary growth, is still impossible with conventional microscopy, both methods rely on grayscale images of cross-sections of fixed samples. Thus, an additional step of sample preparation is required. The approach of Sankar *et al.* (2014) uses high-resolution images of plastic-embedded sections of fixed material, acquired using the tiling/stitching function of a microscope with a motorized stage (Fig. 2A). In contrast, Hall and colleagues use laser scanning confocal images of vibratome sections in which cell borders were outlined by fluorescent staining of the cell wall (Hall *et al.*, 2016). Both strategies have advantages and disadvantages. Sample preparation for the first approach is easier at young developmental stages, and image resolution is higher, whereas the segmentation/pre-processing processes are slightly more difficult compared with confocal images (confocal images have less background and shadows). Moreover, only the procedure of Hall and colleagues allows the measurement of an additional fluorescent signal. A minor limitation of both protocols and still a general issue of secondary growth quantification is that radial growth is normally measured in cross-sections, and thus only in 2D (Lehmann and Hardtke, 2016).

After acquisition, the pre-processing transforms the images to improve the segmentation. This step is tightly linked to the

Table 1. Key steps of ‘quantitative histology’ methods for secondary growth

Step	Description	Sankar <i>et al.</i> (2014)	Hall <i>et al.</i> (2016)
0	Sample preparation	Microtome sections Plastic-embedded tissue	Vibratome sections Calcofluor white staining
1	Image acquisition	Light microscopy Stitching/tiling	Laser confocal microscopy
2	Image pre-processing	Gamma contrast Gaussian blur	Gaussian blur
3	Segmentation and features extraction	Watershed algorithm Morphometric features	Watershed algorithm Morphometric features Fluorescence signal intensity
4	Cell type classification	Machine learning (SVM)	Machine learning (random Forest)

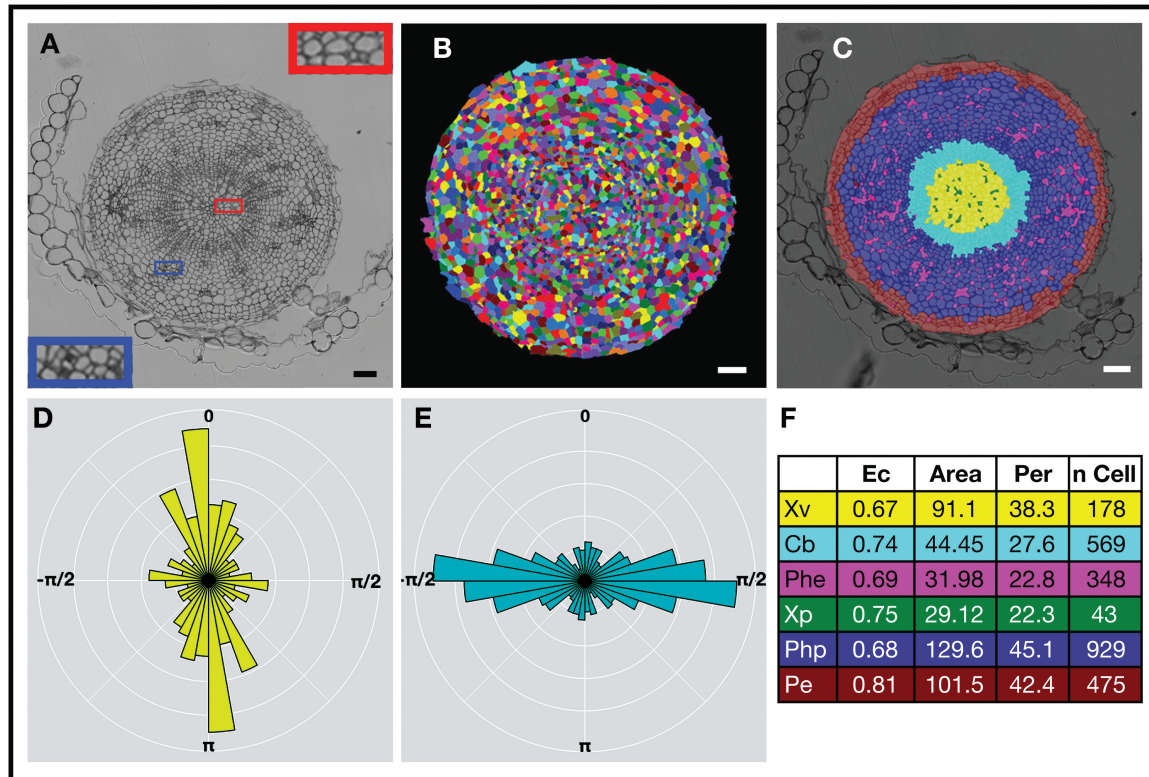


Fig. 2. Example of the ‘quantitative histology’ approach. In (A–C) the same *Arabidopsis* hypocotyl section (Col-0 21 d after germination) is presented. (A) Row image, red box magnification showing details of the xylem, blue box magnification showing details of phloem. (B) Image after pre-processing and segmentation with a watershed algorithm; each color basin represents one cell. (C) Labeled image using a machine learning (ML) approach. Every color represents a cell type: yellow, xylem vessels (Xv); cyan, cambium (Cb); magenta, phloem elements (Phe); green, xylem parenchyma (Xp); blue, phloem parenchyma (Php); brown, periderm (Pe). (D) Rose diagram of the incline angles of the xylem vessels measured in (C). For instance, a value of 0 represents radial/anticlinal orientation, and a value of $\pi/2$ represents orthoradial/periclinal orientation. (E) Rose diagram of the incline angles of the cambial cells measured in (C). (F) Average of some features [eccentricity (Ec), area, perimeter (Per)] and cell numbers (n Cell) for each cell type measured in (C). Scale bar=100 μm .

imaging method and to the segmentation algorithm used. Both methods apply a series of filters to remove or reduce noise and reinforce the contrast. For instance, Sankar *et al.* (2014) use a Gaussian blur to filter out high-frequency noise, followed by a gamma adjustment to improve the general contrast of the image, while Hall *et al.* (2016) use only a blur for denoising.

The segmentation is the process in which objects (in our case cells) are identified and extracted from the background and from each other. More precisely, a label is assigned to every pixel of the image, and pixels with the same label share certain characteristics (i.e. belong to the same cell). The two approaches rely on a common algorithm for the segmentation of grayscale images: the watershed algorithm (Fig. 2B) (Vincent and Soille, 1991; Yoo *et al.*, 2002; Barbier de Reuille *et al.*, 2005, 2015; Pound *et al.*, 2012). Briefly, the watershed algorithm is based on the geographical concept of the watershed and catchment basin. In geography, a catchment basin is a region of a map in which water flows into the same lake or basin, while the watersheds are the limits at which water would enter different catchment basins. An image can be seen as a topographical surface where high pixel intensity corresponds to ‘high’ regions and low pixel intensity refers to ‘low’ regions; thus we can apply the same geographical definitions to this virtual map. For instance, if the cell wall is brighter than the

cell content, we can identify cells as catchment basins for the segmentation process (Fig. 2B) (Vincent and Soille, 1991).

The accuracy of the segmentation is critical, as mis-segmented cells are likely to be wrongly classified. After the segmentation, cellular features/descriptors such as cell area, cell perimeter, position of the cell, and cell eccentricity are computed for every cell. The computation of the features is achieved using conceptually similar toolboxes (Pau *et al.*, 2010) (<http://www.diplib.org/main>). Moreover, the incline angle—the angle formed by the major axis of the cell with the radius of the sample—is calculated in both protocols (Sankar *et al.*, 2014; Hall *et al.*, 2016). In addition, Hall *et al.* (2016) measured cell lumen area, and the cell wall area.

Cell type classification is achieved through an ML approach (Fig. 2C). The basic principle of ML is to teach computers to: (i) analyze existing data effectively; (ii) extract underlying similarity/differences; and (iii) generate a classifier/pattern to apply to new data (Bastanlar and Ozuysal, 2014; Ma *et al.*, 2014; Libbrecht and Noble, 2015; Angermueller *et al.*, 2016; Singh *et al.*, 2016). The first step is the creation of a training set, a set of images that is used to learn the model, in which the cell types of interest are manually labeled. The second step is the choice of the features that better describe each class of cells. Then, different algorithms for supervised classification can be used to create the classifier. Sankar and colleagues used a Support Vectors Machine (SVM)

algorithm, whereas Hall and colleagues reported to have better performances using a random Forest algorithm (please refer to the following reviews for a comprehensive overview on ML algorithms: Bastanlar and Ozuysal, 2014; Ma *et al.*, 2014; Libbrecht and Noble, 2015; Angermueller *et al.*, 2016; Singh *et al.*, 2016). Then, the classifier performances are tested against the so-called test set, a fraction of the training set, until they are satisfactory (several rounds of optimization may be necessary). Finally, the classifier is used to label cells (identify the different cell types) on a running set (a set of segmented images that was not manually labeled) (Fig. 2C). Sankar and colleagues also proposed an automated filter to correct mislabeled cells. Indeed, they reported that at later developmental stages, in some cases xylem identity was assigned to phloem parenchymatic cells. In such cases an automated quality check, based on manually created masks of the total area and of the xylem area, was implemented and used (Sankar *et al.*, 2014).

In summary, the final output of the two approaches regarding identification of the cell type is rather comparable as both methods allow the quantification of similar features and cell types with accuracy >85% (Fig. 2F). However, the choice of the method should be dictated by the research focus/interests. For instance, we recommend the method of Hall and colleagues to study problems related to cell wall integrity, whereas we suggest the method of Sankar *et al.* for temporal analyses (developmental series with several time points).

Current and futures applications of 'quantitative histology'

A proof of concept of 'quantitative histology' approaches is the detailed characterization of two Arabidopsis accessions that display differences in secondary growth progression: Ler and Col-0 (Ragni *et al.*, 2011). The characterization of the morphodynamics between Ler and Col-0 revealed that overall secondary growth is more prominent in Col-0, whereas xylem occupancy is higher in Ler. This is not primarily due to cell size, although xylem cells in Ler are slightly bigger, but rather due to a decrease in phloem proliferation in Ler (Sankar *et al.*, 2014). Another remarkable observation is that the spatio-temporal dynamics of the incline angles reflect the different phases of secondary growth of the Arabidopsis hypocotyl. For instance, at young stages (15 d), the inclines are uniformly distributed. At ~20 d, xylem cells are radial and cambial cells orthoradial, and the overall distribution starts to be bi-modal (Fig. 2D, E) (Sankar *et al.*, 2014). In addition, this type of analysis pointed out some unexpected findings such as that the cambium produces more overall phloem than xylem, even though xylem occupancy is increasing during plant development, and that the enhanced xylem occupancy in Ler is not due to an increase of xylem cell numbers but mainly due to a decrease in phloem area.

Hall *et al.* (2016) validated their approach characterizing *knotted1-like 1* (*knot1*)/*brevipedicellus* (*bp*) loss-of-function mutants. The *knot1* mutant is suitable for a test as it exhibits reduced fiber cell number, combined with a decrease in xylem vessel area and altered cell wall deposition (Liebsch *et al.*, 2014). In addition, they quantified xylan abundance across

different cell types, coupling the intensity of a fluorescent signal (immunostaining of the xylan) with the cell type classification and the morphometric data. Other components of the cell walls (such as cellulose, lignin, and callose), which can be visualized by immunolabeling techniques, could be easily measured together with the cell morphological descriptors, paving the way for the analyses of the chemical composition of the cell wall with spatial resolution (Hall *et al.*, 2016).

Another future application is to combine the automated cellular phenotyping with genome-wide association studies (GWAS). Strikingly, natural variation is still a largely untapped resource for the study of secondary growth. However, a large degree of variability in radial growth-related traits was observed in the hypocotyl of a small collection of Arabidopsis accessions, confirming the potential of this approach (Sibout *et al.*, 2008; Ragni *et al.*, 2011). Another aspect of secondary growth that can be further explored with more accurate phenotyping techniques is how secondary growth is modulated during changes of environmental conditioned and abiotic stresses.

So far, Sankar *et al.* (2014) and Hall *et al.* (2016) have tested their approaches only in the Arabidopsis hypocotyls. However, we expect to see the 'quantitative histology' approaches exploited in other plant species (tomato, poplar, etc.), as they are quite versatile and easy to adapt. For instance, we foresee minor tuning of the segmentation and machine learning parameters for the application to other organisms (as long as the images can be easily segmented). In addition, Hall *et al.* (2016) provide their method as a MATLAB package, with a graphical interface, and thus it does not require any coding by the user. Along the same lines, the 'quantitative histology' approach by Sankar *et al.* (2014) was recently implemented in the open source platform LithoGraphX [www.lithographx.org; a fork of MorphoGraphX (Barbier de Reuille *et al.*, 2015)] to render it accessible to biologists. Other advantages of the implementation on this platform are: (i) the reduced computational time for the segmentation process; (ii) the possibility to use several types of images as input (laser confocal images, grayscale images, and color images) and several pre-processing tools; and (iii) the choice between the two ML algorithms (Barbier de Reuille and Ragni, 2017). Moreover, in LithoGraphX it is possible to perform the Hall *et al.* approach or other protocols, as LithoGraphX was initially developed for the analyses of confocal images and offers a variety of tools for measuring fluorescent signal intensity.

A possible future implementation is to add tissue-specific features to improve cell type classification of problematic tissues. For instance, phloem companion cells and sieve elements are difficult to distinguish from one another (Sankar *et al.*, 2014). In fact the morphology of these cell types is nearly identical, which hampers the ML recognition process. Adding tissue-specific features such as the number of neighboring cells, cell wall thickness, or a particular stain should resolve this problem.

Conclusions and perspectives

In summary, it is fair to conclude that secondary growth characterization will benefit from precise quantification at the

cellular level. ‘Quantitative histology’ paves the way towards the study of secondary growth with good spatio-temporal resolution: it facilitates the measurement of complex traits and mild phenotypes. We foresee that automated cellular phenotyping will boost natural variation studies and will soon be applied to other species.

To date, the rate-limiting step of ‘quantitative histology’ methods is sample preparation/image acquisition. This is especially true for secondary growth studies where sample preparation is laborious and not yet automatized. Any improvements in this direction will contribute to render the ‘quantitative histology’ approaches routine protocols. A major breakthrough will be to image live secondary growth progression. This will open the door to the study of secondary growth in 3D and 4D.

Acknowledgements

This work was supported by a DFG grant (RA-2590/1-1) and by the SystemsX.ch, the Swiss Initiative in Systems Biology. LR is indebted to the Baden-Württemberg Stiftung for the financial support of this research project by the Elite programme for Postdocs. We thank Dr Azahara Barra-Jiménez and Dr Kristine Hill for critical reading.

References

- Agusti J, Herold S, Schwarz M, et al.** 2011a. Strigolactone signaling is required for auxin-dependent stimulation of secondary growth in plants. *Proceedings of the National Academy of Sciences, USA* **108**, 20242–20247.
- Agusti J, Lichtenberger R, Schwarz M, Nehlin L, Greb T.** 2011b. Characterization of transcriptome remodeling during cambium formation identifies MOL1 and RUL1 as opposing regulators of secondary growth. *PLoS Genetics* **7**, e1001312.
- Altamura MM, Possenti M, Matteucci A, Baima S, Ruberti I, Morelli G.** 2001. Development of the vascular system in the inflorescence stem of *Arabidopsis*. *New Phytologist* **151**, 381–389.
- Angermueller C, Pärnamaa T, Parts L, Stegle O.** 2016. Deep learning for computational biology. *Molecular Systems Biology* **12**, 878.
- Barbier de Reuille P, Bohn-Courseau I, Godin C, Traas J.** 2005. A protocol to analyse cellular dynamics during plant development. *The Plant Journal* **44**, 1045–1053.
- Barbier de Reuille P, Ragni L.** 2017. Vascular morphodynamics during secondary growth. *Methods in Molecular Biology* **1544**, in press.
- Barbier de Reuille P, Routier-Kierzkowska A-L, Kierzkowski D, et al.** 2015. MorphoGraphX: a platform for quantifying morphogenesis in 4D. *eLife* **4**, 05864.
- Baştanlar Y, Ozuysal M.** 2014. Introduction to machine learning. *Methods in Molecular Biology* **1107**, 105–128.
- Burton AL, Williams M, Lynch JP, Brown KM.** 2012. RootScan: software for high-throughput analysis of root anatomical traits. *Plant and Soil* **357**, 189–203.
- Chaffey N, Cholewa E, Regan S, Sundberg B.** 2002. Secondary xylem development in *Arabidopsis*: a model for wood formation. *Physiologia Plantarum* **114**, 594–600.
- Chopin J, Laga H, Huang CY, Heuer S, Miklavcic SJ.** 2015. RootAnalyzer: a cross-section image analysis tool for automated characterization of root cells and tissues. *PLoS One* **10**, e0137655.
- De Rybel B, Mähönen AP, Helariutta Y, Weijers D.** 2016. Plant vascular development: from early specification to differentiation. *Nature Reviews. Molecular Cell Biology* **17**, 30–40.
- Dolan L, Roberts K.** 1995. Secondary thickening in roots of *Arabidopsis thaliana*: anatomy and cell surface changes. *New Phytologist* **131**, 121–128.
- Esau K.** 1977. *Anatomy of seed plants*. Chichester, UK: Wiley.
- Etechells JP, Mishra LS, Kumar M, Campbell L, Turner SR.** 2015. Wood formation in trees is increased by manipulating PXY-regulated cell division. *Current Biology* **25**, 1050–1055.
- Etechells JP, Provost CM, Mishra L, Turner SR.** 2013. WOX4 and WOX14 act downstream of the PXY receptor kinase to regulate plant vascular proliferation independently of any role in vascular organisation. *Development* **140**, 2224–2234.
- Etechells JP, Provost CM, Turner SR.** 2012. Plant vascular cell division is maintained by an interaction between PXY and ethylene signalling. *PLoS Genetics* **8**, e1002997.
- Franklin GL.** 1945. Preparation of thin sections of synthetic resins and wood-resin composites, and a new macerating method for wood. *Nature* **155**, 51.
- Furuta KM, Hellmann E, Helariutta Y.** 2014. Molecular control of cell specification and cell differentiation during procambial development. *Annual Review of Plant Biology* **65**, 607–638.
- Hall HC, Fakhzadeh A, Luengo Hendriks CL, Fischer U.** 2016. Precision automation of cell type classification and sub-cellular fluorescence quantification from laser scanning confocal images. *Frontiers in Plant Science* **7**, 119.
- Jouannet V, Brackmann K, Greb T.** 2015. (Pro)cambium formation and proliferation: two sides of the same coin? *Current Opinion in Plant Biology* **23**, 54–60.
- Lartaud M, Perin C, Courtois B, et al.** 2015. PHIV-RootCell: a supervised image analysis tool for rice root anatomical parameter quantification. *Frontiers in Plant Science* **5**, 790.
- Lehmann F, Hardtke CS.** 2016. Secondary growth of the *Arabidopsis* hypocotyl—vascular development in dimensions. *Current Opinion in Plant Biology* **29**, 9–15.
- Libbrecht MW, Noble WS.** 2015. Machine learning applications in genetics and genomics. *Nature Reviews. Genetics* **16**, 321–332.
- Liebsch D, Sunaryo W, Holmlund M, et al.** 2014. Class I KNOX transcription factors promote differentiation of cambial derivatives into xylem fibers in the *Arabidopsis* hypocotyl. *Development* **141**, 4311–4319.
- Ma C, Zhang HH, Wang X.** 2014. Machine learning for Big Data analytics in plants. *Trends in Plant Science* **19**, 798–808.
- Miguel A, Milhinhos A, Novák O, Jones B, Miguel CM.** 2016. The SHORT-ROOT-like gene *PtSHR2B* is involved in *Populus* phellogen activity. *Journal of Experimental Botany* **67**, 1545–1555.
- Montenegro-Johnson TD, Stamm P, Strauss S, Topham AT, Tsagris M, Wood AT, Smith RS, Bassel GW.** 2015. Digital single-cell analysis of plant organ development using 3DCellAtlas. *The Plant Cell* **27**, 1018–1033.
- Muñiz L, Minguet EG, Singh SK, Pesquet E, Vera-Sirera F, Moreau-Courtois CL, Carbonell J, Blázquez MA, Tuominen H.** 2008. ACAULIS5 controls *Arabidopsis* xylem specification through the prevention of premature cell death. *Development* **135**, 2573–2582.
- Nieminen K, Immanen J, Laxell M, et al.** 2008. Cytokinin signaling regulates cambial development in poplar. *Proceedings of the National Academy of Sciences, USA* **105**, 20032–20037.
- Pau G, Fuchs F, Sklyar O, Boutros M, Huber W.** 2010. EBIImage—an R package for image processing with applications to cellular phenotypes. *Bioinformatics* **26**, 979–981.
- Pereira H.** 2011. *Cork: biology, production and uses*. Amsterdam: Elsevier Science.
- Pound MP, French AP, Wells DM, Bennett MJ, Pridmore TP.** 2012. CellSeT: novel software to extract and analyze structured networks of plant cells from confocal images. *The Plant Cell* **24**, 1353–1361.
- Ragni L, Hardtke CS.** 2014. Small but thick enough—the *Arabidopsis* hypocotyl as a model to study secondary growth. *Physiologia Plantarum* **151**, 164–171.
- Ragni L, Nieminen K, Pacheco-Villalobos D, Sibout R, Schwechheimer C, Hardtke CS.** 2011. Mobile gibberellin directly stimulates *Arabidopsis* hypocotyl xylem expansion. *The Plant Cell* **23**, 1322–1336.

- Sankar M, Nieminen K, Ragni L, Xenarios I, Hardtke CS.** 2014. Automated quantitative histology reveals vascular morphodynamics during *Arabidopsis* hypocotyl secondary growth. *eLife* **3**, e01567.
- Sehr EM, Agusti J, Lehner R, Farmer EE, Schwarz M, Greb T.** 2010. Analysis of secondary growth in the *Arabidopsis* shoot reveals a positive role of jasmonate signalling in cambium formation. *The Plant Journal* **63**, 811–822.
- Sibout R, Plantegenet S, Hardtke CS.** 2008. Flowering as a condition for xylem expansion in *Arabidopsis* hypocotyl and root. *Current Biology* **18**, 458–463.
- Singh A, Ganapathysubramanian B, Singh AK, Sarkar S.** 2016. Machine learning for high-throughput stress phenotyping in plants. *Trends in Plant Science* **21**, 110–124.
- Spicer R, Groover A.** 2010. Evolution of development of vascular cambia and secondary growth. *New Phytologist* **186**, 577–592.
- Vincent L, Soille P.** 1991. Watersheds in digital spaces: an efficient algorithm based on immersion simulations. *IEEE Transactions on Pattern Analysis and Machine Intelligence* **13**, 583–598.
- Yoo TS, Ackerman MJ, Lorensen WE, Schroeder W, Chalana V, Aylward S, Metaxas D, Whitaker R.** 2002. Engineering and algorithm design for an image processing Api: a technical report on ITK—the Insight Toolkit. *Studies in Health Technology and Informatics* **85**, 586–592.
- Zhang J, Nieminen K, Serra JA, Helariutta Y.** 2014. The formation of wood and its control. *Current Opinion in Plant Biology* **17**, 56–63.

8.2 Published article 2:

A molecular framework to study periderm formation in Arabidopsis

The research was designed by LR and AW. All experiments were performed by AW, DR, ABJ, SM, KS, MBT and LR. MBT contributes to the paper with stem's serie in the different ecotypes, and in measuring.

The data was analyzed and discussed in collaboration with ABJ and LR. LR wrote the article with the help of ABJ and AW.

Author	Author position	Scientific ideas %	Data generation %	Analysis & interpretation %	Paper writing %
Anna Wunderling (AW)	1	30%	35%	30%	20%
Dagmar Ripper	2		20%		
Azahara Barra-Jimenez (ABJ)	3	10%		20%	15%
Stefan Mahn (SM)	4		5%	5%	
Kathrin Sajak (KS)	5		5%	5%	
Mehdi Ben Targem (MBT)	6		5%	5%	5%
Laura Ragni (LR)	7	60%	30%	35%	60%
Titel of paper: A molecular framework to study periderm formation in Arabidopsis					
Status in publication process: Accepted					

A molecular framework to study periderm formation in *Arabidopsis*

Anna Wunderling¹, Dagmar Ripper¹, Azahara Barra-Jimenez¹ , Stefan Mahn¹, Kathrin Sajak¹, Mehdi Ben Targem¹ and Laura Ragni¹ 

ZMBP-Center for Plant Molecular Biology, University of Tübingen, Auf der Morgenstelle 32, D-72076 Tübingen, Germany

Author for correspondence:

Laura Ragni

Tel: +49 (0)7071 29 76677

Email: laura.ragni@zmbp.uni-tuebingen.de

Received: 18 December 2017

Accepted: 19 February 2018

New Phytologist (2018) **219**: 216–229

doi: 10.1111/nph.15128

Key words: *Arabidopsis thaliana*, endodermis, periderm, phellem, programmed cell death (PCD), secondary growth.

Summary

- During secondary growth in most eudicots and gymnosperms, the periderm replaces the epidermis as the frontier tissue protecting the vasculature from biotic and abiotic stresses. Despite its importance, the mechanisms underlying periderm establishment and formation are largely unknown.
- The herbaceous *Arabidopsis thaliana* undergoes secondary growth, including periderm formation in the root and hypocotyl. Thus, we focused on these two organs to establish a framework to study periderm development in a model organism.
- We identified a set of characteristic developmental stages describing periderm growth from the first cell division in the pericycle to the shedding of the cortex and epidermis. We highlight that two independent mechanisms are involved in the loosening of the outer tissues as the endodermis undergoes programmed cell death, whereas the epidermis and the cortex are abscised. Moreover, the phellem of *Arabidopsis*, as in trees, is suberized, lignified and peels off. In addition, putative regulators from oak and potato are also expressed in the *Arabidopsis* periderm.
- Collectively, the periderm of *Arabidopsis* shares many characteristics/features of woody and tuberous periderms, rendering *Arabidopsis thaliana* an attractive model for cork biology.

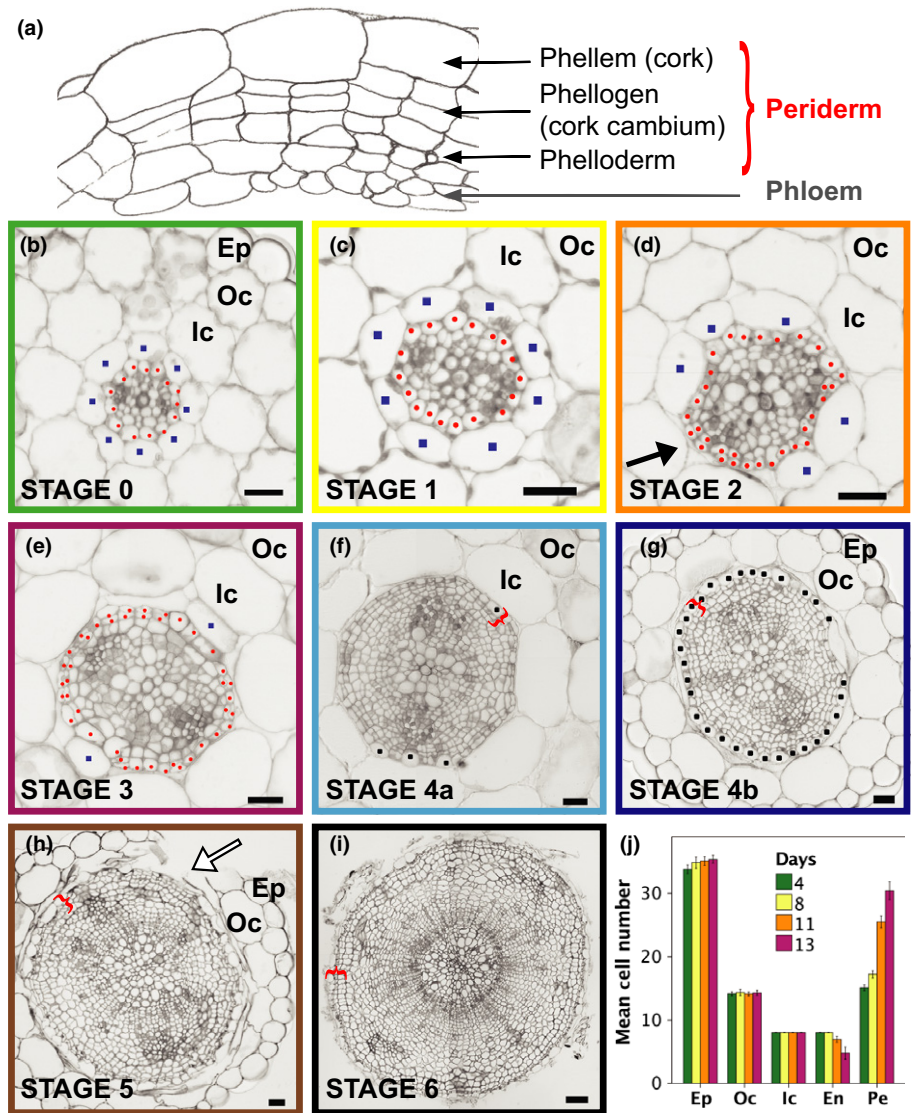
Introduction

Secondary growth, the increase in girth of plant organs, is not only a prerequisite for efficient long-distance transport of water, solutes and photo-assimilates but also shapes the plant body in response to an ever-changing environment. In fact, the emergence of radial thickening contributed to the striking success of vascular plants during evolution (Spicer & Groover, 2010). Moreover, wood represents the major source of biomass accumulation in perennial dicotyledons and gymnosperms (Demura & Ye, 2010). The post-embryonic meristem that drives this process is the vascular cambium. The vascular cambium consists of a ring of undifferentiated meristematic cells that upon division differentiate into xylem (wood) and phloem (bast). Another lateral meristem that contributes to radial thickening and to the protection of the vascular cylinder is the phellogen, also known as cork cambium. The phellogen divides in a strictly bidirectional manner, producing inward the phelloderm and outward the phellem (cork). These three tissues, phellogen, phelloderm and phellem, are collectively referred to as periderm (Fig. 1a).

The periderm is a frontier tissue and its main function is to protect the plant against biotic and abiotic stress, similar to the epidermis during primary development. In particular, it effectively restricts: gas exchange, water loss and pathogen attack (Lulai & Freeman, 2001; Groh *et al.*, 2002; Lenzian, 2006).

Most woody eudicots and gymnosperms form a periderm in the root and the stem, and likewise, underground stems such as potato tubers form an extensive periderm. In the stem of most trees, the first phellogen is formed in the sub-epidermal layer, but in certain species it arises from the epidermis or the phloem. By contrast, in most roots the periderm derives from the pericycle (Esau, 1977). The number of cell layers comprising the periderm varies among species. Usually only one to two layers of phelloderm cell are present in the periderm, whereas several cell layers of phellem differentiate (Esau, 1977; Pereira, 2007). In trees, the phellogen can remain active for several years and/or it can be replaced each year by a new phellogen (Esau, 1977; Pereira, 2007). The phellogen of cork oak, for example, is functional for many years and remains viable throughout the life of a tree, although its activity decreases with age (Waisel, 1995; Pereira, 2007). Furthermore, phellogen activity in trees undergoes seasonal changes and it fluctuates with climatic variations (Waisel, 1995; Caritat *et al.*, 2000; Pereira, 2007). For instance, cold spells and drought cause a decrease in phellogen activity, whereas periods of warm weather result in high activity (Waisel, 1995; Caritat *et al.*, 2000; Pereira, 2007). A 'wound' periderm develops close to damaged or necrotic tissue after mechanical injury (e.g. shedding of branches and leaves) (Tucker, 1975; Thomson *et al.*, 1995; Oven *et al.*, 1999; Neubauer *et al.*, 2012; Khanal *et al.*, 2013) or pathogen infection (Lulai & Corsini, 1998; Thangavel *et al.*, 2016).

Fig. 1 The six stages of periderm development in the *Arabidopsis thaliana* hypocotyl. (a) Illustration of the periderm, which comprises the phellem/cork, the phellogen/cork cambium and the phelloderm. (b–i) Plastic cross-sections of Col-0 hypocotyls, grown in soil under long day (LD) conditions at different time points: (b) 4 d after sowing (das), (c) 8 das, (d) 11 das, (e) 13 das, (f) 16 das, (g) 18 das, (h) 21 das and (i) 27 das. (b) STAGE 0, the stage before the pericycle starts to divide. (c) STAGE 1, the pericycle divides anticlinally and endodermal cells become flatter. (d) vSTAGE 2 is characterized by four to six endodermal cells and by periclinal division in the pericycle, which we refer to as phellogen. (e) STAGE 3: only two endodermal cells in correspondence of the xylem poles subsist. (f) STAGE 4A is characterized by a lack of endodermis and by the differentiation of the first phellem cells. (g) STAGE 4b lacks the inner cortex and exhibits a ring of phellem cells. (h) During STAGE 5, the cortex and the epidermis break and become detached (white arrow). (i) At STAGE 6 the periderm is the outside tissue that protects the vasculature. (j) Quantification of cell number in the epidermis (Ep), outer cortex (Oc), inner cortex (Ic), endodermis (En) and pericycle/periderm (Pe) at different time points (mean cell number \pm 2 SE). Blue squares, endodermal cells; red dots, pericycle/periderm; black dots, phellem cells; red brackets, periderm. Bars, 20 μ m.



To fulfill its barrier role, specialized macromolecules such as suberin are the major components of the phellem cell wall (Pereira, 1988). The chemical and physical properties of phellem have been extensively studied in potato and cork oak, due to the economic importance of improving potato conservation (Neubauer *et al.*, 2013) and of phellem as a material for wine bottle corks and building/insulating. Suberin extracted from the phellem also has industrial applications (Silva *et al.*, 2005) such as the production of hybrid co-polymers (e.g. polyurethanes) (Cordeiro *et al.*, 1999), thermoset resins (Torrón *et al.*, 2014) and high-resistance fibers (de Geus *et al.*, 2010). Suberin is a complex glycerol-based heteropolymer, comprising aliphatic and phenolic fractions and often noncovalently associated waxes (reviewed by Vishwanath *et al.*, 2015). The amount/composition of phellem suberin and waxes varies among species and throughout development; for example, in cork oak it can reach up to 40% of the dry weight (Pereira, 1988; Pinto *et al.*, 2009; Kosma *et al.*, 2015). Lignin is also deposited in the cell wall of the phellem, but it displays a different monolignol composition compared to

wood (Marques & Pereira, 2013; Fagerstedt *et al.*, 2015; Lourenco *et al.*, 2016).

Potato has proven to be a good model to study suberin biosynthesis and periderm water permeability, as periderm can be easily isolated from the tuber in sufficient amounts for chemical analyses. Furthermore, it is possible to measure peridermal transpiration rates (Schreiber *et al.*, 2005). In fact, reverse genetic studies indicate that a reduction of ferulic acid in the potato periderm results in an increased water permeability and defective periderm maturation (Serra *et al.*, 2010). Reducing aliphatic suberin contents results in similar phenotypes, suggesting that both suberin composition and quantity are important for water barrier function (Serra *et al.*, 2009a,b, 2010). Suberin biosynthesis genes have been extensively characterized also in *Arabidopsis*, with particular regard to the chemical composition of the whole root, the endodermis and the seed coat (Beisson *et al.*, 2007; Hofer *et al.*, 2008; Compagnon *et al.*, 2009; Molina *et al.*, 2009; Domergue *et al.*, 2010; Kosma *et al.*, 2012). Furthermore, it has been shown that *ALIPHATIC SUBERIN FERULOYL TRANSFERASE (ASFT)*

and *FATTY ACYL-COA REDUCTASES 1 (FAR1)*, *FAR4* and *FAR5* are expressed in the phellem of roots (Molina *et al.*, 2009; Vishwanath *et al.*, 2013). However, the suberin lamella in the periderm is not disturbed in *asft* mutants (Molina *et al.*, 2009)

Despite the huge progress in understanding the molecular mechanisms underlying cambium and vascular development, very few regulators controlling phellogen establishment and activity have been identified. As far as we know, only the transcription factor (TF) *SHORT-ROOT-like 2B (PttSHRL2B)* has been shown to regulate phellogen activity in poplar (Miguel *et al.*, 2016), whereas it has been suggested that the TF *QsMYB1* (ortholog of Arabidopsis MYB84) coordinates phellogen action in response to drought and heat (Almeida *et al.*, 2013a,b). One possible explanation for this lack of knowledge is that periderm has been mainly studied in nonmodel/amenable species. In contrast to periderm development, our current understanding of the basic mechanisms of cambium activity in woody species is mainly derived from pioneering works in Arabidopsis. In fact, this herbaceous eudicot model plant undergoes secondary growth in the stem, root and hypocotyl and shares common regulatory networks with woody species (reviewed by Barra-Jimenez & Ragni, 2017). The most striking example is the regulatory module involving the receptor-like kinases PHLOEM INTERCALATED WITH XYLEM/TDIF RECEPTOR (PXY/TDR), the small peptide CLV3/EMBRYO SURROUNDING REGION 41/44 (CLE41/CLE44) and the TF WUSCHEL HOMEBOX 4 (WOX4), which controls cambium proliferation in several species including poplar (EtcHELLS *et al.*, 2015; Hirakawa & Bowman, 2015; Kucukoglu *et al.*, 2017).

Here, we propose a framework to study periderm growth in *Arabidopsis thaliana*. We provide a suite of tools to study periderm development, including tissue-specific reporters. In particular, we define distinct stages of periderm growth, considering periderm ontogenesis and the fate of the surrounding tissues. We thus show that periderm growth is tightly connected to the development of the outside tissues and particularly to endodermal programmed cell death (PCD). Finally, we highlight that the Arabidopsis periderm displays characteristics similar to those of a woody eudicot periderm, and that putative regulators are conserved among species. These results are setting the stage for mechanistic insights into periderm growth.

Materials and Methods

Plant material and growth

All lines used are in *A. thaliana* Col-0 background unless otherwise specified. All plants used for confocal microscopy were grown *in vitro* on ½ MS 1% sugar plates under continuous light, unless it is otherwise specified. For the other experiments, light and growing conditions are stated in the text/figure. *GPAT5:mCITRINE-SYP122* (Barberon *et al.*, 2016), *UBQ10:eYFP-NPSN12 (W131Y)* (Geldner *et al.*, 2009), *ASFT:NLS-GFP-GUS*, *GPAT5:NLS-GFP-GUS*, *KCR1:NLS-GFP-GUS*, *RALPH(CYP86B1):NLS-GFP-GUS*, *FAR4:NLS-GFP-GUS*, *HORST:NLS-GFP-GUS*, *DAISY:NLS-GFP-GUS* (Naseer *et al.*,

2012) and *CASP1:CASP1-mCherry* (Vermeer *et al.*, 2014) were gifts from N. Geldner (University of Lausanne, Switzerland). *ESB1:ESB1-mCherry* was kindly provided by D. Salt (University of Aberdeen, UK) and is described by Hosmani *et al.* (2013). *FAR1:GUS*, *FAR5:GUS* were described by Domergue *et al.* (2010) and kindly provided by F. Domergue (CNRS, FR). *PASPA3:H2A-GFP*, *Rxml:H2A-GFP*, *SCPL48:H2A-GFP*, *DPM4:H2A-GFP*, *EXI1:H2A-GFP* were gifts from M. Nowack (VIB, Belgium) and are described by Fendrych *et al.* (2014; Olvera-Carrillo *et al.*, 2015). The *soc1 full* mutants were described by Melzer *et al.* (2008). *SCR:H2B-2xmCherry* (N2106153) was obtained from the NASC and is described by Marques-Bueno *et al.* (2016). The *CASP2:NLS-GFP-GUS* was obtained by the NASC (N69050) and described by Liberman *et al.* (2015).

Histology and staining

Thin plastic sections were obtained as described by Barbier de Reuille & Ragni (2017) and stained with 0.1% toluidine blue and imaged with a Zeiss Axio M2 imager microscope or a Zeiss Axiophot microscope. Vibratome sections (50–80 µm) were obtained, embedding the hypocotyl and/or the root in 6% agarose block, and then cut with a Leica VT-1000 vibratome and collected/visualized in water. For suberin staining, Fluorol yellow 088 (FY) (sc-215052; Santa Cruz, CA, USA) staining was performed as described by Naseer *et al.* (2012). For lignin staining, 0.5% Basic Fuchsin (Sigma) aqueous solution was applied to the root or hypocotyl for 5 min, and samples were then rinsed and mounted in 10% glycerol. Phloroglucinol staining was performed applying a ready solution (26337.180; VWR, Radnor, PA, USA) directly to the vibratome section. For pectin staining, ruthenium red (R2751; Sigma), 0.01% aqueous solution was applied to fresh vibratome sections for 4 min, and sections were then rinsed and mounted in 10% glycerol. Clearing, before autofluorescence detection of the casparian strips, was performed as described by Naseer *et al.* (2012). GUS assays were performed as described by Beisson *et al.* (2007).

Confocal microscopy

All confocal images were acquired as whole-mounts unless specified in the figure legend that vibratome sections were used. Images were acquired with a Leica SP8 with resonant scan or with a Zeiss LSM880 microscope. For FY, green fluorescent protein (GFP) and fluorescein diacetate (FDA): excitation wavelength (ex.) 488 nm; emission (em.) 490–510 nm for yellow fluorescent protein (YFP) and mCherry and Basic Fuchsin: ex. 561 nm; em. 570–630 nm; for phellem autofluorescence: ex. 405 nm; em. 420–500 nm or ex. 405 nm; em. 420–460 nm if combined with GFP or YFP; for phelloderm autofluorescence: ex. 561 nm; em. 576–625 nm. Three-dimensional reconstructions and Ortho Views of a Z-stack were obtained using the ZEN BLACK PRO software.

Image analyses and statistical analyses

The number of cells in the different tissues was quantified using the plug-in CELL COUNTER of FIJI (Schindelin *et al.*, 2012), and cell eccentricity was measured using LITHOGRAPHX (www.lithogra.phx.org) and according to the protocol described by Barbier de Reuille & Ragni (2017). To measure the length of root covered by phellem, whole roots were mounted in water on a microscope slide. Using light microscopy, the point closest to the root tip, where phellem cells begin to be the outside tissue, was marked on the coverslip. The whole root was then traced on the coverslip and the coverslips were subsequently scanned. Phellem length and root length were then measured with the software FIJI (Schindelin *et al.*, 2012). The ratio of phellem length : root length was calculated from at least 15 roots per time point and plant line. To quantify phellem and endodermis cell length and area, Z-stacks of the reporter line *GPAT5:mCITRINE-SYP122* were used. Images were exported with the Ortho View function from the ZEN BLACK PRO software and measured with FIJI (Schindelin *et al.*, 2012). More than 50 cells from at least three independent roots were measured per time point and/or root part. At least three independent experiments were performed and the graphs of one representative experiment each are presented. Statistical analyses were performed using IBM SPSS Statistics version 24. We first tested all datasets for homogeneity of variances using Levene's Test of Equality of Variances. We calculated the significant differences between two datasets using a Welch's *t*-test (not homogenous variance) or a Student's *t*-test (homogeneous variance). The significance threshold was set to $P < 0.05$ (shown by a red asterisk in the figures).

Molecular cloning

The *MYB84* and the *ANAC78* promoters were amplified from genomic DNA with the primers: A-pMYB84F (AACAGGTCTCAACCTCGTGGACTTGGACTTGTTTA) Br-pMYB84R (AACAGGTCTCATGTTACTTGTACTCCTAGTGAAGTC TTG) and A-pANAC78F (AACAGGTCTCAACCTGATCAT TTCAAAGGCATTGTGT) Br-pANAC78R (AACAGGTCTCATGTTCAATCGGTGAAAACCAGAACTTG), respectively, and cloned into pGG-A0 using the GreenGate technology (Lamproulos *et al.*, 2013). The β -glucuronidase coding sequence was recloned into pGG-D0. To obtain the lines *MYB84:NLS-GFP-GUS*, *MYB84:NLS-3xGFP* and *ANAC78:NLS-GFP-GUS*, the final GreenGate reaction was performed including some of the published and publicly available modules: NLS, 3XGFP and GFP (Lamproulos *et al.*, 2013).

Results

Periderm is formed in the root and in the hypocotyl of *Arabidopsis thaliana* under various environmental conditions

To set up a framework to study periderm development, we first investigated in which organs/conditions a periderm is established in *Arabidopsis*. In *Arabidopsis* plants that had undergone

extensive secondary growth, the hypocotyl was fully covered by the phellem (Supporting Information Fig. S1a), whereas in mature primary root, the periderm covered the uppermost part spanning *c.* 20–30% of the root length (Fig. S1b,c). Likewise, a periderm surrounded the oldest part of lateral roots (Fig. S1d). Although most gymnosperms and eudicots produce a periderm in the stem, no periderm has been reported in the *Arabidopsis* stem (Altamura *et al.*, 2001; Agusti *et al.*, 2011; Mazur & Kurczynska, 2012). Consistently, a periderm was not observed at the base of the stem of 12-wk-old plants of commonly used *Arabidopsis* strains such as Col-0, Ler and Ws (Fig. S1e–h). No periderm was detected in the stem of the 24-wk-old *soc1 full1* double mutant (grown under long day (LD) conditions), which is characterized by extended secondary growth and life span (Fig. S1j–l) (Melzer *et al.*, 2008; Davin *et al.*, 2016). Because the periderm is not present in the *Arabidopsis* stem, we continued periderm characterization focusing on the root and hypocotyl.

We analyzed whether periderm development is influenced by photoperiods or growing conditions in the *Arabidopsis* root and hypocotyl. Plants grown *in vitro* (on medium supplemented with (Fig. S2a) or without (Fig. S2b) sugar) in soil (Fig. S2c,d) and under several light conditions (continuous light (CL) (Fig. S2a,b,e), LD (Fig. S2c,f) or short day (SD) conditions (Fig. S2d)) produced a periderm. In general, periderm development reflected plant growth progression: for instance, a periderm was established earlier in plants grown in CL than in LD conditions and in media supplemented with sugar than in media without sugar (Fig. S2). In *Arabidopsis*, flowering has a major influence on secondary growth progression, as it triggers the 'xylem expansion' phase (xylary fiber production and higher xylem-to-phloem ratio) (Sibout *et al.*, 2008). Therefore, we analyzed the temporal relationship between xylem expansion and periderm growth. Under all tested conditions, the periderm was differentiated before flowering occurred and thus establishment of the periderm precedes xylem expansion (Fig. S2g).

Periderm formation follows a predetermined pattern, which can be summarized by six distinct stages

Periderm development in the hypocotyl and in the root was temporally separated, formation occurring much more slowly in the hypocotyl than in the root (Figs 1, S1b,c). As a result, in an 8-d-old plant, the hypocotyl displayed no phellem (Fig. 1c), whereas in the mature part of the primary root (close to the hypocotyl–root junction) some phellem cells were present (Fig. S1b,c). Moreover, as a root represents a gradient of secondary growth, periderm development can be followed along the same root (Fig. 2a), whereas in the hypocotyl it can be analyzed only over time series with plants in different developmental stages (Fig. 1). In both organs the periderm arises from the pericycle – an inner tissue – surrounded by three to four cell layers and it becomes the external tissue once it is fully differentiated. We therefore characterized periderm growth throughout development, considering the fate of the surrounding tissues.

We were able to identify six characteristic stages of periderm development in the hypocotyl and we found that the duration of

each stage was influenced by the growing conditions (Fig. S3a–h). STAGE 0 was designated as the stage before the first division in the pericycle (after hypocotyl elongation occurred). Here, the vasculature was already arranged with a central metaxylem and two phloem poles. The pericycle comprised *c.* 13–14 cells and it was surrounded by eight endodermal, approximately eight inner cortex, *c.* 14 outer cortex and *c.* 33–34 epidermis cells. In the hypocotyl, this stage was present for instance in 3- to 6-d-old plants grown in LD conditions (Fig. 1b,j). In the course of STAGE 1, the pericycle starts to divide (Fig. 1c,j). The first anticlinal divisions occurred at the xylem pole pericycle cells (Fig. S3i). Shortly thereafter, the divisions expanded to the rest of

the pericycle cells. Simultaneously, the endodermal cells became flatter, as shown by a decrease in their eccentricity (Figs 1c, S3j). We defined STAGE 2 as the stage marked by a reduction in the number of endodermal cells (the endodermis comprises four to six cells) as well as by pericycle proliferation (Fig. 1d,j). In more detail, the endodermal cells located at the sites of the phloem poles were missing. The pericycle began to divide periclinally and thus, in some regions, it was possible to distinguish two layers of cells, which hereafter we refer to as phellogen. We classified a periderm to be in STAGE 3 when only one/two endodermal cells located at the xylem poles were still present and the periderm comprised at least two layers of cells. Interestingly, the number of

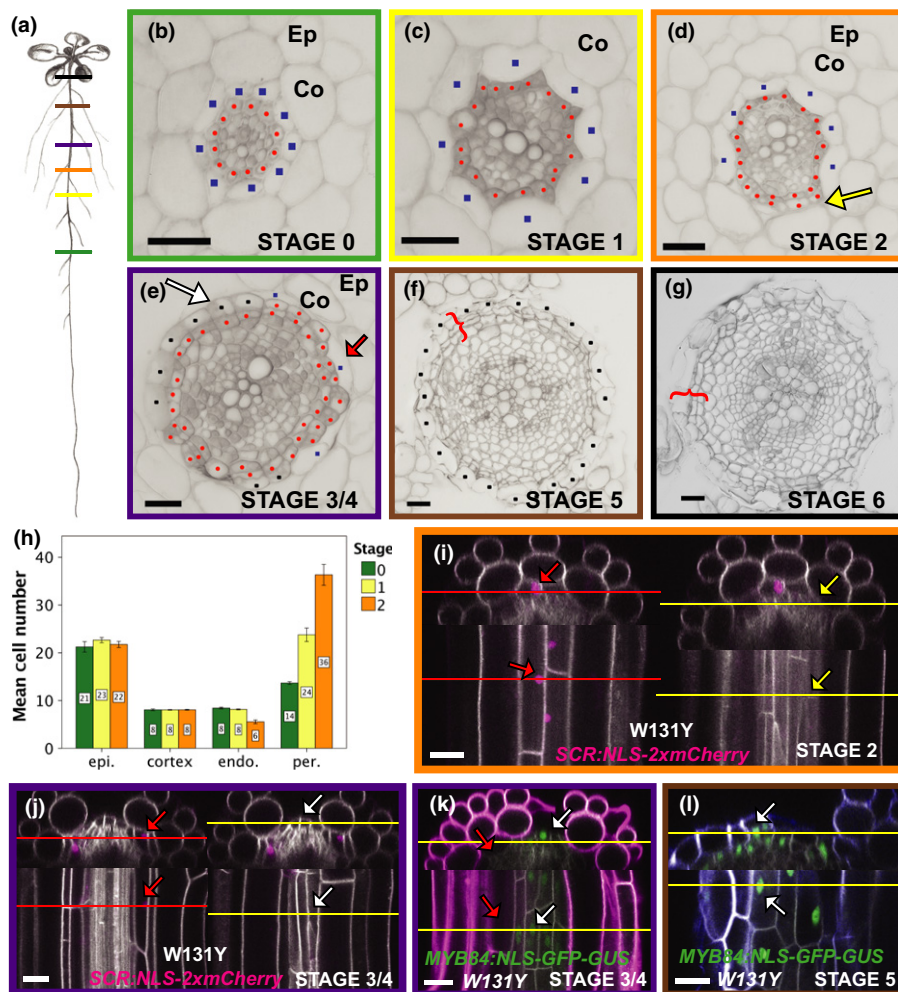


Fig. 2 Periderm development in the *Arabidopsis thaliana* root. (a) Illustration of an *Arabidopsis* root showing the positions corresponding to the different stages. (b–g) Cross-sections of 14-d-old roots (plastic embedding) at different positions of the root corresponding to STAGES 0–6. (b) STAGE 0: the stage before the pericycle starts to divide. (c) STAGE 1: the pericycle divides anticlinally. (d) STAGE 2 is characterized by a reduction in endodermal cells and pericycle proliferation. (e) STAGE 3/4: the cortex and the epidermis break and the periderm is the outmost tissue, whereas some endodermal cells are still present on the opposite side. (f) STAGE 5: the endodermis is no longer present and a ring of phellem cells is visible. (g) STAGE 6: the periderm is the outside tissue. Ep, epidermis; Co, cortex; blue squares, endodermal cells; red dots, pericycle/phellogen cells; black dots, phellem cells; red brackets, periderm. The yellow arrow indicates the absence of an endodermal cell, the red arrow points toward the remaining endodermal cells and the white arrow shows the emerging phellem. (h) Quantification of the cell number in different tissues (epidermis, cortex, endodermis and pericycle) at different periderm stages (0–2). Cross-sections of plants from independent experiments were measured ($n = 33$ STAGE 0; $n = 52$ STAGE 1; and $n = 31$ STAGE 2; error bars are ± 2 SE). (i, j) Ortho View of Z-stacks of *SCR:NLS-2xmCherry* *W131Y* roots at the positions corresponding to (i) STAGE 2 and (j) STAGE 3/4. For each stage, the same cross-section is shown, with the corresponding longitudinal section on endodermal cells (left) and periderm cells (right). (k, l) Ortho View of Z-stacks of *MYB84:NLS-GFP-GUS* *W131Y* roots at the positions corresponding to (k) STAGE 3/4 and (l) STAGE 5. Bars, 20 μ m.

cortical cells and of epidermal cells did not vary (Fig. 1e,j). STAGE 4 was characterized by the absence of the endodermis and the differentiation of first phellem cells from the phellogen. This stage can be divided in two sub-stages: in STAGE 4A, the inner cortex started to disappear from the phloem poles (in the majority of cases; Fig. S3k) and only a few phellem cells are differentiated (Fig. 1f), whereas in STAGE 4B, the inner cortex is missing and a ring of phellem cells starts to be visible (phellem cells are larger and rounder than phellogen cells) (Fig. 1g). At STAGE 5, the epidermis and the outer cortex broke on one side and progressively became detached from the periderm (Fig. 1h). Breaking of the cortex and of the epidermis occurred at random positions (Fig. S3l). Finally, STAGE 6 corresponded to a mature periderm in which the epidermis and the cortex were completely detached, and the periderm was the outer tissue protecting the vasculature (Fig. 1i). In a mature periderm we were able to distinguish four to five cell layers comprising the phellem, the phellogen and the phelloderm.

In roots, periderm development mainly followed the same stages defined for the hypocotyl, although we observed some differences possibly due to the distinct anatomy of the two organs (root at STAGE 0: one cell layer of cortex, hypocotyl at STAGE 0: two cell layers). In fact, the epidermis and the cortex broke and were shed earlier in development of the root. The exact position of each stage within the root and the length of the root corresponding to each stage vary with the age of the plant and the growing conditions (Figs S1b,c, S2e,f).

In roots, STAGE 0 occurred in the region with emerged and elongated lateral roots directly above the lateral root initiation zone (Fig. 2a,b). Similar to the hypocotyl, the vasculature of this region was already arranged with a central xylem axis and two phloem poles. In this part of the root, the pericycle was surrounded by the endodermis (approximately eight cells), the cortex (12–14 cells) and the epidermis (*c.* 23 cells) (Fig. 2b,h). In the region above STAGE 0, the pericycle began to divide at the xylem poles (STAGE 1) (Figs 2c, S3m). STAGE 2 is characterized by the loss of one to two endodermal cells at the phloem poles (in most cases) (Figs 2d, S4n) and by the first periclinal division in the pericycle, which from now can be termed phellogen (Fig. 2d).

In contrast to the hypocotyl, in the root we defined only one large stage, STAGE 3/4, as the events defining stage 3 and 4 cannot be precisely distinguished and often occur coincidentally and stochastically. During STAGE 3/4, the pericycle divided periclinally, while the number of endodermal cells decreased. The cortex and the epidermis broke primarily at the site where the endodermal cells disappeared and, at this location, phellem cells began to be visible (Fig. 2e). At STAGE 5, the periderm was fully differentiated and the phellem was the main external tissue, still partially covered with patches of epidermis and cortex (Fig. 2f). Finally, at STAGE 6 the epidermis and the cortex were completely shed and the periderm comprised three to four cell layers (Fig. 2g). Overall, periderm formation in lateral roots occurs similarly to the main root (Figs S1d, S4a–c).

To corroborate the histological analyses we visualized the most distinctive stages by live imaging. We followed endodermis fate

using the marker *SCR:H2B-2xmCherry* (Di Lorenzo *et al.*, 1996; Marques-Bueno *et al.*, 2016) and tracked periderm growth in *MYB84:NLS-3xGFP* roots (*MYB84* is the Arabidopsis ortholog of *QSMYB1*). Given that PI does not normally penetrate the endodermis, both reporters were crossed to the ubiquitously expressed plasma membrane marker line *W131Y(UBQ10:eYFP-NPSN12)* to outline the different cell types (Geldner *et al.*, 2009; Alassimone *et al.*, 2010). We clearly observed areas of the root where the *SCR* expression domain was interrupted by cells with periderm morphology (Fig. 2i,j) and regions where the periderm marker *MYB84* was flanked by endodermal cells (Fig. 2k), validating our histological analyses. Consistently, in the upper part of the root we could no longer identify endodermal cells (Fig. 2l).

Based solely on morphology and size, phelloderm cells can be difficult to differentiate from phloem parenchyma cells. To address this issue, several staining methods that label phelloderm cells in other species were tested in Arabidopsis. Classical toluidine blue staining, which has been useful in helping to distinguish the three periderm tissues in potato (Sabba & Lulai, 2005), stained uniformly the periderm of Arabidopsis (Fig. S4d). However, a thicker cell wall between two cell layers was visible and may represent the boundary between the periderm and the phloem (Fig. S4e,f). To confirm this, we checked whether we could observe a different degree of esterification of pectins, which is used to distinguish the phelloderm in potato (Sabba & Lulai, 2002), at the presumptive boundary line. In root vibratome sections stained with ruthenium red, a pale red staining was visible in the cell layer below the phellem, whereas it was stronger at the presumptive boundary, supporting our hypothesis (Fig. S4g). These data also fit with the autofluorescence pattern in the red spectrum (ex. 561 nm, em. 570–630 nm), which in roots from 15-d-old plants grown under continuous light showed a strong intracellular autofluorescence mainly in the presumptive phelloderm (Fig. S4h). Together, these results suggested that one layer of phelloderm cells is formed in Arabidopsis, which can be confirmed by the development of tissue-specific markers and/or clonal analyses in the future.

Cortex and epidermis are abscised while endodermis undergoes PCD during periderm growth

We showed that the tissues that surround the periderm are progressively lost following a predefined pattern, so we next investigated the mechanisms underlying this process. In particular, we investigated whether it involves abscission (shedding of plant organs or parts that are no longer necessary), PCD or if the cells simply collapse.

We first studied how the epidermis and the cortex are progressively removed. The breaking of the cortex and epidermis was not an artifact of the embedding methods as we were able to observe it during live cell imaging (Fig. 3a–f). Along a mature root, we observed isolated areas in which the cortex and the epidermis broke and the phellem became the external tissue, followed by a zone where the phellem was the outer tissue with stretches of cortex and epidermis still attached (Fig. 3a,b).

Moreover, most of the epidermal and cortex cells that still surround the periderm after the first break are still alive, as seen by PI and FDA staining (Fig. 3g,h). In fact, PI stains the nuclei of dead cells, whereas FDA becomes fluorescent when cleaved by esterases inside living cells. These results indicate that the epidermis and the cortex are abscised and do not undergo PCD.

We next characterized the course/fate of endodermal cells during periderm growth and assessed the viability of endodermal cells during root development. It was previously shown that 20 min of incubation is sufficient for FDA uptake into the endodermis and stele of the root differentiation zone (Barberon *et al.*, 2016). This was also the case in older root in the regions where lateral roots are emerged and elongated (Figs 4h, S4i). At early STAGE 2, PI was detected in a few nuclei of the endodermis in which FDA was excluded, while the neighboring endodermal cells showed only FDA in the nuclei (Fig. 4a). To better visualize dying vs alive endodermal cells, we repeated the PI staining using the endodermis reporter *CASP2:NLS-GFP-GUS* (*CASPIAN STRIP DOMAIN PROTEIN 2*) (Roppolo *et al.*, 2011). We observed PI staining in the nuclei of endodermal cells, which were flanked by endodermal cells expressing the *CASP2* reporter, confirming our previous results (Fig. 4b). Furthermore, we analyzed the expression of a set of genes whose expression has been associated with developmental PCD (Fendrych *et al.*, 2014; Olvera-Carrillo *et al.*, 2015). The PCD markers *RIBONUCLEASE 3* (*RNS3*), *EXITUS 1* (*EXI1*) and *DOMAIN OF UNKNOWN FUNCTION679 MEMBRANE PROTEIN 4* (*DMP4*) were broadly expressed in the endodermis from STAGE 1 onwards (as long as the endodermis is present) in both root and hypocotyl and only in the inner cortex of the hypocotyl during STAGE 4 (Figs 4c–e, S4j–l, S5a–f). In summary, these data

indicate that the endodermis and the inner cortex (in the hypocotyl) undergo PCD.

Next, we investigated whether the endodermis alters its chemical/physical properties before PCD. The two major features of a mature endodermis are casparian strips (CSs) and suberin lamellae. We first analyzed the expression of the CS markers *ESB1:ESB1-mCherry* (*ENHANCED SUBERINI1*) and *CASP1:CASP1-mcherry* during root development. Both proteins are required for proper CS assembly and accumulate at the plasma membrane domain underlying the CS (casparian strip membrane domain CSD) in the root differentiation zone (Roppolo *et al.*, 2011; Hosmani *et al.*, 2013). A similar pattern was observed for the endodermis in the region of the main root where lateral roots were already emergent and elongated (Figs 4h, S4m,n). Similarly *ESB1* still accumulated at the CSD in mature endodermis (region of the root that precedes endodermis PCD; Fig. 4h) (Fig. S4o), whereas *CASP1* in the mature endodermis was no longer localized to the CSD (Fig. S4p), suggesting that CSs are maintained throughout endodermis development. To confirm that CSs are not degraded before endodermis PCD, we verified whether the typical autofluorescence pattern of CSs (Alassimone *et al.*, 2010) (Fig. 4f) was present in the mature endodermis (Fig. 4g). No difference in the pattern of autofluorescence of the CSs was observed, suggesting that CSs are still present when the endodermis undergoes PCD. The mature endodermis is a highly suberized tissue, and the amount of suberin is modified according to nutrient availability (Barberon *et al.*, 2016) and in response to hormones. For instance, sulfur and potassium deficiency enhances suberization, whereas iron, magnesium and zinc starvation promotes suberin degradation and reduces the expression of suberin biosynthesis genes (Barberon *et al.*, 2016). Because suberin accumulation in the endodermis is a dynamic

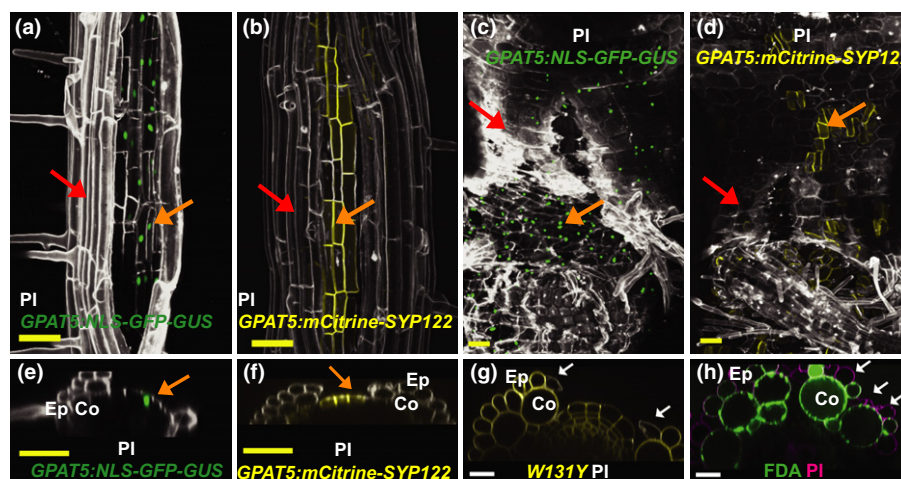


Fig. 3 The epidermis and cortex of *Arabidopsis* root and hypocotyl are abscised together. (a–d) 3D reconstructions of a Z-stack *GPAT5:NLS-GFP-GUS* and propidium iodide (PI), 13-d-old root. (b) *GPAT5:mCITRINE-SYP122* and PI, 13-d-old root. (c) *GPAT5:NLS-GFP-GUS* and PI, 25-d-old hypocotyl. (d) *GPAT5:mCITRINE-SYP122* and PI, 25-d-old hypocotyl. (e) Cross-section (Ortho View of a Z-stack) of (a). (f) Cross-section (Ortho View of a Z-stack) of (b). The cortex and the epidermis become detached in some areas of the root and the hypocotyl. Phellem cells (orange arrow), expressing the suberin biosynthesis gene *GPAT5*, are the outer tissue in certain regions, whereas the flanking areas remain covered by the epidermis and the cortex (red arrow). (g) Cross-section (Ortho View of a Z-stack) of a 17-d-old root, W131Y and PI. (h) Cross-section (Ortho View of a Z-stack) of a 17-d-old root stained with fluorescein diacetate (FDA) and PI. (g, h) Most epidermis and cortex cells are still alive before detachment. Dead cells (white arrow) do not express the W131Y marker (g) and do not show FDA signal (h, green) but are still stained by PI. Bars: (a–f) 50 μ m; (g, h) 20 μ m. Ep, epidermis; Co, cortex.

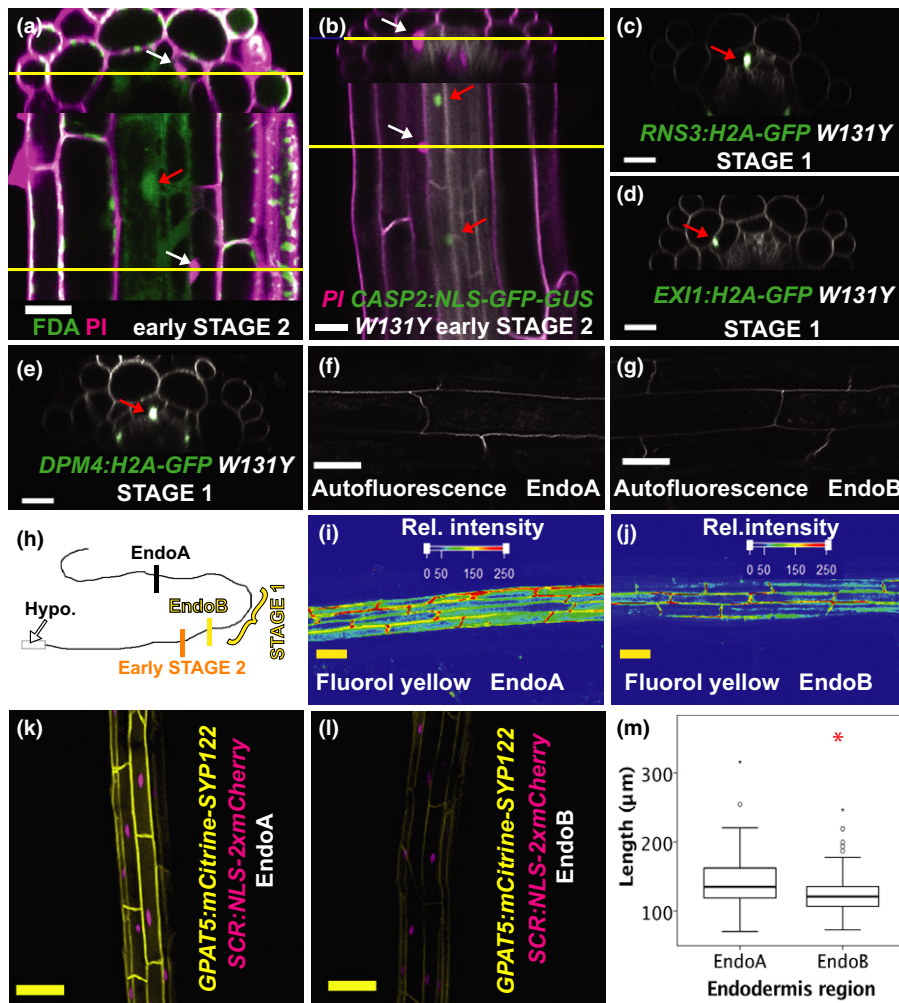


Fig. 4 The endodermis of *Arabidopsis* undergoes programmed cell death (PCD). (a) Cross and longitudinal sections (Ortho View of a Z-stack) of a 13-d-old root stained with fluorescein diacetate (FDA) and propidium iodide (PI) in early STAGE 2. The endodermis is undergoing PCD, as shown by PI staining of the nuclei (white arrow) and absence of FDA in the endodermis. (b) *CASP2:NLS-GFP-GUS W131Y*. Cross and longitudinal section (Ortho View of a Z-stack) of a 13-d-old root stained with PI. (c) *RNS3:H2A-GFP W131Y*. (d) *EXI1:H2A-GFP W131Y*. (e) *DPM4:H2A-GFP W131Y*. (c–e) Developmental PCD markers are expressed in the endodermis before PCD (red arrows indicate GFP signal in the nuclei of endodermal cells). Cross-sections (Ortho View of a Z-stack) of 14-d-old roots in STAGE 1. (f, g) Autofluorescence of the casparian strips (CSs) in the region of the endodermis where lateral roots emerge and become elongated (f; EndoA) and in the region before PCD (g; EndoB). (h) Scheme of an *Arabidopsis* root showing the positions along the root where the images were acquired. (i, j) Relative intensity of fluorol yellow (FY) staining in the region of the endodermis where lateral roots emerge and become elongated (i; EndoA) and in the region before PCD (j; EndoB) of a 14-d-old root, showing a reduction of suberin in the more mature part. (k, l) *GPAT5:mCitrine-SYP122 SCR:NLS-2xmCherry* of 12-d-old roots in the region where lateral roots emerge (k; EndoA) and in the region before PCD (l; EndoB). (m) Quantification of endodermal cell length of 12-d-old roots. Welch's *t*-test (red asterisk: $P \leq 0.001$; $n = 97\text{--}39$). Box plot: the dark line in the middle of the boxes is the median, the bottom and top of the boxes indicate the 25th and 75th percentiles, whiskers (T-bars) are within 1.5 times the interquartile range, the empty dots are outliers and the black stars are extreme outliers. Bars: (a–g) 20 μm ; (h–l) 50 μm .

process, we investigated whether suberin content varies before endodermis PCD. For this, we analyzed FY staining along the root, from the region of emergence of the lateral roots to where the endodermis undergoes PCD. A small decrease in suberin deposition was observed in the uppermost part of the endodermis (Fig. 4i,j). Consistently, a decrease in the expression of the suberin biosynthesis reporter *GPAT5:mCITRINE-SYP122* was detected in the mature endodermis, suggesting that endodermal PCD is promoted by a reduction of suberin (Fig. 4k,l). We also observed that endodermal cells are shorter in the more mature part of the root. A complication here is that suberin biosynthesis genes are expressed in both cell types, and thus the two cell types

are difficult to distinguish at the endodermis–phellem transition zone. Therefore, we confirm a reduction in endodermal cell length before PCD, quantifying cell length in cells expressing both the endodermal marker *SCR:H2B-2xmCherry* and the *GPAT5:mCITRINE-SYP122* (Fig. 4m).

The phellem of *Arabidopsis thaliana* is suberized, lignified and partially composed of dead cells

One of the essential characteristics of phellem is the high degree of suberization, and consequently many suberin biosynthesis genes are expressed in the phellem of cork oak as well as the root

and the hypocotyl of *Arabidopsis* (Molina *et al.*, 2009; Kosma *et al.*, 2012; Vishwanath *et al.*, 2013) (this work) (Figs 3a–d, S6). FY staining decorated the outside surface of phellem cells in both roots (Fig. 5a) and hypocotyls (Fig. S7a,b). However, suberin is not the only polymer present in the phellem, as lignin impregnates the phellem of trees (Marques & Pereira, 2013; Fagerstedt *et al.*, 2015; Lourenco *et al.*, 2016).

To investigate whether the phellem of *Arabidopsis* comprises lignin, we stained phellem cells with Basic fuchsin and Phloroglucinol. These two stains revealed the presence of lignin in the phellem and the lignin deposition patterns partially matched the suberin impregnation (Figs 5b,c, S7c–e,g,i). Phellem cells were characterized by a strong extracellular autofluorescence in the blue–green spectrum (ex. 405 nm and em. 425–500 nm) that coincided with the lignin/suberin deposition pattern (Figs 5d, S7d,f–i). This particular chemical composition renders the phellem an impermeable barrier because dyes such as PI were unable to enter the phellem tissue (Fig. 3e,f). Given that the outer phellem cell layers die and peel off in woody species, we investigated whether it also occurs in *Arabidopsis*. Indeed, the developmental PCD marker genes *RNS3*, *EX11* and *DPM4* were also expressed in phellem cells (Fig. 5e–g). Moreover, the aspartic

protease *PASPA3* and *SERINE CARBOXY- PEPTIDASE-LIKE48* (*SCPL48*) genes were expressed in phellem, as well (Fig. 5h,i). Phellem cell viability was then analyzed by FDA/PI staining, and indicated that most phellem cells were alive as shown by the FDA fluorescence (Fig. 5j). However, we observed a few cells where FDA was excluded while PI stained the nuclei. These cells were larger, suggesting that morphological changes might anticipate phellem cell death (Fig. 5j). Thus, phellem cell size was investigated in more detail. Although phellem cell length was fairly homogeneous (Fig. S7j), when we quantified phellem length in the uppermost region of the root of 12- and 17-d-old plants, we observed a reduction of phellem cell length with age (Fig. 6a–c,e). Consistently, we detected a reduction in cell length when we compared the lower and upper part of the phellem (Fig. 6a,c,d,f). By contrast, phellem cell area was more heterogeneous with most cells having an area of 200–300 μm^2 and few cells with an area larger than 500 μm^2 (Fig. S7j). Moreover, the number of cells with a ‘large’ area increased with periderm development (Fig. 6g,h). As both cell length and cell area vary during phellem maturation, we estimated the volume. Although phellem cell volume was highly variable (Fig. 6i,j) we observed that cells with an area of > 500 μm^2 were associated with a large volume

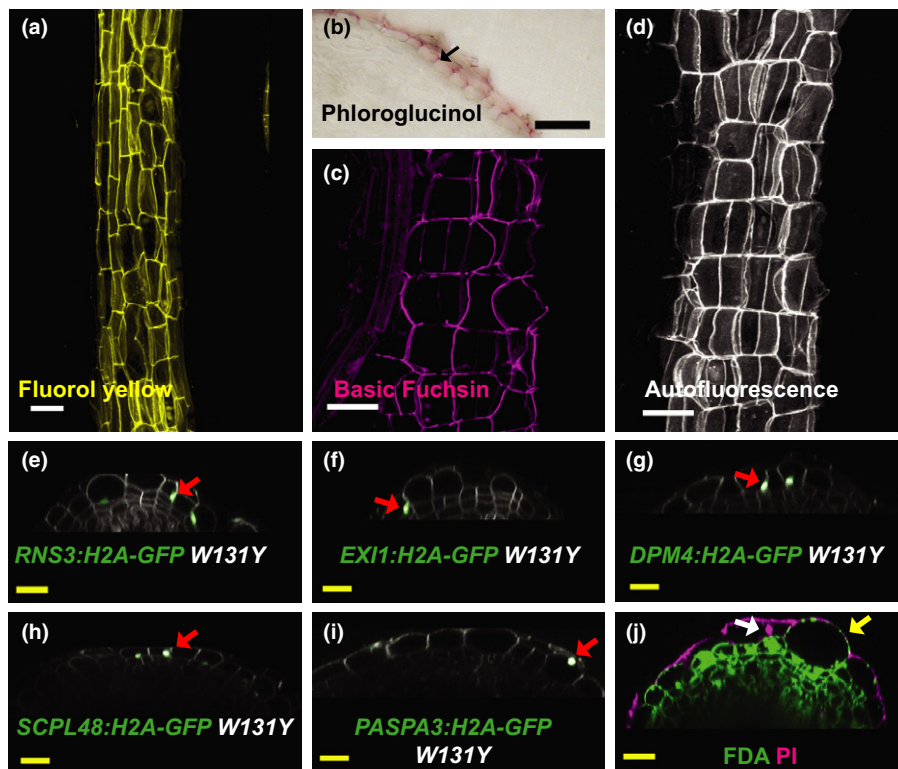


Fig. 5 Chemical composition and morphology of the phellem in the *Arabidopsis* root. (a) The phellem is suberized as shown by fluorol yellow (FY) staining of the uppermost part of a 17-d-old root (3D reconstruction of a Z-stack). (b) Vibratome section of the uppermost part of a 20-d-old root stained with Phloroglucinol (lignin staining). The black arrow indicates lignin staining of phellem cells. (c) The phellem contains lignin as shown by Basic Fuchsin staining of the uppermost part of a 17-d-old root (3D reconstruction of a Z-stack). (d) Autofluorescence (excitation wavelength (ex.) 405 nm; emission (em.) 420–500 nm) of phellem cell of the uppermost part of a 17-d-old root (3D reconstruction of a Z-stack). (e–i) Developmental PCD markers are expressed in phellem cells (red arrows indicate GFP signal in the nuclei of phellem cells). Cross-sections (Ortho View of a Z-stack) of the phellem region of 12-d-old roots. (e) *RNS3:H2A-GFP W131Y*. (f) *EX11:H2A-GFP W131Y*. (g) *DPM4:H2A-GFP W131Y*. (h) *SCPL48:H2A-GFP W131Y*. (i) *PASPA3:H2A-GFP W131Y*. (j) Phellem cells die (white arrow) and peel off, as shown by fluorescein diacetate (FDA) and propidium iodide (PI) staining in the uppermost part of a 14-d-old root (Ortho View of a Z-stack). Yellow arrow indicates a large living phellem cell. Bars: (a, c, d) 50 μm ; (b) 100 μm ; (e–j) 20 μm .

and with the most mature part of the phellem, suggesting that an increase in volume preceded phellem death (Fig. 6i,j).

Conservation of periderm regulators in *Arabidopsis thaliana*

The periderm of *Arabidopsis* seems to share features with the phellem of trees, but it is not known if this conservation persists at the molecular level. Very few regulators of periderm growth have been identified so far, and no specific expression data for the phellogen and phelloderm exists. Nevertheless, several transcriptome datasets noted the importance of some TF families such as the MYBs and the NACs in phellem (Soler *et al.*, 2007, 2011; Ginzberg *et al.*, 2009; Rains *et al.*, 2017; Vulavala *et al.*, 2017). For instance, in cork oak, *QsMYB1/MYB84/RAX3* is expressed in the phellem and expression

responds to drought and heat stress (Almeida *et al.*, 2013b). Moreover, the expression of these genes is enriched in the phellem of poplar (Rains *et al.*, 2017).

We analyzed the expression of *MYB84/RAX3* and *ANAC78* throughout the *Arabidopsis* periderm. *MYB84/RAX3* was expressed in the whole periderm circumference (Figs 2k,l, 7a,d) whereas *ANAC78* was expressed in the periderm and in the phloem of the hypocotyl and root (Fig. 7b,e). The suberin/wax biosynthesis genes *GPAT5*, *KCR1*, *HORST*, *DAISY*, *RALPH* and *ASFT*, which are expressed in the phellem of oak, potato and poplar (Soler *et al.*, 2007, 2011; Serra *et al.*, 2009a,b, 2010; Rains *et al.*, 2017), were expressed in the *Arabidopsis* phellem in both root and hypocotyl (Molina *et al.*, 2009) (Figs 7c,f–l, S6a,e). Thus, it seems that a certain degree of conservation exists between *Arabidopsis* and other species.

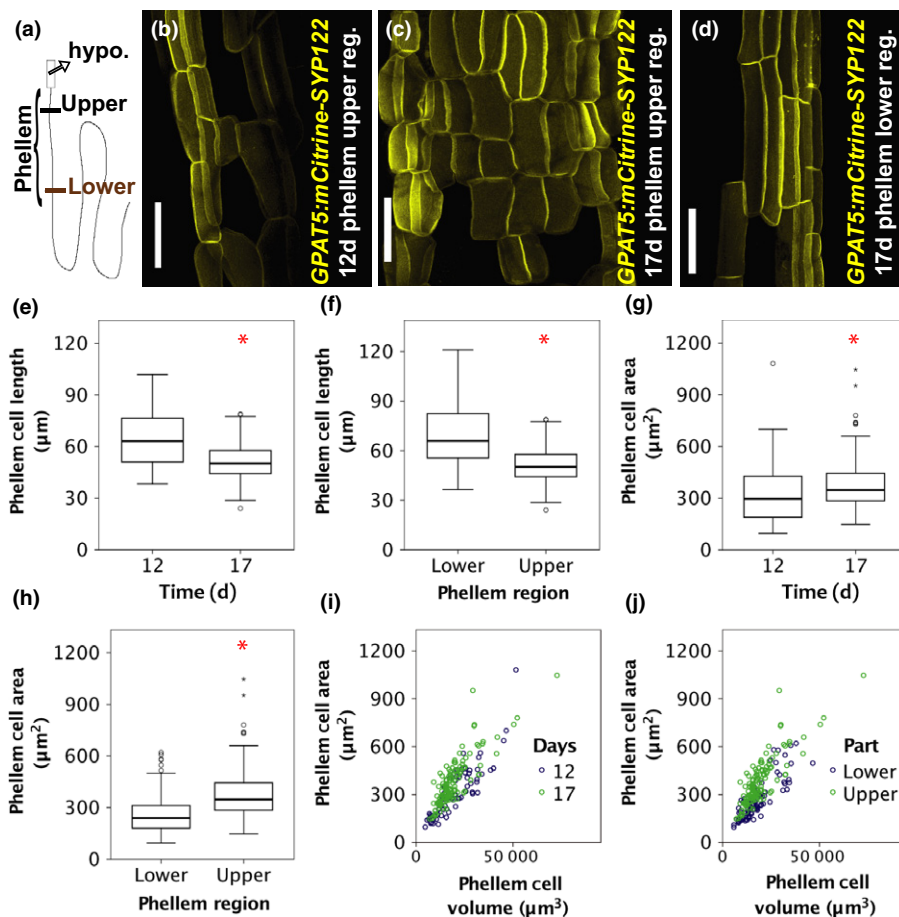


Fig. 6 Phellem cell morphology in *Arabidopsis* root. (a) Scheme of a root showing the upper and the lower phellem regions. (b–d) 3D reconstructions of Z-stacks of *GPAT5:mCITRINE-SYP122* roots. *GPAT5:mCITRINE-SYP122* is used to visualize phellem cells. Phellem cells at different developmental stages showing how phellem cell length decreases with age. (b) Upper region of the phellem of a 12-d-old root. (c) Upper region of the phellem of a 17-d-old root. (d) Lower region of the phellem of a 17-d-old root. (e) Quantification of phellem cell length measured in the upper region of the phellem of 12- and 17-d-old roots, showing that phellem length decreased during development. Welch's *t*-test (red asterisk: $P \leq 0.001$; $n = 69-125$). (f) Quantification of phellem cell length measured in the upper and lower region of the phellem of 17-d-old roots, showing that phellem cell length decreases with age. Welch's *t*-test (red asterisk: $P \leq 0.001$; $n = 89-125$). (g) Quantification of phellem cell area measured in the upper region of the phellem of 12- and 17-d-old roots, showing that the number of phellem cells of large area increases during development. Student's *t*-test (red asterisk: $P = 0.012$; $n = 69-125$). (h) Quantification of the phellem cell area measured in the upper and lower region of the phellem of 17-d-old roots, showing that the number of phellem cells of large area increases during development. Student's *t*-test (red asterisk: $P = 0.001$; $n = 89-125$). (e–h) Box plots: the dark line in the middle of the boxes is the median, the bottom and top of the box indicates the 25th and 75th percentiles, whiskers (T-bars) are within 1.5 times the interquartile range, the empty dots are outliers and the black stars are extreme outliers. (i, j) Plots of phellem cell volume vs phellem cell area. Bars, 50 μm.

Discussion

Periderm development in *Arabidopsis thaliana* root and hypocotyl

In this study, we set up a means to study periderm biology in *Arabidopsis thaliana*, providing a suite of tools and a detailed characterization of periderm growth in the form of identifiable stages. It was previously reported that a periderm is established in the root and in the hypocotyl of *Arabidopsis*. Consistently, we show that the stems of the most commonly used *Arabidopsis* strains lack a periderm. In addition, enhanced longevity and secondary growth do not trigger periderm formation in the stem of *soc1 full1* plants grown in standard growing conditions, indicating that the epidermis in stems can adapt to a large amount of radial expansion. However, we cannot rule out that in extreme growing conditions or in other strains, which push the life span of *Arabidopsis* even further, a periderm could be produced in the stem.

In *Arabidopsis* hypocotyl and root, periderm growth is not a minor localized process, as the periderm covers one-third of the

length of a mature primary root, the uppermost part of lateral roots and the whole hypocotyl of a flowering plant. Periderm growth occurs under different photoperiods and growing conditions and it mainly follows plant growth progression, in the sense that it is formed earlier in plants in which growth is accelerated. This combination of features makes *Arabidopsis* a robust model to study the molecular mechanisms of phellogen establishment and maintenance. In both root and hypocotyl, the periderm arises from an inner tissue to become an external barrier, which can be considered to be a complex process. For a better understanding of this process, we visualized periderm growth and defined a set of six stages that cover several intermediate steps from the onset of pericycle divisions that establish the meristematic phellogen to phellem maturation. These stages will help to compare periderm growth in different genetic backgrounds, paving the way for understanding the periderm regulatory network.

In woody species, phellem cells are characterized by lignin in addition to a higher content of suberin and undergo a maturation process that leads to death and peeling off. The presence of lignin, suberin and associated waxes in the phellem gives the

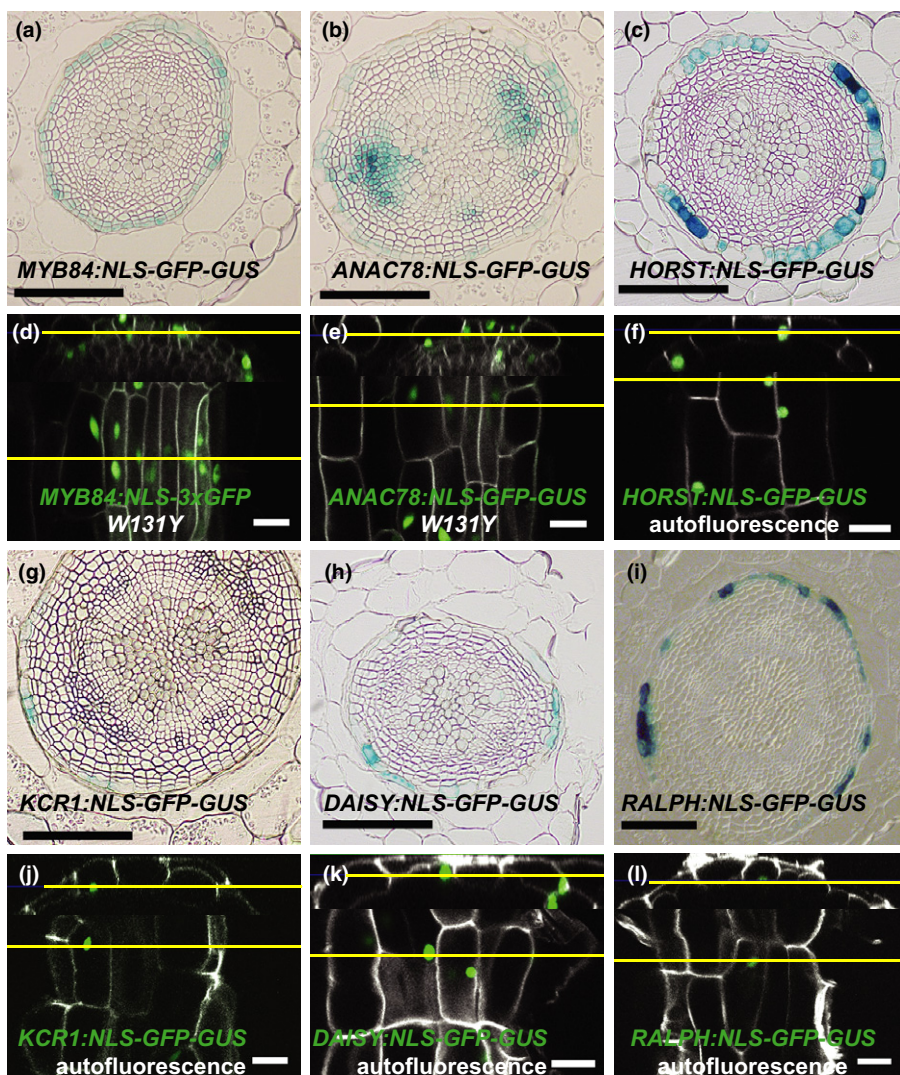


Fig. 7 Periderm-associated gene expression in *Arabidopsis*. (a–c, g–i) Plastic cross-sections of GUS staining of 17- to 19-d-old hypocotyls (STAGE 4). (d–f, j–l) Cross and longitudinal sections (Ortho View of a Z-stack) of 12- to 15-d-old roots (STAGE 5/6). (d, e) The *MYB84* and the *ANAC78* reporters lines were crossed to the *W131Y* line, to outline all cells. (f, j–l) Autofluorescence (excitation wavelength (ex.) 405 nm, emission (em.) 420–460 nm) is used to visualize the phellem. (a, d) *MYB84* is specifically expressed in the periderm of the hypocotyl (a) and the root (d). (b, e) *ANAC78* is expressed in the phellem and the phloem of the hypocotyl (b) and the root (e). (c, f) *HORST* is expressed in the phellem of the hypocotyl (c) and the root (f). (g, j) *KCR1* is expressed in the phellem of the hypocotyl (g) and the root (j). (h, k) *DAISY* is expressed in the phellem of the hypocotyl (h) and the root (k). (i, l) *RALPH* is expressed in the phellem of the hypocotyl (i) and root (l). Bars: (d–f, j–l) 50 μ m; (a–c, g–i) 100 μ m.

periderm barrier properties. It offers protection against pathogens (Lulai & Corsini, 1998; Thangavel *et al.*, 2016) and it reduces water and solute losses (Beisson *et al.*, 2007). For instance, a somaclonal variant of potato resistant to pathogenic *Streptomyces* is characterized by an increased number of phellem cell layers and suberin deposition (Thangavel *et al.*, 2016).

As in trees, in *Arabidopsis*, the phellem is highly suberized and many of the genes coding for suberin biosynthesis enzymes are expressed in this tissue (Molina *et al.*, 2009; Vishwanath *et al.*, 2013) (this work) and therefore can be used as reporters for the phellem. Similarly, we show that *Arabidopsis* phellem is also lignified and it undergoes a maturation process that results in an increase of cell volume and ultimately in cell death, keeping a constant number of phellem cell layers. In summary, *Arabidopsis* can be used in pioneering works to study phellem biology in response to biotic and abiotic stresses for breeding programs.

Only a few transcription factors are known to regulate phellogen and phellem production in trees. Remarkably they are also expressed in *Arabidopsis*, suggesting a conserved gene core that controls periderm growth. Among them, *QsMYB1/MYB84/RAX3* is upregulated in the phellem of cork oak upon heat and drought stress (Almeida *et al.*, 2013b) and it also accumulates in the poplar phellem (Rains *et al.*, 2017). In *Arabidopsis*, it was previously reported that *MYB84/RAX3* regulates axillary meristem formation together with its closest homologs *MYB37/RAX1* and *MYB38/RAX2* (Muller *et al.*, 2006) and it may control lateral root formation (Feng *et al.*, 2004). The specific expression pattern and conservation among species renders *MYB84/RAX3* a good marker to study periderm development and it will be interesting to further study its function in the *Arabidopsis* root.

PCD shapes periderm growth

Many plant developmental programs, for example xylem vessel and anther differentiation, involve a step of PCD (Olvera-Carrillo *et al.*, 2015). Here, we reveal that PCD is a crucial event during periderm development. As the periderm arises from the pericycle to become the outer protective barrier, the epidermis, the cortex and the endodermis have to accommodate periderm growth and are finally removed. This process follows a predetermined pattern and includes two independent mechanisms: PCD and abscission.

In the root, the endodermis undergoes PCD, whereas the epidermis and the cortex break and are abscised from the periderm. Consistently a set of genes, identified as developmental PCD markers (Olvera-Carrillo *et al.*, 2015), were expressed exclusively in the endodermis and the phellem (which is also dying) and the epidermis and cortex were still alive when they become detached from the periderm. Endodermal PCD is a gradual event as it does not occur in all endodermal cells at the same time and it is preceded by a reduction in cell length and suberin deposition. Remarkably, in the hypocotyl both the endodermis and the inner cortex undergo PCD sequentially, whereas the outer cortex and the epidermis are detached. PCD starts in the endodermal cells located at the phloem poles, it expands to the neighboring

endodermal cells, it then occurs in the endodermal cells at the xylem poles and finally it reaches the inner cortex. These successive steps suggest a complex mechanism of regulation and communication between tissues. Mechanical tensions may play a key role, as suggested by the elliptical shapes of the hypocotyl. In fact, the phloem poles (where PCD starts) can be considered as the foci of the ellipse. Future studies directed to the alteration of the physical/chemical properties of the cell walls of the outer tissues may highlight the mechanical regulation of this process. Moreover, the cortex in the hypocotyl represents the ideal cell type to study this communication aspect because the two cell layers of the same tissue (same cell identity) share different fates: the inner cortex undergoes PCD while the outer cortex is abscised.

Acknowledgements

L.R. is indebted to the Baden-Württemberg Stiftung for financial support of this research project by the Elite program for Postdocs. This work was supported by the DFG (grant RA-2590/1-1). We thank Marja Timmermans for critical reading of the manuscript.

Author contributions

A.W. and L.R. designed the research; A.W., D.R., A.B.-J., S.M., K.S., M.B.T. and L.R. performed the experiments; A.W., A.B.-J. and L.R. analyzed and discussed the data; L.R. wrote the paper with the help of A.W. and A.B.-J.

ORCID

Azahara Barra-Jimenez  <http://orcid.org/0000-0002-4676-2436>

Laura Ragni  <http://orcid.org/0000-0002-3651-8966>

References

- Agusti J, Lichtenberger R, Schwarz M, Nehlin L, Greb T. 2011. Characterization of transcriptome remodeling during cambium formation identifies *MOL1* and *RUL1* as opposing regulators of secondary growth. *PLoS Genetics* 7: e1001312.
- Alassimone J, Naseer S, Geldner N. 2010. A developmental framework for endodermal differentiation and polarity. *Proceedings of the National Academy of Sciences, USA* 107: 5214–5219.
- Almeida T, Menendez E, Capote T, Ribeiro T, Santos C, Goncalves S. 2013a. Molecular characterization of *Quercus suber* MYB1, a transcription factor up-regulated in cork tissues. *Journal of Plant Physiology* 170: 172–178.
- Almeida T, Pinto G, Correia B, Santos C, Goncalves S. 2013b. *QsMYB1* expression is modulated in response to heat and drought stresses and during plant recovery in *Quercus suber*. *Plant Physiology and Biochemistry* 73: 274–281.
- Altamura MM, Possenti M, Matteucci A, Baima S, Ruberti I, Morelli G. 2001. Development of the vascular system in the inflorescence stem of *Arabidopsis*. *New Phytologist* 151: 381–389.
- Barberon M, Vermeer JE, De Bellis D, Wang P, Naseer S, Andersen TG, Humbel BM, Nawrath C, Takano J, Salt DE *et al.* 2016. Adaptation of root function by nutrient-induced plasticity of endodermal differentiation. *Cell* 164: 447–459.
- Barbier de Reuille P, Ragni L. 2017. Vascular morphodynamics during secondary growth. *Methods in Molecular Biology* 1544: 103–125.

- Barra-Jimenez A, Ragni L. 2017. Secondary development in the stem: when Arabidopsis and trees are closer than it seems. *Current Opinion in Plant Biology* 35: 145–151.
- Beisson F, Li Y, Bonaventure G, Pollard M, Ohlrogge JB. 2007. The acyltransferase GPAT5 is required for the synthesis of suberin in seed coat and root of *Arabidopsis*. *Plant Cell* 19: 351–368.
- Caritat A, Gutiérrez E, Molinas M. 2000. Influence of weather on cork-ring width. *Tree Physiology* 20: 893–900.
- Compagnon V, Diehl P, Benveniste I, Meyer D, Schaller H, Schreiber L, Franke R, Pinot F. 2009. CYP86B1 is required for very long chain omega-hydroxyacid and alpha, omega-dicarboxylic acid synthesis in root and seed suberin polyester. *Plant Physiology* 150: 1831–1843.
- Cordeiro N, Belgacem MN, Gandini A, Pascoal Neto C. 1999. Urethanes and polyurethanes from suberin 2: synthesis and characterization. *Industrial Crops and Products* 10: 1–10.
- Davin N, Edger PP, Hefer CA, Mizrachi E, Schuetz M, Smets E, Myburg AA, Douglas CJ, Schranz ME, Lens F. 2016. Functional network analysis of genes differentially expressed during xylogenesis in *sociol* woody Arabidopsis plants. *Plant Journal* 86: 376–390.
- Demura T, Ye Z-H. 2010. Regulation of plant biomass production. *Current Opinion in Plant Biology* 13: 298–303.
- Di Lorenzo L, Wysocka-Diller J, Malamy JE, Pysch L, Helariutta Y, Freshour G, Hahn MG, Feldmann KA, Benfey PN. 1996. The SCARECROW gene regulates an asymmetric cell division that is essential for generating the radial organization of the Arabidopsis root. *Cell* 86: 423–433.
- Domergue F, Vishwanath SJ, Joubès J, Ono J, Lee JA, Bourdon M, Alhattab R, Lowe C, Pascal S, Lessire R *et al.* 2010. Three Arabidopsis fatty acyl-coenzyme A reductases, FAR1, FAR4, and FAR5, generate primary fatty alcohols associated with suberin deposition. *Plant Physiology* 153: 1539–1554.
- Esau K. 1977. *Anatomy of seed plants*. New York, NY, USA: John Wiley & Sons.
- Ethchells JP, Mishra LS, Kumar M, Campbell L, Turner SR. 2015. Wood formation in trees is increased by manipulating PXY-regulated cell division. *Current Biology* 25: 1050–1055.
- Fagerstedt KV, Saranpaa P, Tapanila T, Immanen J, Serra JA, Nieminen K. 2015. Determining the composition of lignins in different tissues of silver birch. *Plants* 4: 183–195.
- Fendrych M, Van Hautegeem T, Van Durme M, Olvera-Carrillo Y, Huysmans M, Karimi M, Lippens S, Guerin CJ, Krebs M, Schumacher K *et al.* 2014. Programmed cell death controlled by ANAC033/SOMBRERO determines root cap organ size in *Arabidopsis*. *Current Biology* 24: 931–940.
- Feng C, Andreasson E, Maslak A, Mock HP, Mattsson O, Mundy J. 2004. Arabidopsis MYB68 in development and responses to environmental cues. *Plant Science* 167: 1099–1107.
- Geldner N, Denervaud-Tendon V, Hyman DL, Mayer U, Stierhof YD, Chory J. 2009. Rapid, combinatorial analysis of membrane compartments in intact plants with a multicolor marker set. *Plant Journal* 59: 169–178.
- de Geus M, van der Meulen I, Goderis B, van Hecke K, Dorschu M, van der Werff H, Koning CE, Heise A. 2010. Performance polymers from renewable monomers: high molecular weight poly(pentadecalactone) for fiber applications. *Polymer Chemistry* 1: 525.
- Ginzberg I, Barel G, Ophir R, Tzin E, Tanami Z, Muddarangappa T, de Jong W, Fogelman E. 2009. Transcriptomic profiling of heat-stress response in potato periderm. *Journal of Experimental Botany* 60: 4411–4421.
- Groh B, Hubner C, Lenzian KJ. 2002. Water and oxygen permeance of phellements isolated from trees: the role of waxes and lenticels. *Planta* 215: 794–801.
- Hirakawa Y, Bowman JL. 2015. A role of TDIF peptide signaling in vascular cell differentiation is conserved among euphyllophytes. *Frontiers in Plant Science* 6: 1048.
- Hofer R, Briesen I, Beck M, Pinot F, Schreiber L, Franke R. 2008. The Arabidopsis cytochrome P450 CYP86A1 encodes a fatty acid omega-hydroxylase involved in suberin monomer biosynthesis. *Journal of Experimental Botany* 59: 2347–2360.
- Hosmani PS, Kamiya T, Danku J, Naseer S, Geldner N, Guerinot ML, Salt DE. 2013. Dirigent domain-containing protein is part of the machinery required for formation of the lignin-based Casparian strip in the root. *Proceedings of the National Academy of Sciences, USA* 110: 14498–14503.
- Khanal BP, Grimm E, Knoche M. 2013. Russetting in apple and pear: a plastic periderm replaces a stiff cuticle. *Arabidopsis* 5: pls048.
- Kosma DK, Molina I, Ohlrogge JB, Pollard M. 2012. Identification of an Arabidopsis fatty alcohol:caffeoyle-coenzyme A acyltransferase required for the synthesis of alkyl hydroxycinnamates in root waxes. *Plant Physiology* 160: 237–248.
- Kosma DK, Rice A, Pollard M. 2015. Analysis of aliphatic waxes associated with root periderm or exodermis from eleven plant species. *Phytochemistry* 117: 351–362.
- Kucukoglu M, Nilsson J, Zheng B, Chaabouni S, Nilsson O. 2017. WUSCHEL-RELATED HOMEBOX4 (WOX4)-like genes regulate cambial cell division activity and secondary growth in *Populus* trees. *New Phytologist* 215: 642–657.
- Lampropoulos A, Sutikovic Z, Wenzl C, Maegele I, Lohmann JU, Forner J. 2013. GreenGate – a novel, versatile, and efficient cloning system for plant transgenesis. *PLoS ONE* 8: e83043.
- Lenzian KJ. 2006. Survival strategies of plants during secondary growth: barrier properties of phellements and lenticels towards water, oxygen, and carbon dioxide. *Journal of Experimental Botany* 57: 2535–2546.
- Lieberman LM, Sparks EE, Moreno-Risueno MA, Petricka JJ, Benfey PN. 2015. MYB36 regulates the transition from proliferation to differentiation in the Arabidopsis root. *Proceedings of the National Academy of Sciences, USA* 112: 12099–12104.
- Lourenco A, Rencoret J, Chemetova C, Gominho J, Gutierrez A, Del Rio JC, Pereira H. 2016. Lignin composition and structure differs between xylem, phloem and phellem in *Quercus suber* L. *Frontiers in Plant Science* 7: 1612.
- Lulai EC, Corsini DL. 1998. Differential deposition of suberin phenolic and aliphatic domains and their roles in resistance to infection during potato tuber (*Solanum tuberosum* L.) wound-healing. *Physiological and Molecular Plant Pathology* 53: 209–222.
- Lulai EC, Freeman TP. 2001. The importance of phellogen cells and their structural characteristics in susceptibility and resistance to excoriation in immature and mature potato tuber (*Solanum tuberosum* L.) periderm. *Annals of Botany* 88: 555–561.
- Marques AV, Pereira H. 2013. Lignin monomeric composition of corks from the barks of *Betula pendula*, *Quercus suber* and *Quercus cerris* determined by Py-GC-MS/FID. *Journal of Analytical and Applied Pyrolysis* 100: 88–94.
- Marques-Bueno MDM, Morao AK, Cayrel A, Platre MP, Barberon M, Caillieux E, Colot V, Jaillais Y, Roudier F, Vert G. 2016. A versatile Multisite Gateway-compatible promoter and transgenic line collection for cell type-specific functional genomics in Arabidopsis. *Plant Journal* 85: 320–333.
- Mazur E, Kurczynska E. 2012. Rays, intrusive growth, and storied cambium in the inflorescence stems of *Arabidopsis thaliana* (L.) Heynh. *Protoplasma* 249: 217–220.
- Melzer S, Lens F, Gennen J, Vanneste S, Rohde A, Beeckman T. 2008. Flowering-time genes modulate meristem determinacy and growth form in *Arabidopsis thaliana*. *Nature Genetics* 40: 1489–1492.
- Miguel A, Milhinhos A, Novak O, Jones B, Miguel CM. 2016. The SHORT-ROOT-like gene PtSHR2B is involved in *Populus* phellogen activity. *Journal of Experimental Botany* 67: 1545–1555.
- Molina I, Li-Beisson Y, Beisson F, Ohlrogge JB, Pollard M. 2009. Identification of an Arabidopsis feruloyl-coenzyme a transferase required for suberin synthesis. *Plant Physiology* 151: 1317–1328.
- Muller D, Schmitz G, Theres K. 2006. Blind homologous R2R3 Myb genes control the pattern of lateral meristem initiation in Arabidopsis. *Plant Cell* 18: 586–597.
- Naseer S, Lee Y, Lapierre C, Franke R, Nawrath C, Geldner N. 2012. Casparian strip diffusion barrier in Arabidopsis is made of a lignin polymer without suberin. *Proceedings of the National Academy of Sciences, USA* 109: 10101–10106.
- Neubauer JD, Lulai EC, Thompson AL, Suttle JC, Bolton MD. 2012. Wounding coordinately induces cell wall protein, cell cycle and pectin methyl esterase genes involved in tuber closing layer and wound periderm development. *Journal of Plant Physiology* 169: 586–595.
- Neubauer JD, Lulai EC, Thompson AL, Suttle JC, Bolton MD, Campbell LG. 2013. Molecular and cytological aspects of native periderm maturation in potato tubers. *Journal of Plant Physiology* 170: 413–423.

- Olvera-Carrillo Y, Van Bel M, Van Hautegeem T, Fendrych M, Huysmans M, Simaskova M, van Durme M, Buscaill P, Rivas S, Coll NS *et al.* 2015. A conserved core of programmed cell death indicator genes discriminates developmentally and environmentally induced programmed cell death in plants. *Plant Physiology* 169: 2684–2699.
- Oven P, Torelli N, Shortle WC, Zupančič M. 1999. The formation of a ligno-suberised layer and necrophylactic periderm in beech bark (*Fagus sylvatica* L.). *Flora* 194: 137–144.
- Pereira H. 1988. Chemical composition and variability of cork from *Quercus suber* L. *Wood Science and Technology* 22: 211–218.
- Pereira H. 2007. *Cork biology production and uses*. Amsterdam, the Netherlands: Elsevier.
- Pinto PCRO, Sousa AF, Silvestre AJD, Neto CP, Gandini A, Eckerman C, Holmbom B. 2009. *Quercus suber* and *Betula pendula* outer barks as renewable sources of oleochemicals: a comparative study. *Industrial Crops and Products* 29: 126–132.
- Rains MK, Gardiyehewa de Silva ND, Molina I. 2017. Reconstructing the suberin pathway in poplar by chemical and transcriptomic analysis of bark tissues. *Tree Physiology* 1: 1–22.
- Roppolo D, De Rybel B, Denervaud Tendon V, Pfister A, Alassimone J, Vermeer JE, Yamazaki M, Stierhof YD, Beeckman T, Geldner N. 2011. A novel protein family mediates Casparian strip formation in the endodermis. *Nature* 473: 380–383.
- Sabba RP, Lulai EC. 2002. Histological analysis of the maturation of native and wound periderm in potato (*Solanum tuberosum* L.) tuber. *Annals of Botany* 90: 1–10.
- Sabba RP, Lulai EC. 2005. Immunocytological analysis of potato tuber periderm and changes in pectin and extensin epitopes associated with periderm maturation. *Journal of the American Society for Horticultural Science* 130: 936–942.
- Schindelin J, Arganda-Carreras I, Frise E, Kaynig V, Longair M, Pietzsch T, Preibisch S, Rueden C, Saalfeld S, Schmid B *et al.* 2012. Fiji: an open-source platform for biological-image analysis. *Nature Methods* 9: 676–682.
- Schreiber L, Franke R, Hartmann K. 2005. Wax and suberin development of native and wound periderm of potato (*Solanum tuberosum* L.) and its relation to peridermal transpiration. *Planta* 220: 520–530.
- Serra O, Hohn C, Franke R, Prat S, Molinas M, Figueras M. 2010. A feruloyl transferase involved in the biosynthesis of suberin and suberin-associated wax is required for maturation and sealing properties of potato periderm. *Plant Journal* 62: 277–290.
- Serra O, Soler M, Hohn C, Franke R, Schreiber L, Prat S, Molinas M, Figueras M. 2009a. Silencing of *StKCS6* in potato periderm leads to reduced chain lengths of suberin and wax compounds and increased peridermal transpiration. *Journal of Experimental Botany* 60: 697–707.
- Serra O, Soler M, Hohn C, Sauveplane V, Pinot F, Franke R, Schreiber L, Prat S, Molinas M, Figueras M. 2009b. *CYP86A33*-targeted gene silencing in potato tuber alters suberin composition, distorts suberin lamellae, and impairs the periderm's water barrier function. *Plant Physiology* 149: 1050–1060.
- Sibout R, Plantegenet S, Hardtke CS. 2008. Flowering as a condition for xylem expansion in *Arabidopsis* hypocotyl and root. *Current Biology* 18: 458–463.
- Silva S, Sabino M, Fernandes E, Correló V, Boesel L, Reis R. 2005. Cork: properties, capabilities and applications. *International Materials Reviews* 50: 345–365.
- Soler M, Serra O, Fluch S, Molinas M, Figueras M. 2011. A potato skin SSH library yields new candidate genes for suberin biosynthesis and periderm formation. *Planta* 233: 933–945.
- Soler M, Serra O, Molinas M, Huguet G, Fluch S, Figueras M. 2007. A Genomic approach to suberin biosynthesis and cork differentiation. *Plant Physiology* 144: 419–431.
- Spicer R, Groover A. 2010. Evolution of development of vascular cambia and secondary growth. *New Phytologist* 186: 577–592.
- Thangavel T, Tegg RS, Wilson CR. 2016. Toughing it out – disease-resistant potato mutants have enhanced tuber skin defenses. *Phytopathology* 106: 474–483.
- Thomson N, Evert RF, Kelman A. 1995. Wound healing in whole potato tubers: a cytochemical, fluorescence, and ultrastructural analysis of cut and bruise wounds. *Canadian Journal of Botany* 73: 1436–1450.
- Torrón S, Semlitsch S, Martinelle M, Johansson M. 2014. Polymer thermosets from multifunctional polyester resins based on renewable monomers. *Macromolecular Chemistry and Physics* 215: 2198–2206.
- Tucker SC. 1975. Wound regeneration in the lamina of magnoliaceous leaves. *Canadian Journal of Botany* 53: 1352–1364.
- Vermeer JE, von Wangenheim D, Barberon M, Lee Y, Stelzer EH, Maizel A, Geldner N. 2014. A spatial accommodation by neighboring cells is required for organ initiation in *Arabidopsis*. *Science* 343: 178–183.
- Vishwanath SJ, Delude C, Domergue F, Rowland O. 2015. Suberin: biosynthesis, regulation, and polymer assembly of a protective extracellular barrier. *Plant Cell Reports* 34: 573–586.
- Vishwanath SJ, Kosma DK, Pulsifer IP, Scandola S, Pascal S, Joubes J, Dittich-Domergue F, Lessire R, Rowland O, Domergue F. 2013. Suberin-associated fatty alcohols in *Arabidopsis*: distributions in roots and contributions to seed coat barrier properties. *Plant Physiology* 163: 1118–1132.
- Vulavala VKR, Fogelman E, Rozental L, Faigenboim A, Tanami Z, Shoseyov O, Ginzberg I. 2017. Identification of genes related to skin development in potato. *Plant Molecular Biology* 94: 481–494.
- Waisel Y. 1995. Developmental and functional aspects of the periderm. In: Iqbal M, ed. *The cambial derivatives*. Stuttgart, Germany: Gebrüder Borntraeger Verlagsbuchhandlung, 293–315.

Supporting Information

Additional Supporting Information may be found online in the Supporting Information tab for this article:

Fig. S1 Periderm formation in *Arabidopsis*.

Fig. S2 Periderm establishment in the hypocotyl and in the root grown under different conditions.

Fig. S3 Stages of periderm development in the hypocotyl of plants grown under different conditions.

Fig. S4 Periderm formation in lateral roots, phelloderm stainings and programmed cell death in the root endodermis.

Fig. S5 Programmed cell death in the hypocotyl during periderm growth.

Fig. S6 Several suberin biosynthesis genes are expressed in the phellem.

Fig. S7 Chemical composition of hypocotyl phellem cells.

Please note: Wiley Blackwell are not responsible for the content or functionality of any Supporting Information supplied by the authors. Any queries (other than missing material) should be directed to the *New Phytologist* Central Office.